

CHAPTER 1

INTRODUCTION

1.1 Introduction

Total knee replacement (TKR) is a surgical procedure performed when severe degeneration of the knee joint is present [1]. Knee replacement surgery is a routine procedure performed on over 400 000 people worldwide each year [2]. TKR has become one of the most common orthopaedic procedures performed on older persons. In the past 20 years, the rates of knee replacement procedures have increased approximately eightfold [3]. Over 90% of people who have had a TKR experience an improvement in knee pain and function [4]. The average joint replacement patient is around 65-70 years old; however people of all ages have received knee implants. Studies have consistently shown knee implants are functioning well in 90-95% of patients between 10 and 15 years after surgery [5].

TKR originated with the hinged prosthesis over 100 years ago, the modern era of TKR began as a result of the combined work of a number of engineers and surgeons who developed the condylar-style implant between the years of 1969 and 1980 [6]. The goal of any knee replacement procedure is to alleviate pain and restore functionality to the patient. This knee must be stable yet allow varied movements associated with activities of daily living. Climbing up stairs or rising from a chair are increasingly difficult activities when the knee is not functioning properly.

Knee implant system involves two bones; distal femur (the bottom end of the femur) and proximal tibia (the upper end of the tibia). It has three components; femoral, tibial, and patellar components as shown in Figure 1.1. Femoral component has a convex shape which is a large plate bent to help the curvatures of the femoral condyles (located at distal femur). This plate is often fabricated from Cobalt-Chromium (CoCr) alloy or titanium. The tibial component is a plate made of Ultra High Molecular Weight Polyethylene (UHMWPE). This plate is enclosed in a stemmed metallic back-up which is often made of Titanium. Patellar component is fabricated from Polyethylene [7, 8].

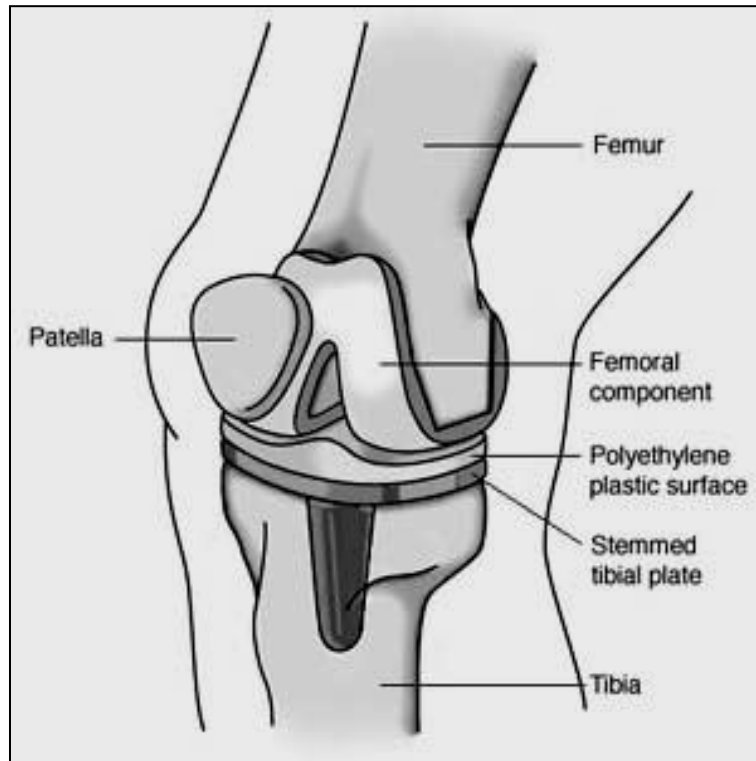


Figure 1.1 knee implant components [9]

TKR is a surgical procedure performed when severe degeneration of the knee joint is present [10]. TKR has become one of the most common orthopaedic procedures performed on older persons. In the past 20 years, the rates of knee replacement procedures have increased approximately eightfold [11, 12].

Total knee arthroplasty (TKA), also referred to as total knee replacement (TKR), is a surgical procedure where worn, diseased, or damaged bone and cartilage, from the surfaces of knee joint, are removed from the distal end of the femur, proximal end of the tibia, and the back surface of the patella (if needed) and replaced with artificial surfaces that try to mimics the natural knee function and motion [13].

1.2 Motivation

Conventional knee implants give a satisfactory result in many cases that bring the patient back to a near-normal and active lifestyle. However, in some cases, conventional knee implant

components are not sufficient because of abnormal joint anatomy or postoperative complications [14, 15]. In such cases, a custom design of knee implants for human is necessary. The proposed custom design of implants has become possible with advancements in medical imaging, bio-modeling, reverse engineering, rapid prototyping, and advanced CAD modeling. Computed Tomography (CT) scan data was converted into CAD model, and using advanced CAD modeling functions, a patient knee implant was designed.

Younger patients have a lower success rate than older patients when conventional standard implant components are used [16]. Aseptic loosening is the most common cause for premature failure in younger patients [17]. It has been suggested that a more active lifestyle in younger patients is the major cause for premature failure. For this reason, many countries try to delay the surgery until the patient has reached the age of 65 [18].

Aseptic Loosening of the knee components is usually caused by micromotions that prevent appropriate bone ingrowth or bone remodeling due to uneven stress distribution on the bone implant surface [19]. The uneven stress distribution is caused by the design of bone-implant interface that has been restricted by the surgical techniques currently available. The bones are reshaped to fit the implant components by planar straight five cuts using an oscillating saw and cutting guides. The resultant bone shape is squared-off, rather than rounded as is its original shape. Thus, the forces generated due to the patient's weight and activities are distributed in such a way that the newly created "corners" of the distal femur take a disproportionate amount of stress, rather than the forces being evenly distributed over the rounded ends of a natural femur. This can lead to bone remodeling and loosening of the prosthetic joint. Aseptic loosening of prosthetic components may eventually lead to pain, instability and loss of function, and thus constitutes a failure as shown in Figure 1.2.

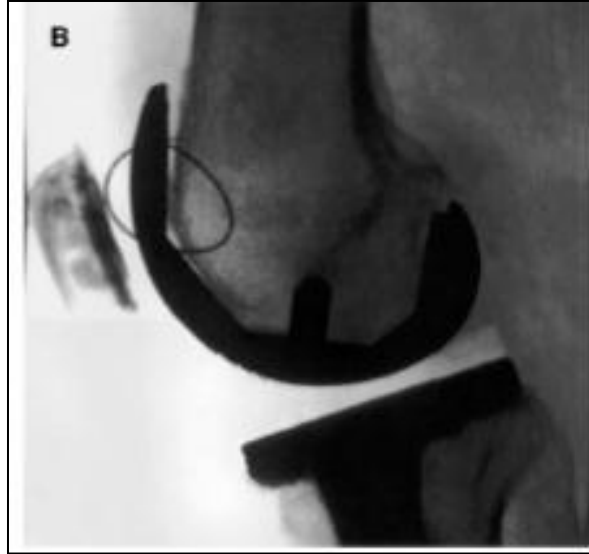


Figure 1.2 femoral component loosening [20].

The proximal tibia is reshaped using a single planar straight cut, and the tibial tray is normally secured using a stem configuration. While loading the tibial tray, high stress concentrations are caused by the stem; the cancellous bone can collapse, leaving a void around the stem. If the tibial component is not properly sized and if the tibial component does not have enough cortical bone supporting it, then the component can protrude into the cancellous bone and create an implant failure [21].

The Ultra High Molecular Weight Polyethylene (UHMWPE)-bearing component can also cause failures leading to revision surgery and replacement of all components. In many cases, the bearing surface is completely worn through; and metal-on-metal contact between the femoral component and the tibial tray causes discomfort and loss of motion. In other cases the wear particles cause osteolysis; and a revision surgery is required to address the pain, discomfort, and lack of mobility [22].

Many other factors (such as loosening of femoral and tibial components, sacrificed or torn ligaments, and mobile bearing components) can increase the wear rate of the bearing surface, which will decrease the component's longevity and increase the risk for osteolysis [22, 23].

Also, the articulating surface of a conventional knee implant component is of generic shape while every individual patient has a unique shape of knee joint and this causes the problems mentioned earlier. Most patients' gaits are altered after a total knee arthroplasty (TKA) and proper walking and ambulation has to be relearned due to the change in surface geometry.

Owing to the generic shape of the femoral component and the patellar groove, it is common to resurface the patella in order to prevent dislocation, even though the patella is not affected by osteoarthritis. Studies have shown that resurfacing of a healthy patella can cause unnecessary postoperative anterior pain for the patients [24]. According to the same study, a correctly designed femoral component with a sufficient patellar groove can avoid the resurfacing and reduce the risk for postoperative pain. Today, many implant companies offer implant components that are customized according to size and shape [24].

1.3 Objectives

Every individual has a unique shape of knee joint. The use of a standard implant is a compromise of shape, cost, inventory and time to manufacture it. Current research has led to the development of custom designed implant components to accommodate for the great variations in size and shape of the knee joint among individuals and to prevent aseptic loosening [25, 26 and 27]. This study will provide a new proposed customized knee implant system that could provide a better result for younger patients and patients with an abnormal joint anatomy. The proposed custom design process can be used for a wide variety of implants and is not restricted to knee-implant components. The main objective of this study is to design custom made implant as smooth surface of femoral implant component with maintain the articulating surface of femoral as natural knee. The external articulating surface with tibial component and patellar component were maintained.

The implant design shall include optimization of thickness and development of methodology to get from a CT scan of the knee to final implantation in a patient. This shall be achieved by:

- Converting CT data into CAD model
- Designing the implant using the original human femur specific data with the help of different 3D modeling softwares.

Design verification shall be done by comparing custom designed implant and conventional standard design. Finite element analysis used to examine the stress distribution in the implant-bone interface for the custom implant and conventional implant design and to compare between the two models.

1.4 Structure of thesis

The thesis consists of seven chapters:

Chapter 1 is the introduction of total knee replacement, motivation, objectives and the structure of the thesis.

Chapter 2 introduces the structure of a knee joint. Motion of the knee joint and forces in the knee joint during the gait cycle are described, with structure and mechanical property of bones.

Chapter 3 introduces the total knee replacement arthritis and diseases. In this chapter, Implantation of femoral component knee joint and Failure model of total knee prosthesis are reviewed from literature review.

Chapters 4-6 are presented as separate projects with methodology, finite element analysis, results and discussion as follow:

- ✓ **Chapter 4** describes the methodology of custom design femoral component.
- ✓ **Chapter 5** describes the design of the femoral implant in details including the required Finite Element Analysis to test and examine the custom implant.
- ✓ **Chapter 6** presents the results which show the stress distributions under different load conditions. Also, Conclusions are presented in.

Finally in Chapter 7, all the research questions are answered and conclusions for this work are given, also present the future work about custom design knee joint.

CHAPTER 2

THE KNEE JOINT

Chapter 2 introduces the anatomy and physiology of the knee joint as well as the Structure and mechanical property of bones. Motion of the knee joint and forces in the knee joint during the gait cycle are described in this chapter.

2.1 Anatomy of the knee joint

The human lower limb is adapted for weight-bearing, locomotion and maintaining the unique, upright, bipedal posture [28]. The knee joint is the middle joint of the lower limb. It works in conjunction with the hip and ankle joint, for supporting and moving the body during a variety of both routine and difficult activities. The weight of the body, inertia forces and muscle forces are transmitted to the ground through the knee, which has to bear compressive forces up to six times body weight during daily life activities [29, 30].

The knee is one of the most important and most studied joints in the human body [31]. Dynamically, it works in conjunction with the hip joint and ankle to support and move the body during a variety of both routine and difficult activities. It has an important role either in human locomotion as in static erect posture. As it can be seen in Figure 2.1 the knee is composed of two distinct articulations located within a single joint capsule, sharing the same articular cavity: the tibiofemoral joint, the articulation between the distal femur and the proximal tibia; and the patellofemoral joint – the articulation between the posterior patella and the femur [32, 33].

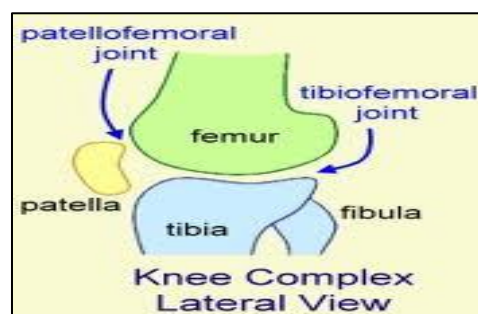


Figure 2.1 tibio-femoral and patello-femoral joints [34]

The knee joint is the middle joint of the lower limbs of the human body. It is the largest, most complex and most heavily-loaded joint of the human body and is regularly subjected to stress [35, 36]. As it can be seen in Figure 2.2, it is formed by a combination of hard tissue (bone) and soft tissues (ligaments, muscle, synovial fluid and cartilage). The bone parts that form the knee joint are the distal end of the femur, through the femoral condyles, the proximal end of the tibia, through tibial condyles and the patella. The soft tissue parts that sustain and move the bone structure are: the ligaments, connecting bone to bone (e.g. anterior cruciate and posterior cruciate ligament – ACL and PCL; lateral and medial collateral ligaments – LCL and MCL); the muscles that contribute to the stabilization of the joint and participate in the angular (rotatory) motion (flexion/extension, medial/lateral rotation and abduction/ adduction); and the tendons, which attach muscle to bone (e.g. quadriceps tendon). Other soft tissue parts are: the menisci (lateral and medial) that are interarticular cartilages, act as shock absorbers and improve the congruence between articular surfaces; the articular cartilage that covers the ends of the bones (distal end of the femur, the top of the tibia, and the back of the patella) with a smooth surface that allows easy gliding movement, facilitating motion; and the synovial liquid that have shock absorbing and lubricating functions. The anatomical fitting of the articular surface to the articular capsule, i.e., the topology of articular surfaces, along with the combination of actions from ligaments and cartilages, create the passive stabilizer system of the joint. Various muscles and their tendons form the knee's dynamic stabilizers [36, 37].

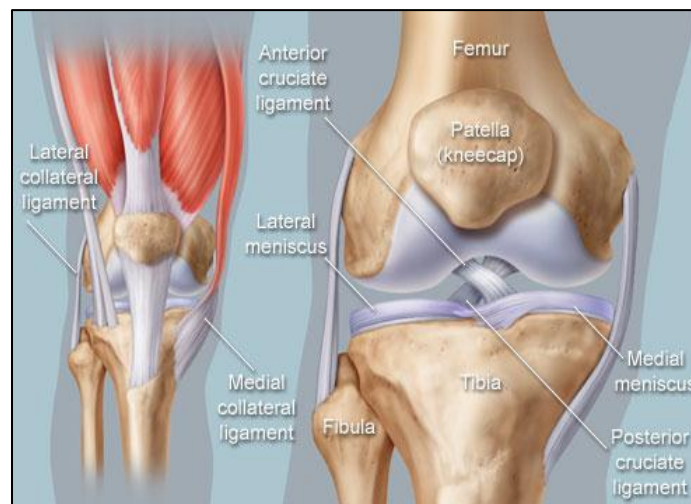


Figure 2.2 Anatomy of the knee joint: anterior medial view [38]

2.1.1 Bones of the knee joint

The knee is a hinge joint made up of three bones held firmly together by ligaments. These bones are the femur (upper leg bone), the tibia (shin bone) and the patella (knee cap). The tibial plateau and two condyles on the distal end of the femur make contact with the patella as shown in figure 2.3.

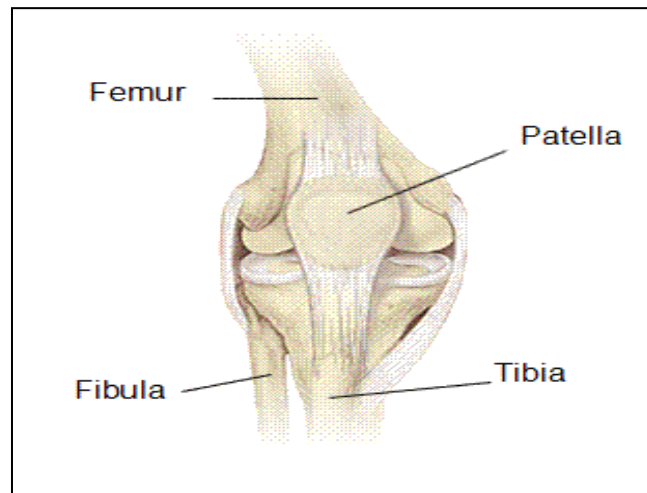


Figure 2.3 Bones of the knee joint. [39]

The anatomy of the knee is important for the design of the total knee replacement prosthesis. The orientation, shape and kinematics of the knee depend on the morphological shape of the distal femur.

2.1.1.1 The femur

In human anatomy, the femur, or thighbone, is the longest, largest, strongest and heaviest bone [35, 36]. As can be seen in Figure 2.4, the distal femur is composed of two convex protrusions, the medial and the lateral femoral condyles. The condyles are separated posteriorly by an intercondylar fossa and are joined anteriorly by the femoral trochlear groove or surface. At its distal end, its major weight-bearing articulation is with the tibia, at the inferior and posterior surfaces of the femur's condyles (which constitute the surface for articulation with the corresponding condyles of the tibia and menisci). It also articulates anteriorly with the patella, at the trochlear groove [32, 33].

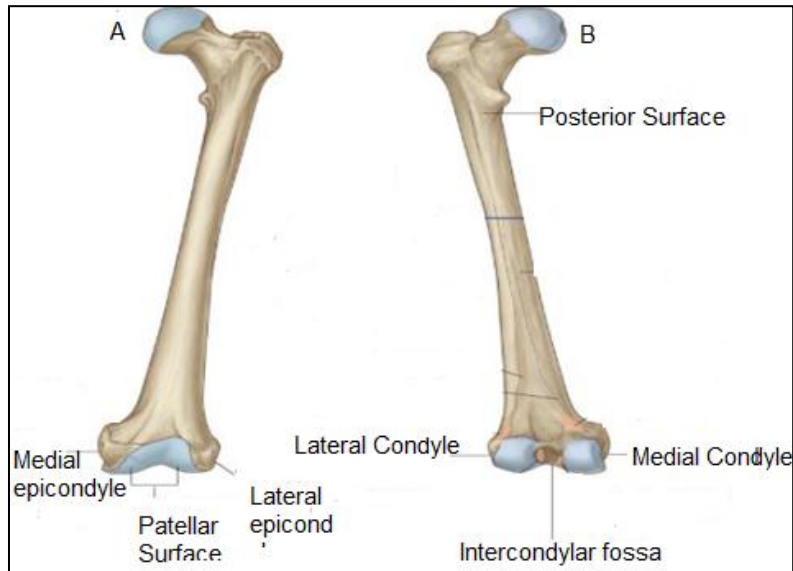


Figure 2.4 Shaft and distal end of femur. A. Anterior view. B. Posterior view.

2.1.1.2 The tibia

The tibia is the second largest bone of the human body after the femur. It is the medial one of the two lower leg bones (tibia and fibula), and is the only one that articulates with the femur at the knee joint [33, 35]. The proximal tibia is expanded in the transverse plane for weight-bearing reasons, and it is formed by the medial and lateral condyles or plateaus which constitute the distal articular surface of the knee joint. The tibial condyles are separated by an intercondylar region, which is constituted by a roughened area and two bony spines called intercondylar eminence (that serves as attaching points for the cruciate ligaments and for menisci) [36], as it can be visualized in Figure 2.5.

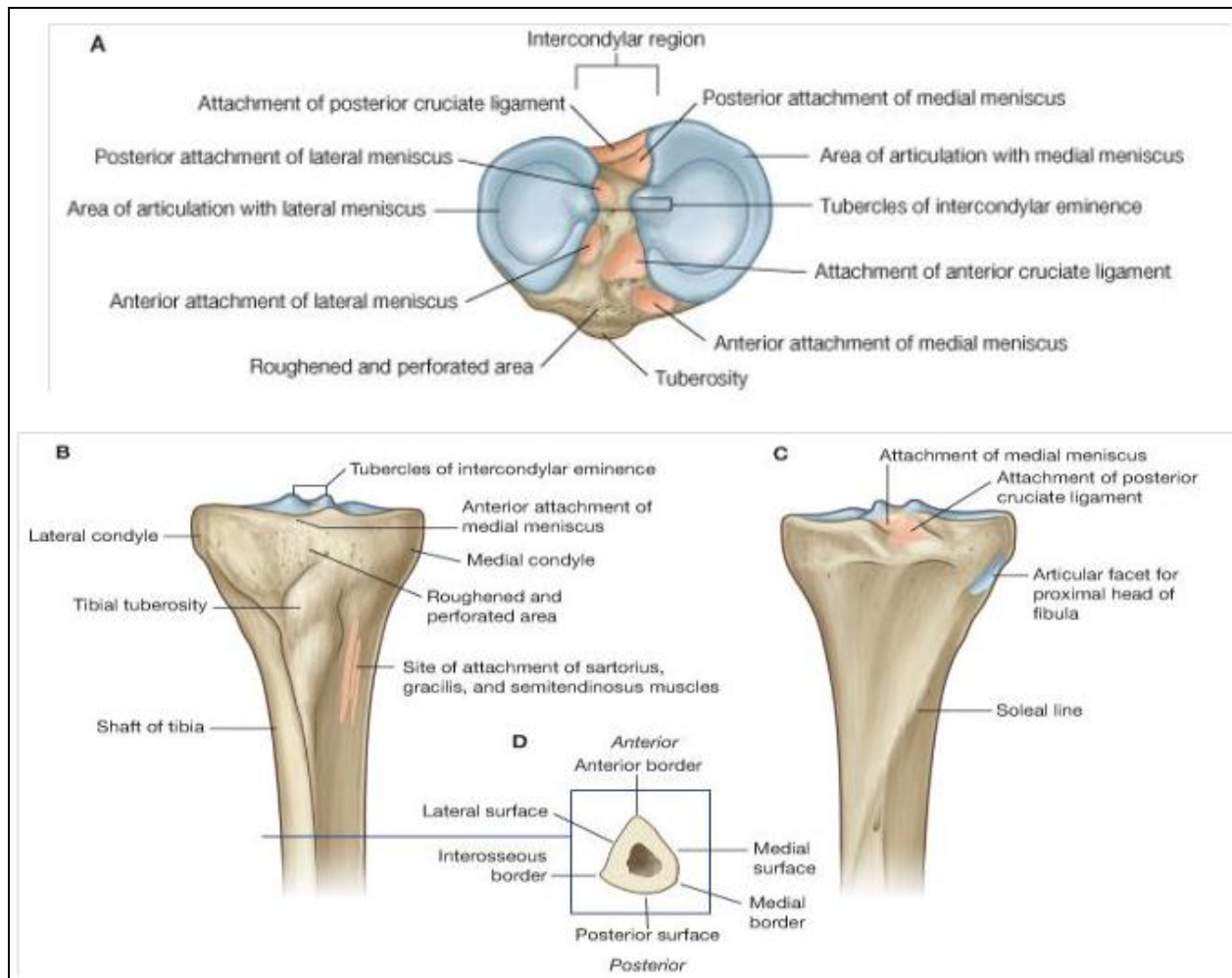


Figure 2.5 Proximal extremity of the tibia. A. Superior view – tibial plateau. B. Anterior view. C. Posterior view. D. Cross-section through the shaft of tibia [33].

The central part of the tibial condyles articulates with the corresponding lower and posterior parts of the femur's condyles that constitute the knee articulation. The outer margins of the surfaces are the regions in contact with the interarticular cartilages (menisci). The tibial plateaus are predominantly flat, with a slight convexity at the anterior and posterior margins, suggesting that this bony architecture does not match up well with the convexity of the femoral condyle. Thus, accessory joint structures (menisci) are necessary between articular surfaces to improve joint congruency and bony stability, obliterating the intervals between the tibial and the femoral surfaces in their various motions and compensating for any superficial irregularities [36].

Together the articular surfaces of the tibial condyles and the intercondylar region form a 'tibial plateau', which articulates with and is anchored to the distal end of the femur. During knee extension, the intercondylar eminence of the tibia becomes lodged in the intercondylar fossa of the femur, helping to prevent rotation [35].

2.1.1.3 The patella

The patella (knee cap) is a flat, triangular bone situated on the front of the knee joint. This bone is the largest sesamoid bone in the body and is embedded in the tendon of the quadriceps femoris muscle – see Figure 2.6. This tendon crosses anterior to the knee joint to insert on the tibia (via patellar ligament, connecting patella to the tibia) [33]. The patella increases the leverage of the tendon, maintains its position when the knee contracts and acts as a shield towards the front of the knee joint, as it is composed mainly of dense cancellous tissue. Protection and muscular attachment are the main functionalities of the patella. During flexion and extension of the knee, the patella slide up and down in the patellar groove or surface [33, 35].

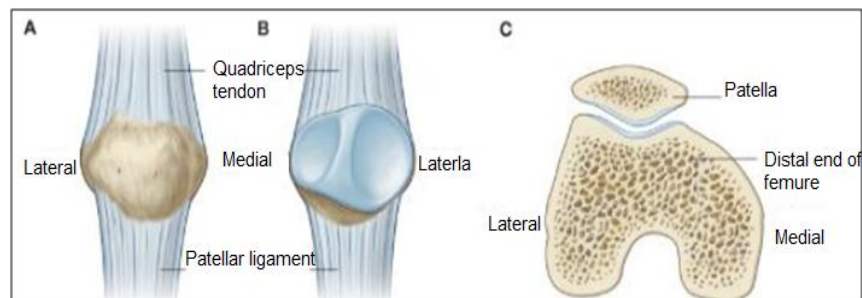


Figure 2.6 Patella. A. Anterior view. B. Posterior view. C. Superior view [35].

2.1.2 Menisci

The menisci are two semicircular shape fibrocartilages that are located on top and circumference of the tibial condyles, covering one half to two thirds of the articular surface of the tibial plateau as shown in Figure 2.7. They serve to deepen the surfaces of the head of the tibia for articulation with the condyles of the femur (forming concavities into which the femoral condyles sit), improving the congruence and increasing the contact area at the tibiofemoral joint. This way, the

menisci distribute the weight-bearing loads from the femur to the tibia more evenly and stabilize the knee joint preventing the translation (sliding) of the femur with respect to the tibia. Additionally, they are a shock absorbing media that protects the joint and serve as lubricant providing for very low friction between the articular surfaces [35].

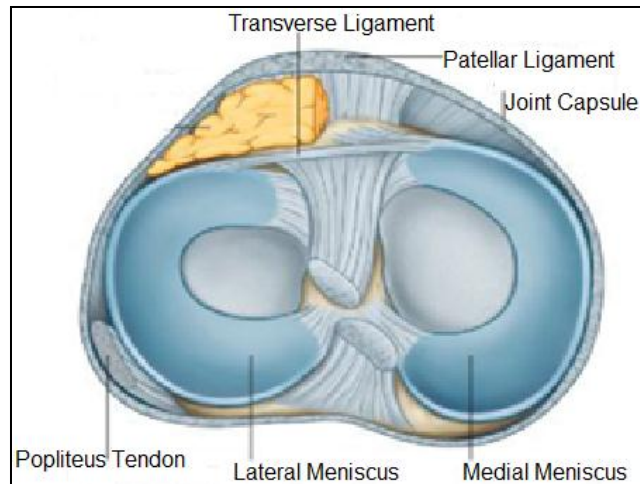


Figure 2.7 Menisci of the knee joint, superior view [39].

2.1.3 Ligaments

Ligaments connect one bone to another, usually at or near a joint. Ligaments and tendons associated with synovial joints play an important role in keeping joint surfaces together (providing stability for the joint) and guiding motion (allowing and limiting mobility).

There are four major ligaments in the knee joint: two cruciate and two collateral ligaments, which assist in tibiofemoral joint stability as shown in figure 2.8. The two cruciate ligaments are located inside the knee joint between the femur and the tibia, in the intercondylar region, and ensure anterior-posterior stability of the joint. The anterior cruciate ligament (ACL) prevents anterior displacement of the tibia relative to the femur (forward sliding), while the posterior cruciate ligament (PCL) restricts posterior displacement (sliding backwards) [33, 36].

The collateral ligaments are located on the outer surfaces of the knee, one on each side of the joint, and stabilize the hinge-like motion of the knee, providing for varus–valgus stability throughout the range of motion of the joint (impede sideways motion on the frontal plane). The medial collateral ligament (MCL) is placed at the inner part of the joint and is the primary

restraint to excessive abduction (valgus - outward angulation of the distal segment) and lateral rotation stresses at the knee, while the lateral collateral ligament (LCL) (connecting the fibula to the femur) is primarily responsible for limiting varus (inward angulation of the distal segment) motion and limit excessive lateral rotation of the tibia [33].

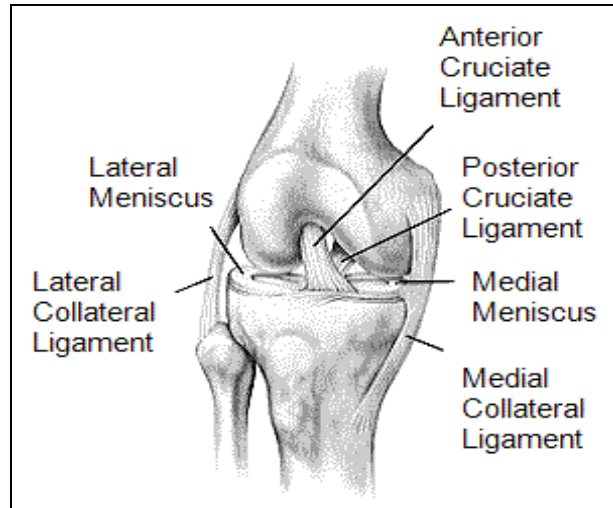


Figure 2.8 Ligaments of knee joint. [40]

2.1.4 Mechanical axis of the knee

The mechanical axis is a static weight bearing axis which can be drawn on a radiographic image of the limb. The mechanical axis is defined in the frontal (coronal) plane and the sagittal plane. The anatomical planes of the human body are can be seen in Figure 2.9. The mid-sagittal plane divides the body into right and left halves. Frontal (coronal) planes are drawn perpendicular to the sagittal lines and divide the body into anterior and posterior sections. Horizontal (transverse) planes divide the body into upper (superior) and lower (inferior) sections.

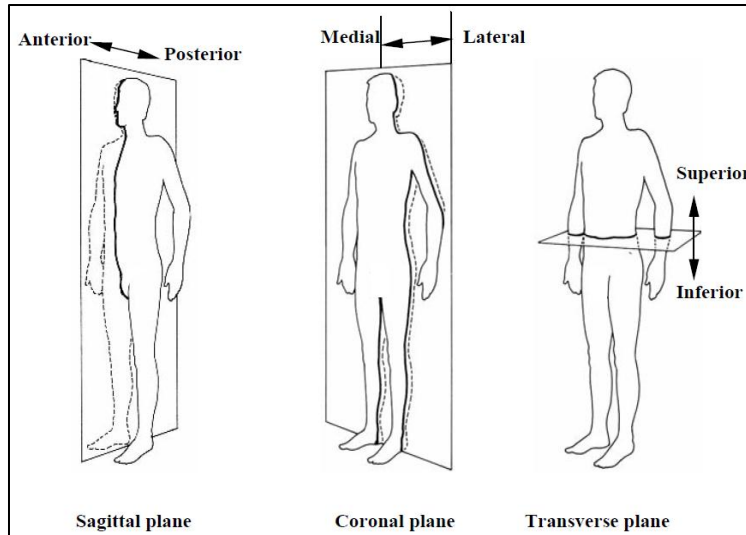


Figure 2.9 Anatomical planes of the human body

The mechanical axis of the lower limb in the frontal plane is defined as a line drawn from the centre of the femoral head to the centre of the ankle joint, see Figure 2.10. In the sagittal plane, the normal mechanical axis runs from the centre of gravity to the centre of the ankle joint. This line is practically perpendicular to the ground. It therefore runs just behind the femoral head and just in front the knee.

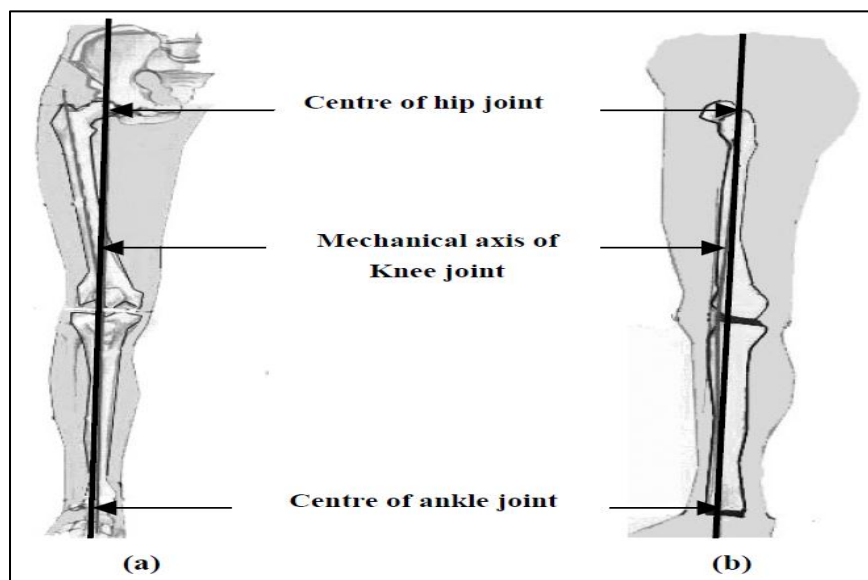


Figure 2.10 Mechanical axis of the knee joint: (a) mechanical axis in frontal plane; (b) mechanical axis in sagittal plane

2.1.5 Deformity (mal-alignment) of knee joint

Deformity in the limb may occur in any plane, not just the anatomical sagittal or frontal planes. The common situation is for deformity to occur between these anatomical planes. In other words, angular deformity or mal-alignment may occur in any direction; medial or lateral, anterior and posterior or anywhere in between. Furthermore rotational deformity (internal or external) and translational deformity may coexist.

In a healthy, well-aligned knee joint, the mechanical axis passes through the middle of the knee in the frontal plane. In condition of abnormal alignment, the mechanical axis does not pass through the centre of the knee joint. As can be seen in Figure 2.11, **Varus deformity** (mal-alignment) often involves collapse of the medial condyles of the tibia and femur (The tibia adducted with respect to the femur is defined as varus deformity); and **valgus deformity** that of the lateral condyles (the tibia abducted with respect to the femur is defined as valgus deformity).

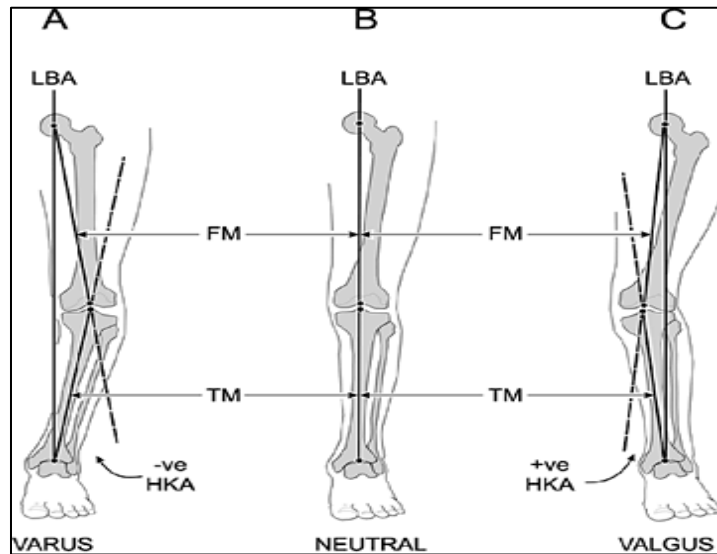


Figure 2.11 malalignment of the knee, Varus (A), Natural (B), Valgus(C). [41]

In many knee joint diseases, the mechanical axis is disturbed and does not pass through the centre of the joint. This disturbance results in overload of distinct areas of the knee joint leading to damage. The patella does not lie symmetrically in its groove. The surgeon must restore the mechanical axis of the knee joint during the total knee replacement surgery, i.e. the new knee

joint must be put in such a position that the mechanical axis passes through the middle of the new knee joint.

2.2 Kinematics of the Knee

The basic mechanism of movement between the femur and the tibia is a combination of rolling, gliding and spinning during flexion and extension [35]. The basic kinematic principle of motion in the knee joint can be represented by a mechanism called the crossed four-bar linkage as shown in figure 2.12 [42].

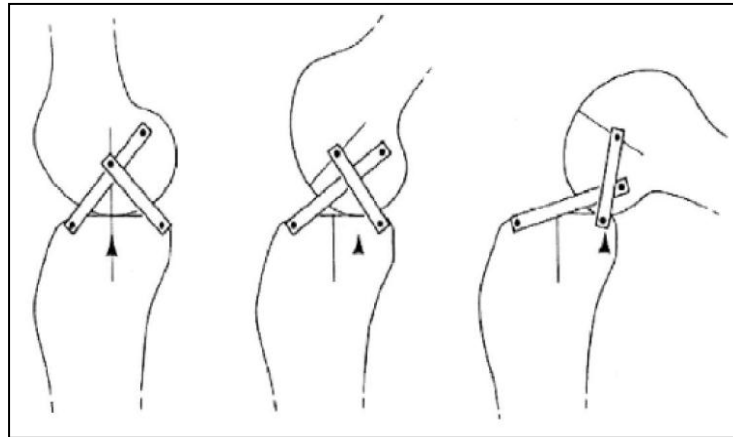


Figure 2.12 Four-bar linkages. [42]

This is only a schematic representation because the cruciate ligaments are not rigid bars and can stretch under load. Although the cruciate ligaments play an important role in the motion of the knee joint, the shape of the distal femur is largely responsible for the movement. The distal articulating surface of the femur could be described as being composed of three circular surfaces [43]:

1. An anterior circle representing the floor of the patellar groove.
2. A posterior circle representing the posterior femoral condyles.
3. A middle circle with a larger radius representing the distal femoral condyles.

The lateral and medial condyles of the distal femur are asymmetric in a number of morphological features [44]. The lateral condyle is flattened distally and has a larger radius than the medial condyle. The medial condyle can be viewed as a sphere and is somewhat constrained to a ball-in-

socket joint. Minimal anterior/posterior translation occurs on the medial side of the femur. The posterior medial and lateral condyles are circular in shape and have an almost equal radius as shown in figure 2.13 [45].

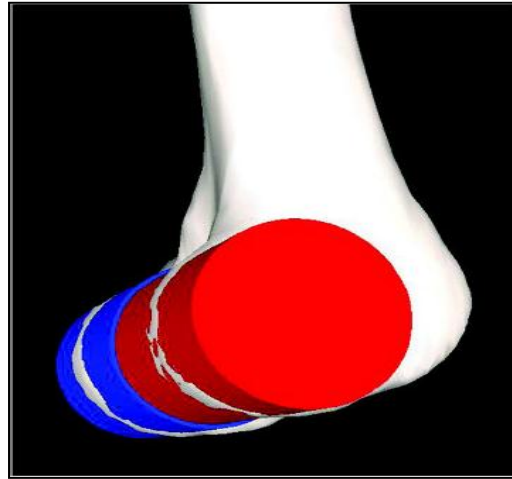


Figure 2.13 Circular posterior condyles. [45]

2.2.1 Tibial Plateau

There exists a difference between the medial and lateral side of the tibial plateau. The medial plateau is slightly concave, whereas the lateral is convex [46].

The tibial plateau only affects the kinematics of the knee and not the dimensions of the distal femur [47].

2.2.2 Patella

The trochlear groove in which the patella moves is relevant to the dimensions of the distal femur. The forces of the quadriceps muscles are guided around the distal end of the femur with a sesamoid bone called the patella [48]. The tracking of the patellofemoral joint is an important anatomical consideration of a total knee arthroplasty [49]. The patellar groove position of the femoral component should be equal to the healthy knee. There are a few factors of the trochlear groove and patella which should be accounted for when designing knee prosthesis. These factors include the trochlear radius, depth of groove and the angle between the groove and the anatomical axis.

2.3 Normal gait cycle

The gait cycle is defined as the period from heel contact of one foot to the next heel contact of the same foot. Each gait cycle is divided into two periods, stance and swing as shown in figure 2.14. Stance is the time when the foot is in contact with the ground, constituting 62 percent of the gait cycle. Swing denotes the time when the foot is in the air, constituting the remaining 38 percent of the gait cycle.

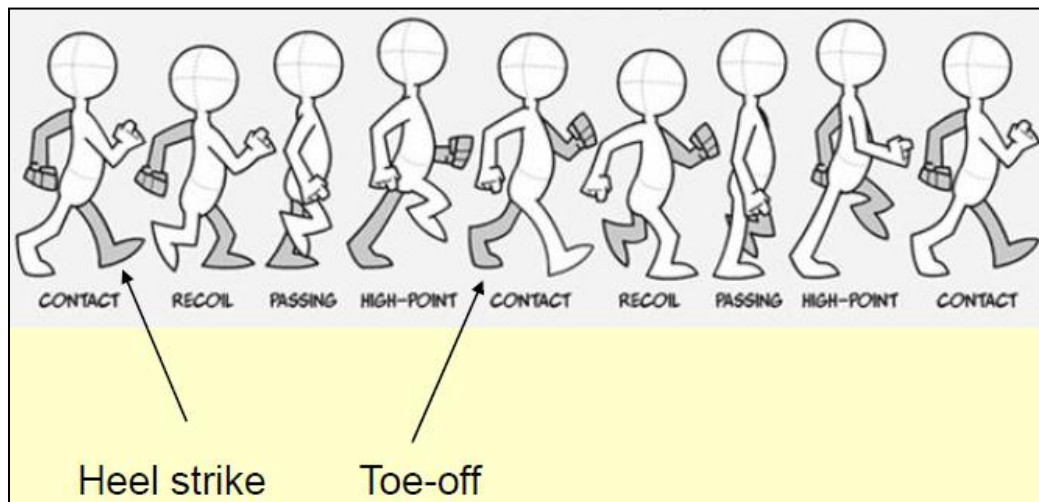


Figure 2.14 walking gait cycle

2.4 Forces in knee joint

The determination of in-vivo forces acting at the human knee and in-vivo torques acting across the tibio-femoral joint is of great value to clinicians, researchers and implant designers. The forces acting in the knee during activity were calculated in the late 1960s using a knee model with the input of gait analysis and force-plate data, together with geometrical measurements of the limb [50]. The highest forces were obtained for descending stairs or a slope and then ascending, and the lowest for level walking. The more vigorous the activity, the higher the forces, as shown for active subjects walking down hill where forces of 8 body-weights (BW) were obtained [51]. In walking activities, where the flexion angles in stance are about 20° , the patello-femoral forces are less than 2 BW, but, in higher flexion, forces as high as 7 BW have been calculated.

2.4 Structure and mechanical property of bones

2.4.1 Anatomy and Physiology of Bone

Bone is a complex and dynamic living organ constituting the skeletal system together with other connective tissues such as ligaments, tendons, and cartilages. Its mechanical functions are providing the structural framework for the body, protection for the vital internal organs, and assistance in movement by acting as a lever system to transfer forces [52, 53].

Majority of bones can fall into five different bone types based on its shape: long (for example, humerus and femur), short (for example, wrist bone), flat (for example, cranial bones), irregular (for example, vertebra), and sesamoid bone (for example, patella) [49]. Its mechanical functions vary depending on this shape of bone. The function of the long bone, for example femur, is to act as a stiff lever and to transmit muscle generated forces over joints. On the other hand, the function of flat bone, for example skull bones, is focused to provide protection for the internal organ such as brain [53]. The bone studied in this study, femur bone, falls into the long bone type.

Structurally, the bone consists of a number of components. The long bone consists of diaphysis, epiphyses, metaphyses, articular cartilage, periosteum, medullary cavity, and endosteum. This structure of the long bone is shown in Figure 2.15. A long cylindrical shaft in the middle part is called *diaphysis*. The distal and proximal ends of the bone are called *epiphyses* which are partly covered by the *articular cartilage* [53].

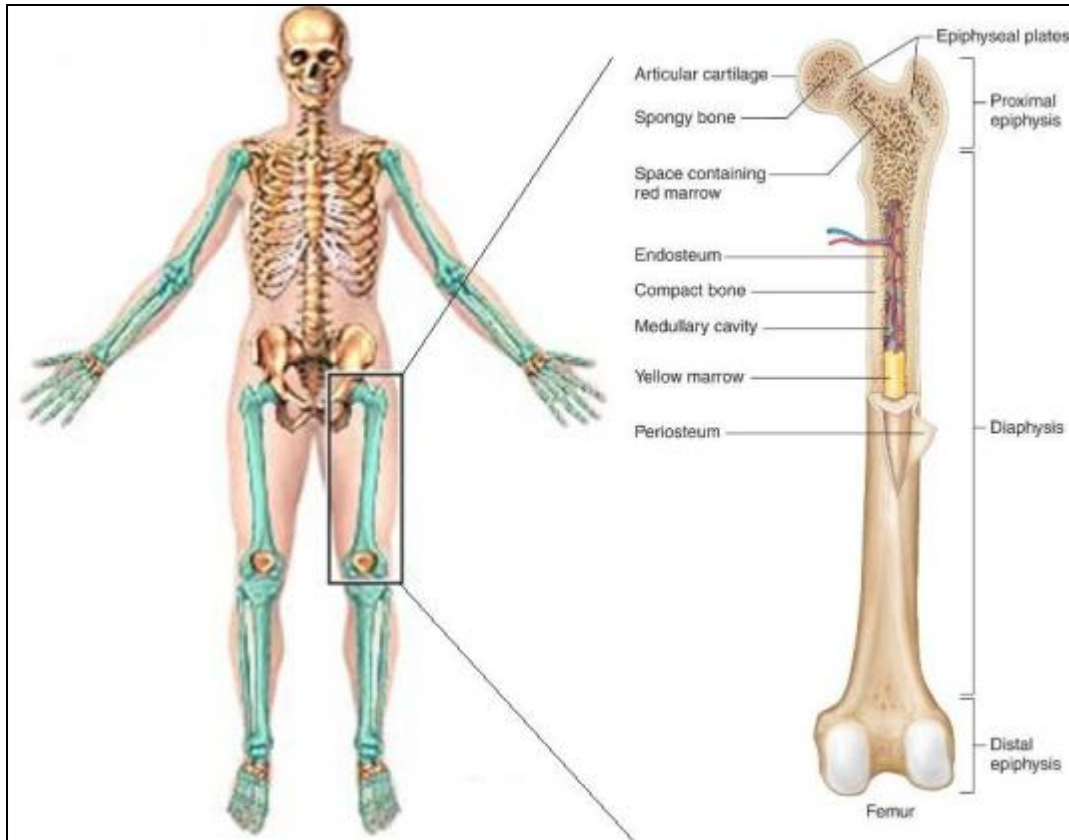


Figure 2.15 Structure of the long bone [54]. Light Green colored bones at left side of figure are long bones in the human skeletal system. The right figure shows the structure of the long bone, femur.

Rather being completely solid, bone has a large number of spaces between cells and matrix components. Density and size of these spaces varies from one region to another. Based on this, bone can be also categorized into either compact bone called cortical bone or spongy bone called trabecular bone, which are shown in Figure 2.16.

Cortical bone or spongy bone called trabecular bone are shown in Figure 2.16. As the name indicates, the cortical bone contains fewer spaces in its matrix and provides rigid protection, support, and resistance for the mechanical stresses from weight and movements. The hard outer layer of bone is made of this cortical bone with porosity of 5-30% [55]. The total mass of all cortical bone in our body accounts for 80% of the total bone mass of an adult skeleton. The basic unit of the compact bone is called osteon or Haversian system [42].

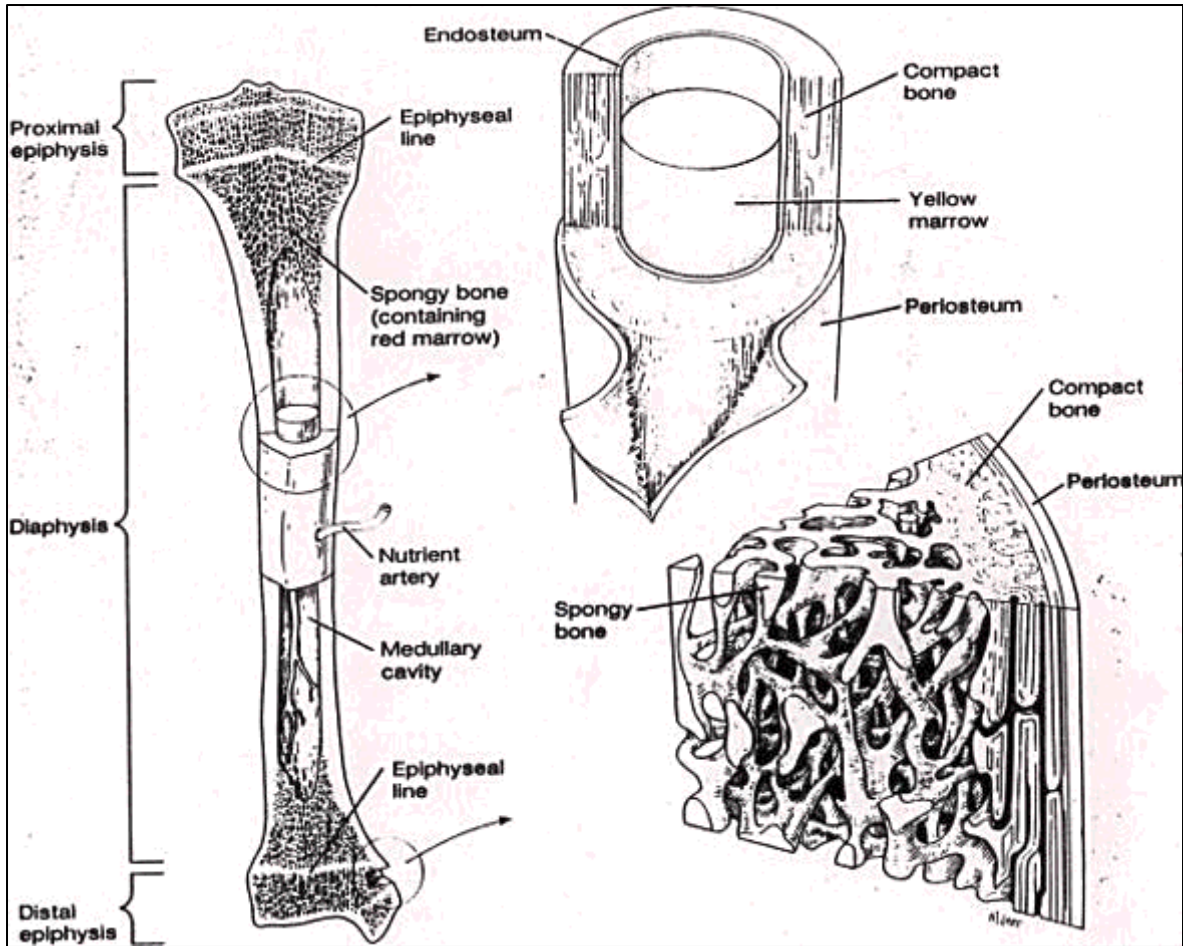


Figure 2.16 cortical and trabecular bone in the femur [56]

On the other hand, the trabecular bone contains much more spaces in its matrix. The inside of some of the bones are filled with this trabecular bone with porosity ranging from 30% up to 90% depending on the location of bone. This trabecular bone accounts for 20% of total bone mass [55, 56]. Differing from the cortical bone, the basic unit of the trabecular bone is called trabeculae, an irregular latticework of thin columns of bone. Trabecular bone also helps bones resisting mechanical stresses and transfer forces without breaking. Importantly, this trabecular bones contribute to reduce the overall weight of a bone [42]. The femur bone studied in this thesis falls into the long bone type. Long bones are built of high amounts of compact bone tissues in their diaphyses.

2.4.2 Material properties of bone

Bone is an *anisotropic* and *inhomogeneous* material. Its mechanical properties vary depending on the direction of the force applied and location in the bone [53].

Material can fall into two categories based on the mechanical behavior in response to the direction of force applied: isotropic and anisotropic material. Isotropic material has identical material behavior in all directions while anisotropic material has different behavior in all directions. Due to its structure, bone has anisotropic material behavior. Table 2.1 summarizes the properties and includes longitudinal (Elastic Modulus) and Poisson’s ratio.

Table 2.1 Material properties of (femur) bone. Left column shows type of material while the middle and the right columns show values in unit and comments respectively (bone location and cadaveric bone age). [55, 57, 59, 60, 61, 62, 63, and 64]

Human Cortical Bone			
Longitudinal Modulus (Elastic Modulus)		15.6 – 17.7 GPa 15.7 – 19.9 GPa	femur, age 20-89 femur, age 54-85
Density		1.8 g/cm ³	not available
Poisson’s ratio		0.2-0.5 (average 0.3)	not available
Human Trabecular Bone			
Longitudinal Modulus (Elastic)		1-20 GPa	various bone, n/a
Apparent Density		0.35-0.75 g/cm ³ (average 0.56)	mean age 69
Poisson’s ratio		0.01-0.35 (average 0.12)	not available

Many researchers found the mathematical equations for the elasticity-density relationship based on their empirical studies. Table 2.2 shows selected equations from literature, which have high determination coefficient. In Table 2.2, the elastic modulus is expressed as E (GPa for the cortical bone and MPa for the trabecular bone) while the apparent density is shown as ρ (g/cm³). Due to its high determination coefficient, two equations from literature were adopted and used to obtain values of Young’s modulus in this thesis along with density values from Table 2.1

Table 2.2 Empirical mathematical relationship between the modulus (longitudinal) and apparent density of cortical and trabecular bone.

Equation	Determination coefficient	Anatomical Location	Other relevant information
Human Cortical Bone			
$E = -13.43 + 14.261\rho$	0.67	Femoral Metaphysis	[66]
$E = 3.891\rho^{2.39}$	0.75	Tibial Diaphysis	[67]
$E = -.142 + 14\rho^b$	0.77	Femur	[65]
Human trabecular bone			
$E = 1310\rho^{1.4}$	0.91	Femoral Neck	[68]
$E = 6850\rho^{1.49}$	0.85	Femoral Neck	[69]
$E = 0.58\rho^{1.3}$ a.b	0.94	Femur	[66]

a Unit of the apparent density only for this equation is kg/m^3 .

b These equations were used to obtain Young's moduli for the cortical and trabecular bone in this thesis.

CHAPTER 3

LITERATURE REVIEW-TOTAL KNEE REPLACEMENT

A literature review was done for better understanding Arthritis and disease of the knee joint, Implantation of femoral component knee joint as well as the Failure models of a total knee replacement are described in this chapter. Also introduce one of the latest technologies in Rapid Tooling is Electron Beam Melting (EBM) to producing metal parts directly from 3D CAD models.

3.1 Arthritis, A common disease

Arthritis is the most common of all joint diseases. Before the 1940's, little could be done to cure this disease. Treatment consisted of some sort of walking aid and pain reliving medicines. Health care analysts have calculated that every year 750,000 new patients suffer from arthritis, and the number is increasing [70]. "Arthritis" comes from "Arth" means "joint", "itis" meaning "inflammation." Dan Alexander et al. studied arthritic disease and found that friction causes bodily joints to become inflamed. According to the study, the joints rub against each other, and a grinding action sets in with the damage of soft tissue. The bony structure becomes damaged leading to Arthritis [71].

Enzymes damage the structural molecules of the cartilage and tiny pieces may flake off into the joint cavity. The result is a change in the contours of articular surface, eventually leading to bone-to-bone contact. This mechanism can be compared with a damaged gasket leading to metal-to-metal contact in a machine, which increases mechanical friction and irritation. Figure 3.1 shows the process of arthritis in joints over a period of time.

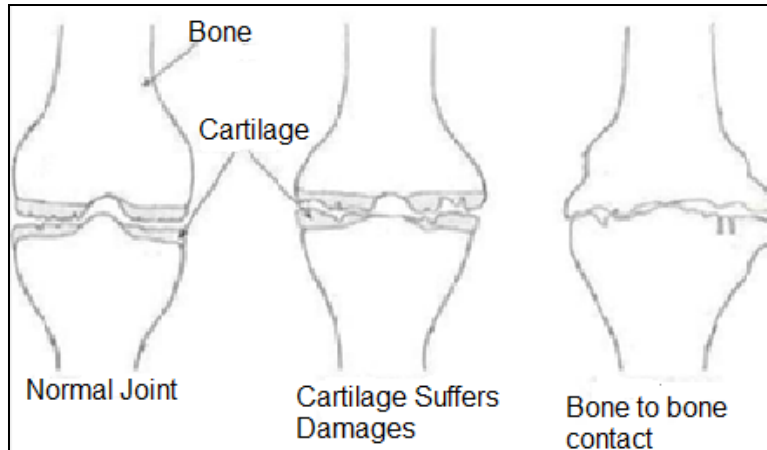


Figure 3.1 Process of arthritis over time

The advent of radiography made it feasible to clean abnormal looking joints using surgery and to remove any spur or loose bodies near the joint [72]. This technique did not address the basic problem that caused the degenerative arthritis. With the development of technology as well as knowledge of the disease, treatment for arthritis was developed. John Charnley and other pioneers developed joint implants, and an era of joint arthroplasty (joint replacement) began. Hip implants were the first to be developed in 1960s by Charnley using metallic and plastic materials as a replacement for the joint [73]. Knee replacement was developed in the 1970's. Gunston in 1971 developed the polycentric knee arthroplasty, and this was followed by total knee replacement by Coventry in 1972 [74, 75]. Very soon this technique became common and was developed for other joints like elbow, ankle, wrist, fingers, shoulders and foot.

Clinical interest in joint replacement increased, and it was soon realized that further research was required in the development of materials, better design, and biomechanics.

Science and engineering collaborated to develop more rigid and reliable designs of joint replacement. This also led to improvement of manufacturing technologies used and development of biocompatible materials. The design of implants played a very important role in this development. Biologic fixation of implant components became evident, and a new technique of fixation of implant to bone was developed [76].

Today, joint replacement is very common. Total hip replacement and total knee replacement have almost become part of older age. According to statistics published by Centers for Disease Control and Prevention, 43 million persons had arthritis in 1997 [70] and many underwent joint

surgery. The study also indicated that all age groups were affected, including working age populations, and the rate increased with age.

There are many possible causes for arthritis such as obesity, genetic factors, hormones, repetitive high stress on the joint, and other metabolic diseases. Initial treatment with medication can help the joint regain its original function; however, many times at a later stage of the disease, surgery is required and the joint has to be replaced by artificial joints. Osteoarthritis of the knee joint is a very common problem in elderly people and is also increasing in young patients [70]. With actual cartilage repair still remaining difficult to evaluate, one of the common remedies is through the use of knee implants.

3.2 Total Knee Replacement

Knee joint replacement surgery due to arthritis is common in human beings. Knee implants were developed in 1970s [74, 76]. Since its use knee implant design has come a long way. Different knee implant manufacturers constantly develop new designs, and continuous improvement has been observed in these designs. Several surgical techniques have been developed for Total Knee Arthroplasty (TKA) and noted in journal publications. There are more than 20 patents on TKA design by different implant manufacturers and authors. [77, 78, 79, 80]

Over last two decades, many studies have been done on design, function and procedures for knee implant components, and surgical methods. The overall goal of most studies is to improve the Total Knee Arthroplasty. The design of a knee replacement is an end result of the overall goals, whether these goals are explicitly stated or not. It was in the 1970's when cemented metal-plastic designs started with restoration of normal joint mechanics [75] Gunston introduced design factors such as geometry of joint surfaces, ligament length patterns, location of contact points, and other implant stability functions in the design. According to Peter Walker, a design goal has to be set for designing the knee implant. The most important design goal is to provide durability and comfort to the patient i.e., pain relief [81]. This is achieved by a rigid design with no sliding between the implant and tissue surface. According to Walker, durability depends on the materials used, the fixation method, the avoidance of adverse bone and tissue remodeling, and the achievement of correct alignment. Also, to achieve normal joint mechanics, the surface of the joint replacement should be very close to the anatomical structure of the joint.

Fixation of implant with bone should be durable and rigid. Today, this can be achieved by using of either cement or a bone ingrowth surface. Many experiments have been done in this area to determine which is better, and both of the techniques are still used [82].

3.2.1 Implantation of femoral component knee joint

There are two different methods used when implanting the femoral component on the distal femur. The selected size can differ depending on the type of method used [83]. In both these methods the distal cut is done before the other cuts. It is made perpendicular to the mechanical axis resecting the same thickness as that of the prosthesis [84]. As presently mentioned, due to the 3° tibia varus, more bone is usually removed on the lateral side. The first method is called *flexion spaced-balancing* (Anterior referencing) [85]. In this method the anterior cut is made, followed by the posterior cut. The anterior cut is made the same thickness as the anterior thickness of the implanted prosthesis. The required prosthesis distance is then measured from the anterior cut to make the posterior cut. Therefore the posterior cut is the variable dimension to ensure the correct flexion space. The second method is called the *size-matched resection* (Posterior referencing) [86]. In this method the posterior cut is first made to the thickness of the posterior part of the prosthesis. The anterior cut is then made to the correct prosthesis internal dimension. Thus the thickness of the anterior cut is changed according to the size of the selected prosthesis [87].

3.2.2 Failure model of total knee prostheses

Total knee replacement (TKR) is an extremely successful surgery, more than 22,000 cases (3-7%) are required to be revised annually [88, 89]. In a retrospective series of 212 total knee cases that required revision, as shown in figure 3.4 the causes for revision were as follows: Polyethylene wear (25%), loosening (24%), instability (21%), infection (18%), arthrofibrosis (15%), malalignment (12%), extensor mechanism deficiency (7%), avascular necrosis patella (4%), periprosthetic fracture (3%), isolated patellar resurfacing (1%) [88].

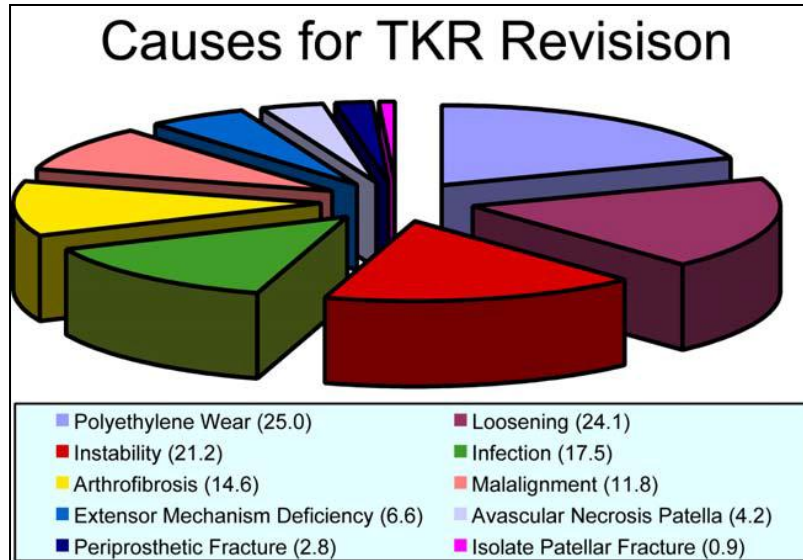


Figure 3.2 Causes for TKR Revision [89]

In fact, in many cases the true etiology of revision TKR is multifactorial. Regardless of the failure mechanism the following three recommendations are consistently cited to reduce the number of failures:

- 1) Improved design.
- 2) Better materials, and
- 3) More accurate surgical technique.

3.3 Rapid Tooling and Manufacturing

Rapid tooling and manufacturing is an important part of Rapid Prototyping, which deals with producing tools or final usable metal parts directly from 3D CAD models. This process eliminates all the intermediate manufacturing functions and reduces the time from concept to manufacturing.

Much research has been conducted in the field of Rapid Tooling (RT), and many new techniques have been developed. One of the latest technologies in Rapid Tooling is Electron Beam Melting (EBM).

3.3.1 Electron Beam Melting

One of the latest technologies in Rapid Tooling is Electron Beam Melting (EBM). Arcam (Arcam, Sweden) has developed this technology, which involves firing an electron beam at metal powder, thereby melting the powder using the kinetic energy of electrons [90]. By controlling and directing the electron beam, the machine can melt a powder layer as thin as 0.1mm. Once a layer has melted, a new layer of metal powder is added over the previous one, and the procedure is repeated. Finally, detail is built up on thin metal slices melted together to form a desired solid. Figure 3.6 shows a schematic diagram of EBM technology. Different materials can be used to manufacture 100% solid parts using this technology. Once the parameters are developed for a specific material, any complex part can be build on this machine. Recently titanium has been added to the list of available materials, which can be produced on the EBM Machine. This new development will enable manufacture of biomedical implants directly on EBM.

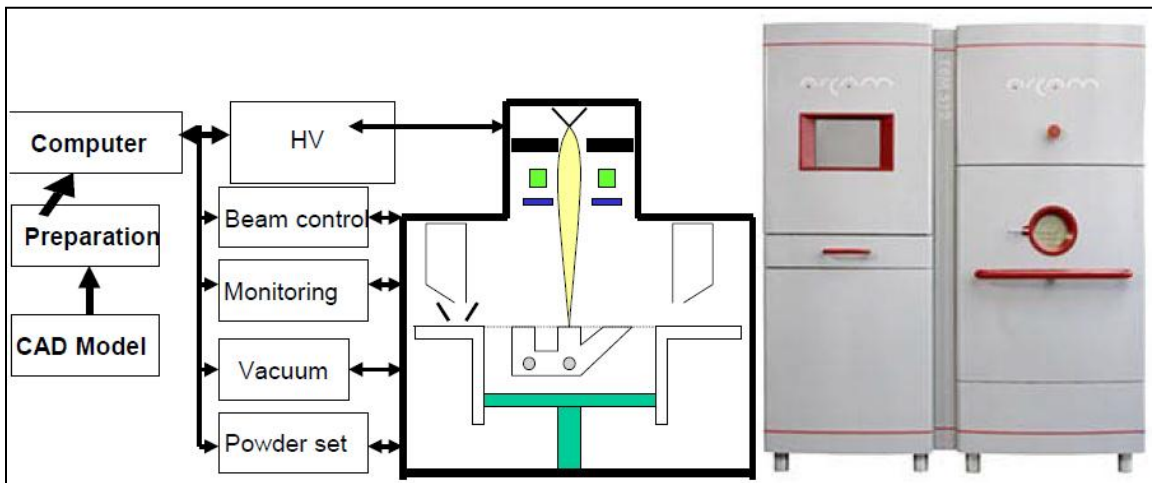


Figure 3.3 Schematic diagram of EBM machine by Arcam

Today most of the complex medical parts such as biomedical implants are produced using investment casting. Use of technology such as EBM will reduce the time to produce these parts. Certain complex geometries, which were previously not feasible / affordable, may now be produced quickly and accurately using this technology.

CHAPTER 4

METHODOLOGY

Chapter 4 explains the segmentation procedures of knee joint and how the 3D femur models are created using programs such as MIMICS 10.01 and Preprocessing CAD Model was done by using Geomagic studio 2012 software. After that using the CAD software such as solid works 2012 to design the custom smooth bone-implant interface femoral component of knee joint.

4.1 Specific aim of this work

The articulating surface of a conventional standard femoral knee implant is of generic shape and causes the problems mentioned earlier. Most patients' gaits are altered due to the change in distal femur geometry. The ease of adapting to the new gait can vary widely but does present a problem for many patients. The patella resurfacing is an additional surgical intervention that requires an implant component as well, but a more important consideration is that many patients suffer from postoperative pain due to the procedure [91]. The patellar groove position of the femoral component should be equal to the healthy knee.

As mentioned in chapter one, the conventional standard femoral components have a very simple bone-implant interface of five cut surface. The sharp edges on the implant-bone surface create stress concentration under load, which will lead to bone remodeling and an increase in bone density. The flat area between the sharp edges is stress shielded, which will lead to bone loss and loosening of component.

Today, many implant companies offer implant components that are customized according to size and shape. This research introduces a new approach to custom mode design femoral component of knee implants. The proposed custom femoral component design presented in this thesis has addressed all the above problems and the problems which were discussion in the first chapter. It will provide a new proposed customized implant system that could provide a better result for younger patients and patients with an abnormal joint anatomy. It can be used for a wide variety of implants and is not restricted to knee-implant components. As mentioned in the literature

review, human younger patients are subject to more strenuous activities, which lower the chances for successful Total Knee Arthroplasty (TKA).

4.2 Functional Requirements of the femoral Implant Design

One of the most important functional requirements of any femoral knee implant is its ability to replicate joint motion as closely as possible. Compromise on any motion or degree of freedom will be a suboptimal design. The following are other major functional requirements for design of the femoral knee prosthesis:

1. To provide easy insertion of femoral component on bone during surgery.
2. The size of the implant should be as close to the normal as possible to minimize any tissue damage and to avoid compromise on any change in motion.
3. The material used to manufacture such an implant should be biocompatible.
4. The bone-implant interface should be porous to promote bone ingrowth.

4.3 Proposed methodology

Based on the above-mentioned functional requirements and aims of this work, the components of a femoral knee implant are designed for the same is proposed. The following is the breakdown of the proposed methodology:

1. Selection of patient
2. Computed Tomography scan
3. Image reconstruction
4. Three dimensional reconstruction
5. Creation 3D model for finite element analysis
6. Preprocessing CAD model for design
7. Design of human knee implant
 - a) Custom parametric smooth design of femoral component
 - b) Custom parametric straight cut design of femoral component

Each of the above steps involved in the design of custom femoral knee implants is now discussed in detail. The following section discusses steps 1 through 5 (i.e., selection of patient to

preprocessing CAD model for design). Details on implant design are elaborated in Chapter 4 (Design of Implant), and Chapter 5 discusses about the finite element analysis to examine the stress distribution on the implant-bone interface.

4.3.1 Selection of patient

A 30-year- old male was selected for this research. CT scan of this patient was taken at the hospital of the Near East University (NEU) at North Cyprus.

4.3.2 Computed Tomography Scan

The first step for the design of custom femoral knee implant is to obtain the geometric data of the joint. CT scanning is a commonly used imaging technique for any medical examination requiring 3D visualization. During the scan, x-rays are emitted from one direction and received on the opposite direction. Multiple x-rays are emitted and received in a plan with specific intensity level. Helical (spiral) scanning is now commonly used since it gives better results with low radiation exposure. During this process, continuous spiral scanning is done, and the final data are a continuous helical image. After the scan, a calculation is done on the data, converting it into two-dimensional images.

CT scan data was acquired at the radiology department in Near East University. Helical computed tomography scan of the distal portion of the right thigh was performed. These scanned data were retro-reconstructed into 1mm slices with 0 degree gantry tilts and transferred to a CD.

4.3.3 Image reconstruction

The image from the CT scan is a group of 2D images taken at every 1 mm step as explained in the previous section. Figure 3.1 shows an example of a 2D image taken from Patient. Merging of all the 2D slices to a complete 3D model can be done by software using an algorithm which will add the thickness and merge all the images to define a 3D model. Several software packages are available to perform this conversion. MIMICS from Materialize were used for this research.



Figure 4.1 human knee being CT scanned

The DICOM (Digital Imaging and Communications in Medicine) file format is the standard method for the transmission of medical images and their associated information. These DICOM image files were captured from the CT scanner workstation and copied on a CD. The files were then imported into MIMICS. Each image contains header information including the patient's name and table position for that specific image. MIMICS detect this table position from each image and automatically rearrange the images to obtain a uniform image sequence. Figure 4.2 shows a set of images ready to be imported into MIMICS.

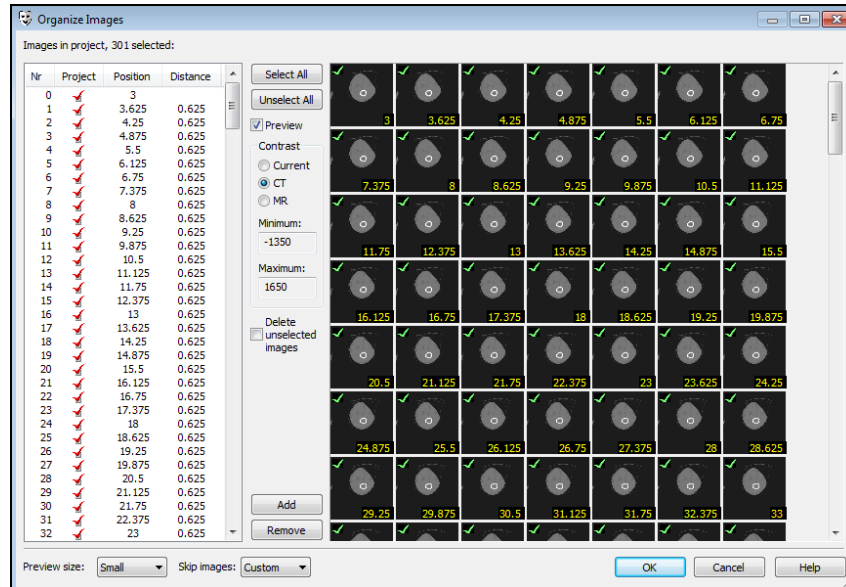


Figure 4.2 CT images imported into MIMICS

Once the images are imported, the next stage is to select the correct threshold as shown in **Appendix A**. By using a built in function called the profile line, an appropriate threshold of the bone can be determined throughout the scan. This important step enhances the image and focuses only on the area of interest.

4.3.4 Three dimensional reconstruction

MIMICS 10.01 software is used to convert CT image into a 3D model as shown in figure 4.3. From the menu following commands are used to convert CT image into a 3D model organizing images, Thresholding, Edit Masks, Region Growing, Calculate 3D from the “Segmentation” Menu as shown in **Appendix A**.

Then MIMICS software generates automatically axial, coronal and sagittal views and the results as shown in Figure 3.2. These views consisted of varying pixel intensities, with the light being hard material and low intensity for softer material.

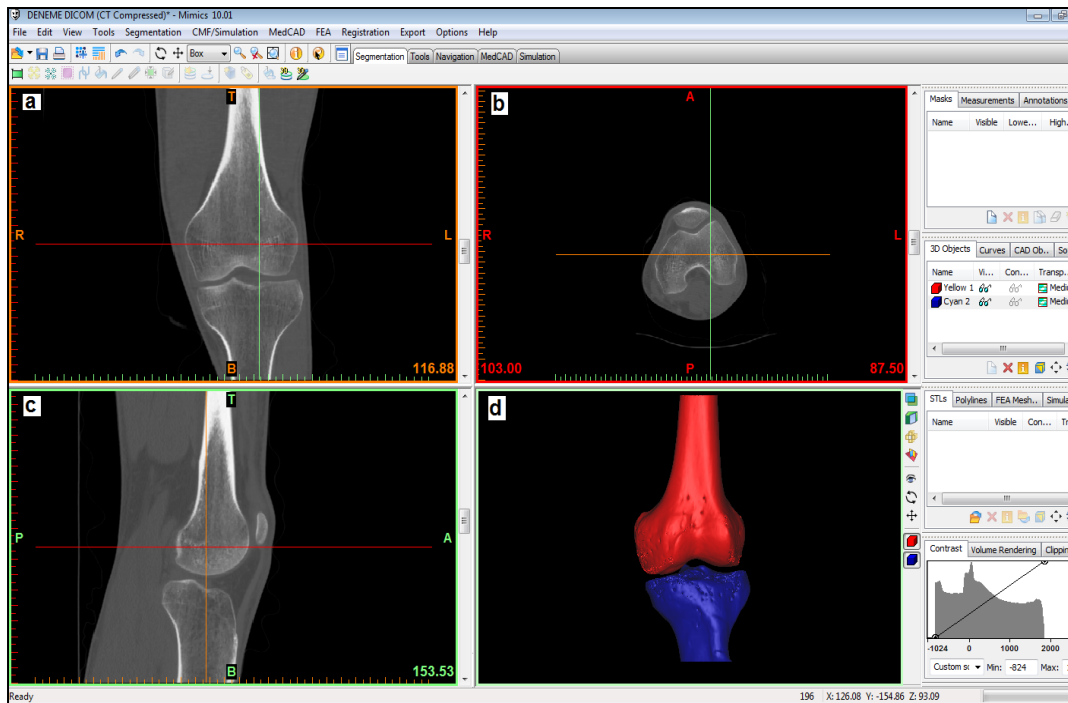


Figure 4.3 MIMICS user interface with imported CT scan: A: front view (coronal); b: top view (axial); c: side view (sagittal); d: 3D view

After the mentioned views have been created, a pixel intensity threshold was selected which represents the cortical bone structures. All the pixels that fell outside this interval were ignored. The pixels that were in the interval were added to a mask. MIMICS used different masks to separate different items. In the older versions of MIMICS, the threshold interval limits was selected manually. The newer versions contained certain preset threshold intervals that could be selected, depending on the type of tissue that was investigated. Therefore the 3D models were created automatically.

The *Bone CT* threshold interval was selected, creating a mask which represents the bone structures in all images. This mask included the femur, tibia, and patella. The different bones were then separated with method called region growing. It will eliminate noise and separate structures that are not connected. Because the distal femur, the proximal tibia, and the patella are not connected, multiple region growing were applied using different masks and colors. Each mask was converted into a 3D model using the "*calculate 3D*" function as shown in figure 4.4. Because of the thresholding function, some of the cancellous bone was not included; and this

created unwanted internal voids in the model. A complete solid model was desired for the custom design phase, and editing of the masks was necessary.

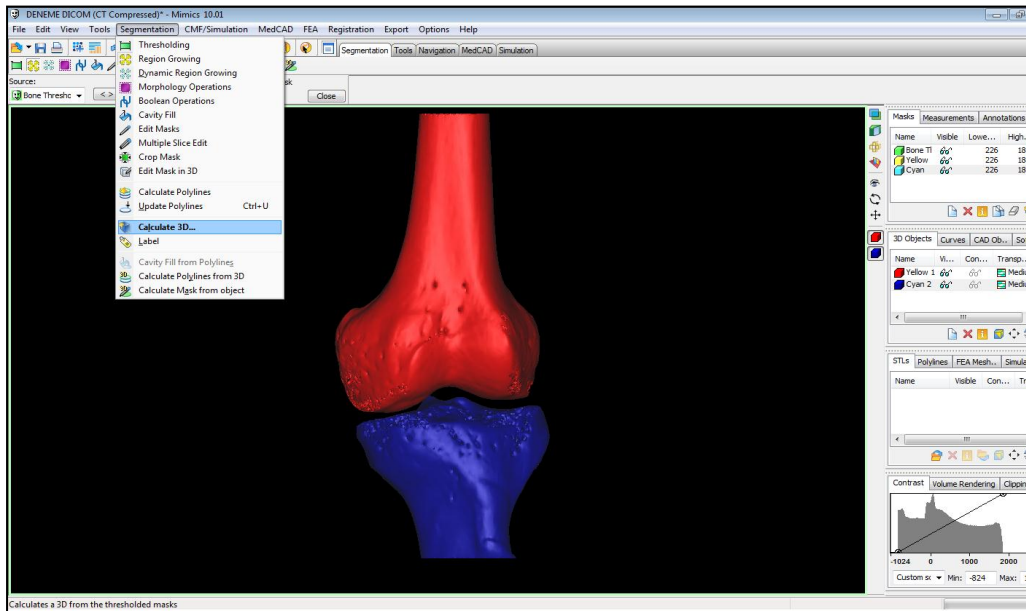


Figure 4.4 Three- dimensional CAD model of knee generated in MIMICS

The generated 3D model is now ready to be exported to other software for further processing and design of the implant. The 3D data generated are converted into a standard file format used in the rapid prototyping industry and to measure the dimension for using to design standard human knee joint. There are four different formats in which the 3D data can be exported for further design, namely STL, IGES, VRML or DXF. The most commonly used file format for such application is STL. The smoothing function was used to make rough surfaces smoother. Finally the 3D reconstructed data is exported in STL format with desired parameters.

4.3.5 Creation of finite element model (Remeshing)

After creation of the 3D model, tool called MIMICS remesher is used to improve the quality and speed of finite element analysis on STL modules. It is used to smooth the surface of the implant to an optimum level and optimize the quality of triangles for the finite element analysis. MIMICS remesher starts with smoothing operation with the factor of 0.4 as shown in figure 4.5. Height/base (A)

parameter was used to check the qualities of the triangles with good triangles contain the quality of one and bad triangles contain the quality of zero.

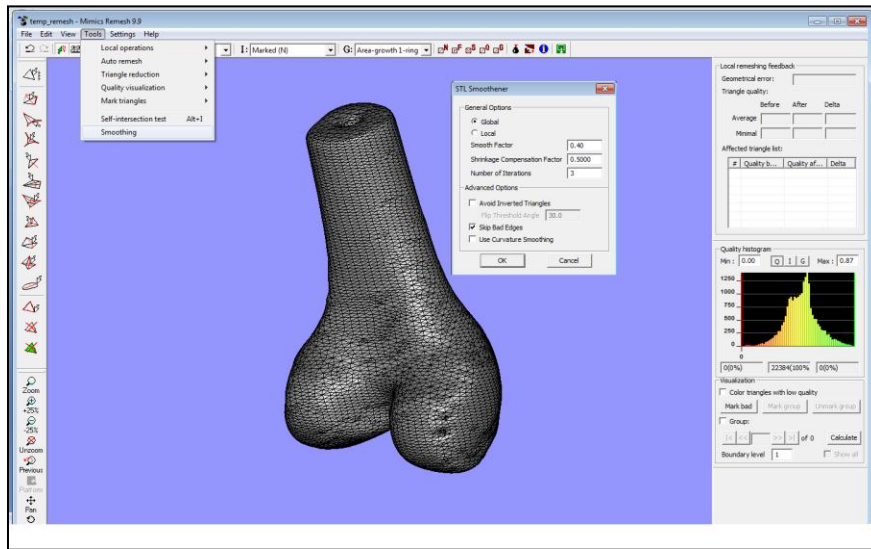


Figure 4.5 Mimics remesher starts with smoothing operation

Part quality sheet was enabled in order to fix the histogram value accordingly and arrange the triangles quality data. Initially after surface calculation numbers of triangles presented in the surface were very high to perform any FE task, triangle reduction was done using normal method in two consecutive steps for edge and point reduction as shown in Figure 4.6.

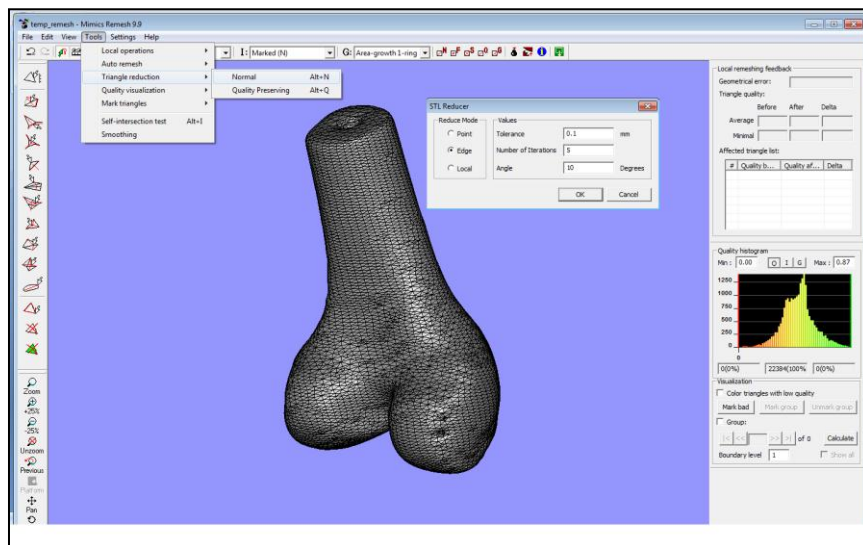


Figure 4.6 triangle reduction in mimics remesher

Parameter chosen for the point reduction and edge reduction were chosen as tolerance of 0.1 with angle 15(degrees) and the number of iteration as 5. Split based method was selected for auto remeshing where the minimum edge length and maximum edge length was assigned to 2.5 and 4 respectively as shown in figure 4.7.

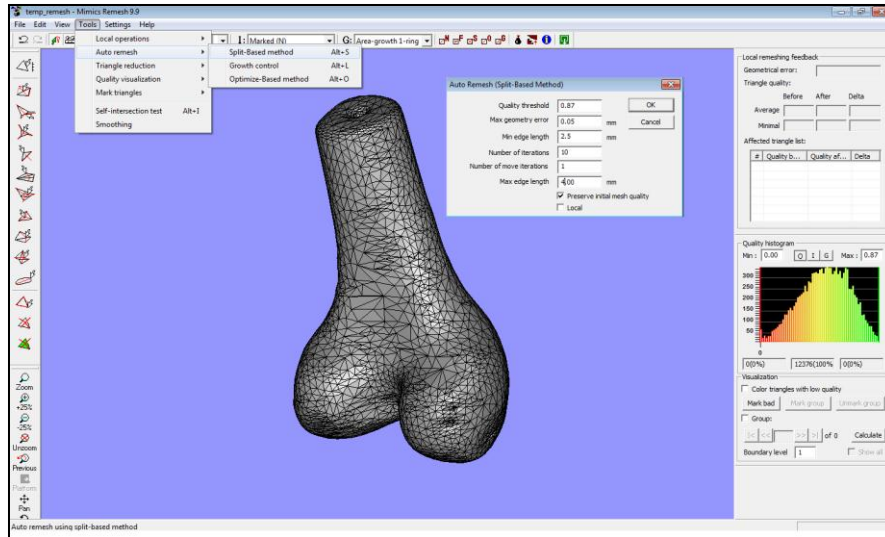


Figure 4.7 auto remeshing in MIMICS remesher

After satisfying with mesh quality self intersection test was called in case of intersection triangle as shown in figure 4.8, the mesh was successfully exported into the MIMICS again.

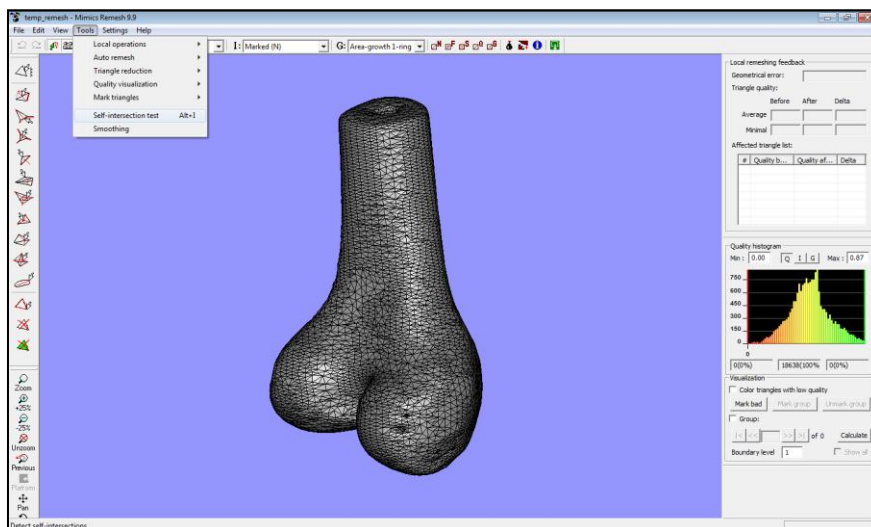


Figure 4.8 Remeshing operation using MIMICS remesher tools.

4.3.6 Preprocessing CAD Model for Design

After creating 3-D models in MIMICS and MIMICS remesher used to improve the quality of the 3d model and to speed of finite element analysis, surface mesh is generated as shown in figure 4.8. Unfortunately MIMICS does not currently have the ability to export the 3D-model into a CAD format that can be manipulated by standard CAD packages.

The most efficient method for the required data manipulation was to convert the 3D-model into a STL-file format (i.e., a format designed for stereolithography) that could be converted into a 3D CAD format by another software package. The STL-file format is a triangular surface mesh used by the rapid prototyping industry as a standard file format. STL-file generated by MIMICS based on the mask information contains a large number of triangles with various sizes and shapes.

The STL file exported from MIMICS is now ready for further processing. Geomagic Studio 2012 was used in this research for smoothing and preparation of the model. Using the mesh Doctor and Rewrap function, the model was repaired the surface. Also using the *Reduce noise*, *Relax grid* and *Sandpaper functions*, the model was smoothed as shown in Figure 4.9.

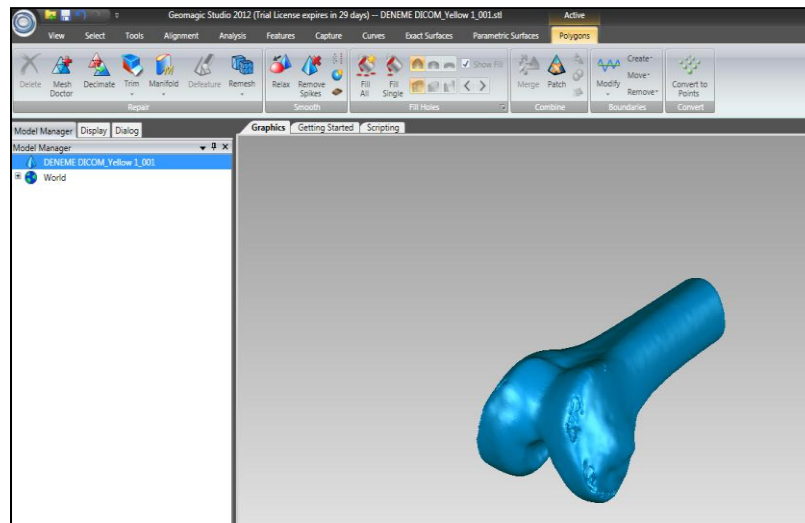


Figure 4.9 Smooth femoral knee implant CAD model from Geomagic studio

The model is now ready for femoral component design, however, it was decided that the best 3D CAD model file would be in STEP format. Geomagic Studio cannot directly convert STL files into STEP files. This process involves generating closed NURBS (Non Uniform Rational B-

Spline) surfaces. The NURBS surface requires some process such as de-noising, smoothing, filling of gaps, removing spikes, repairing intersections to convert CAD models Using an automatic NURBS surface generation command, a solid CAD model in the STEP file format was generated as shown in Figure 4.10.

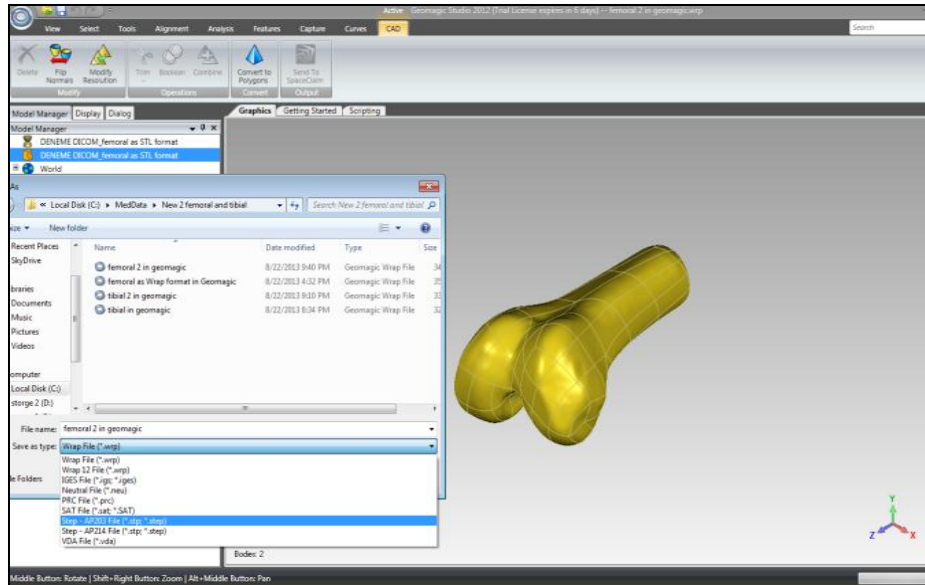


Figure 4.10 Solid model as STEP format generated from Geomagic studio

4.3.6 Design of Implant

The CAD model of the distal femur derived from the CT images was used as the base for the implant design. To address the problems with gait change and patellar resurfacing, the original shape of the articulating surface can be preserved. The design of femoral implants can be performed using any standard CAD modeling software such as Pro Engineer, Solidworks, AutoDesk Inventor or Solid Edge. Based on the powerful feature options and availability, Solidworks (Solidworks, USA) was selected for this research. The 3D model of the femur knee joint as shown in Figure 4.10 was imported into Solidworks. From the 3D model, a custom knee implant was designed. The design considered all the functional requirements of implant as discussed in section 4.2 of this chapter.

Two different types of a custom femoral component were designed. The external articulating surface with tibial component and the patellar component was maintained; however the femoral bone-implant interface was:

- a) Custom designed with a smooth parametric custom bone-implant interface
- b) Custom designed with planner bone-implant interface.

The first design with smooth bone-implant surface considered the bone ingrowth in the implant and a uniform stress distribution to avoid any stress concentration. However, since there are no commercial femoral implants available as smooth bone-implant interface for human, a standard implant was also designed for comparison purposes. The custom design was based on specific thickness from CT scan, custom articulation, and a parametric bone-implant interface. The next chapter focuses on the design of the above mentioned implants.

CHAPTER 5

DESIGN OF IMPLANTS AND FINITE ELEMENT ANALYSIS

Current research is an advancement of this human knee implant design and uses a custom surface. It is believed that this design will improve the stress distribution over the bone-implant interface surface, enabling uniform bone ingrowth and optimize patello-femoral tracking. This chapter focuses on the development of custom knee implants with parametric inner surface by using CAD software such as solidworks 2012, and ANSYS workbench to development the femur bone surface as well as to test the proposed custom design.

5.1 Proposed Methodology for the Design of Custom femoral component implants

The design of a custom femoral knee implant is proposed. As explained in the methodology section (Chapter 4), the following are the major steps involved during the design process:

1. Selection of patient
2. Computed Tomography scan
3. Image reconstruction
4. Three dimensional reconstruction
5. Creation 3D model for finite element analysis
6. Preprocessing CAD model for design
7. Design of femoral implant

A thirty-year- old male was selected for this research. CT scan of this patient was taken at the hospital of the Near East University at North Cyprus. The 2D images from a CT scan were converted into 3D CAD model using Mimics and Mimics remesher. The rough computer model was then smoothed using Geomagic Studio, and the final 3D model of the femur was obtained.

This femur model was imported into Solidworks for further design of the implant. For comparison purposes, two designs were proposed:

- a) A custom design with smooth parametric custom bone-implant interface

b) A standard design with straight cuts and pegs.

The standard implant was designed for comparison purposes only. The design approach for both types of implants remains similar; however, both are discussed separately for better understanding.

5.2 Design of femoral implant with smooth custom bone-implant interface

The intent behind this design is to have a smooth, parametric interface between the femoral component of the implant and the femur. This will have the following advantages:

- Uniform load distribution over the bone-implant interface surface
- Stimulation of bone ingrowth all over the interface

In this research, two major design factors are considered for the design of a custom knee implant. They are:

- Specific implant thickness
- Stability of implant after the surgery

Each of these design factors is discussed in detail in the following sections.

5.2.1 Selection of thickness in femoral implant design

An important step in the implant design is to decide on the thickness of the femoral implant. The thickness should be as uniform as possible to avoid any concentrated stress-failure. There are two main thickness selection factors to be considered, namely

- Implant must be thick enough to prevent mechanical failure
- The implant should promoting bone ingrowth at bone-implant interface

5.2.1.1 Mechanical failure thickness criterion

Mechanical failure of the implant would occur at the smallest cross section. As shown in figure 5.1(a), two condyles merge together at Section A-A. This section has two small areas and is at higher risk of failure. Since the force acting on the joint will not pass through this section, a

moment will be created. Under this condition, the failure mode at this section shall be due to bending moment.

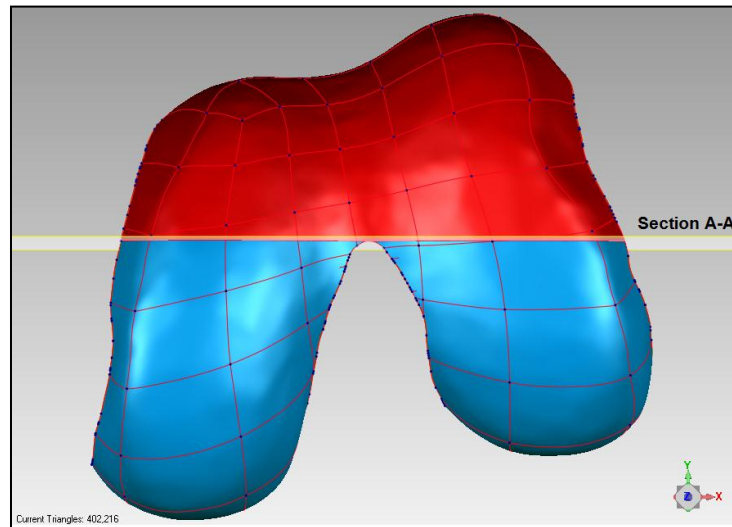


Figure 5.1(a) Implant failure site

This mechanism could be compared with a cantilever beam, with section A-A as fixed. The maximum force acting on this cantilever shall be the impact load while running. Patient's human are difference in a weight. For design purpose we shall use the actual weight of patient 70 Kg (154 lb) where lb is pound, ($1\text{ kg} = 2.2\text{ pounds}$). Weight of human = 154 lb

Considering the normal load on implant as half the total load of human and load being equally distributed on both the condyles, the cantilever action of condyle can be explained as shown in Figure 5.1(b). The length of cantilever (0.5) shall be equal to distance between the section plane and the center of the condyle surface area, which articulates the joint (Not shown in figure).

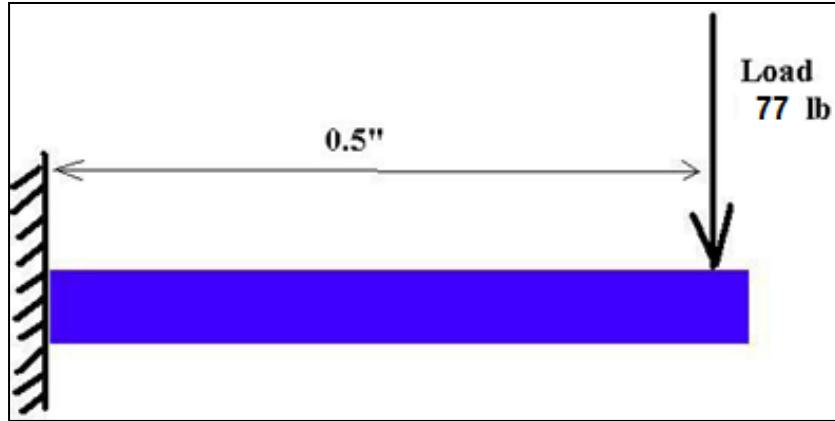


Figure 5.1(b) Cantilever load on one condyle

The thickness of the implant could be adjusted based on material choice (titanium or cobalt-chromium) as well as patient weight and activity level. Let the material used in this study is Titanium alloy Ti6Al4V.

Material properties for Titanium alloy Ti6Al4V [105] are

- a) Bending Modulus = 14.5×10^6 lb/ in²
- b) Maximum bending stress $\sigma = 150\,000$ lb/in²

We know that Maximum Stress

$$\sigma = \frac{\text{Bending Moment } (M) \times \text{deflection } (y)}{\text{Moment of Inertia } (I)} \quad (1)$$

$$\text{Bending moment } (M) = \text{Force} \times \text{moment arm} \quad (2)$$

Where

$$\text{Force} = 77 \text{ lb}$$

$$\text{Moment of arm} = 0.5 \text{ in}$$

$$\text{Bending moment } (M) = 77 \times 0.5 = 38.5 \text{ lb.in} \quad (3)$$

$$\text{deflection } (y) = \frac{t}{2} \quad (4)$$

where t is thickness of condyle.

From the CT data, the width of proposed implant at section A-A of figure 4.1(a) is calculated to be 0.5”.

Moment of Inertia for rectangular cross section

$$\text{Moment of Inertia } (I) = \frac{bh^3}{12} \quad (5)$$

Where

$b = 0.5$ in

$h = t/2$ [in], for implant not to fail in bending,

Substitute the values of maximum bending stress, Eq. 3, Eq. 4 and Eq. 5 into Eq. 1.

The minimum thickness “t” of the implant at mid-section A-A ≥ 0.157 ” i.e. $t_{min} \geq 0.157$ inch” ($t_{min} \geq 3.99$ mm) at section A-A, where (1 *inch* = 25.4 *millimeter*). Thus the thickness of implant should be greater than or equal to 3.99 mm.

5.2.1.2 Bone ingrowth promoting thickness criterion

Based on previous research, it was found that the implant in the vicinity of cancellous bone has the maximum bone ingrowth probability [92]. Hence it was decided to have the thickness of the implant such that the inner surface is in the vicinity of porous cancellous bone. However, it is important to note that the cancellous bone may not be strong enough to support the implant and could cause implant failure. A study needs to be carried out on failure mode and bone ingrowth with the proposed design, which would be the part of design optimization, once such implant is developed. The 2D image from CT scan revealed in ‘MIMICS 10.01’ that the thickness of the sclerotic subchondral bone at the femur articulation is approximately 4 mm on the side and 7.7 mm at the articulation. Figure 5.1(c) shows the 2D image of cortical bone along with subchondral bone with thickness distribution over the femur region. Hence the implant should have thickness equal to or larger than this thickness of sclerotic subchondral bone.

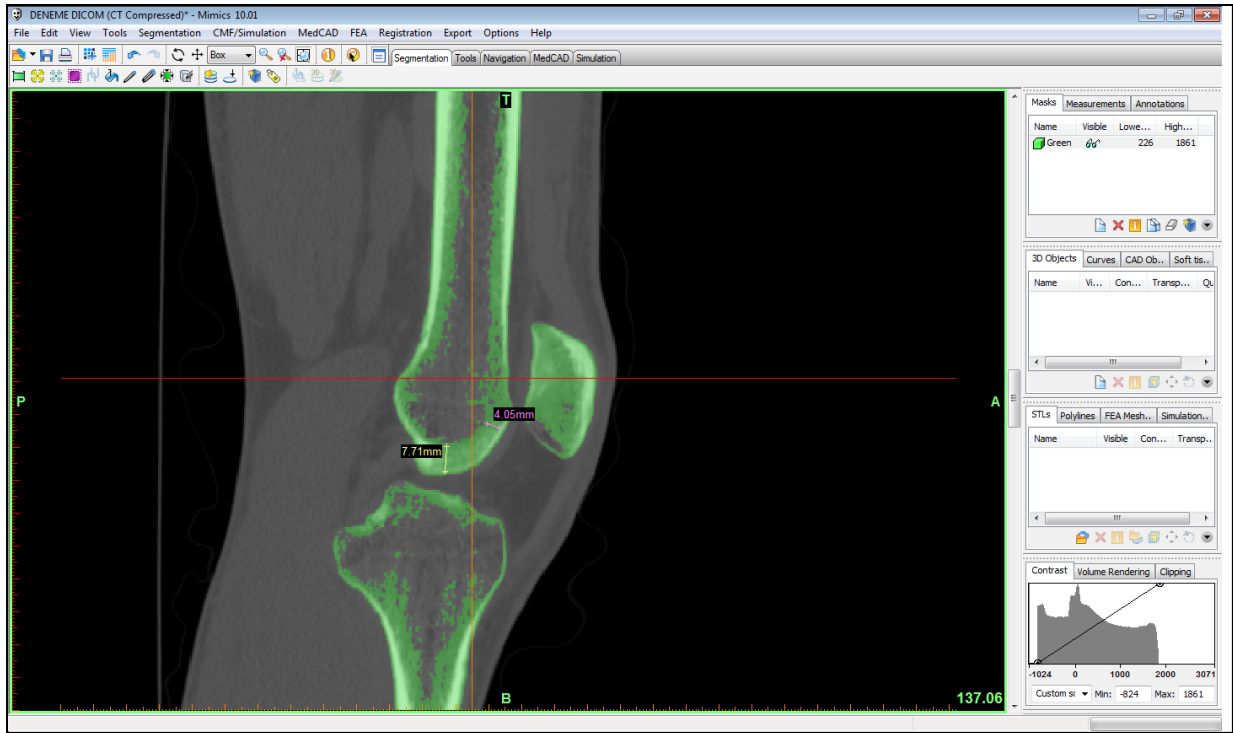


Figure 5.1(c) Thickness of cortical bone in human femur

5.2.2 Implant Stability after Surgery

From previous research in implant design, it was noted that the implant must be stable immediately after the surgery [92]. The standard femoral implant design used pegs to avoid any tangential displacement and to increase stability [92]. Interestingly, the pegs gave bone ingrowth only in cancellous bone. To obtain a uniform bone ingrowth over a cancellous bone surface, it was decided to have a parametric inner surface. A schematic sketch of this inner surface is shown in Figure 5.1(d)

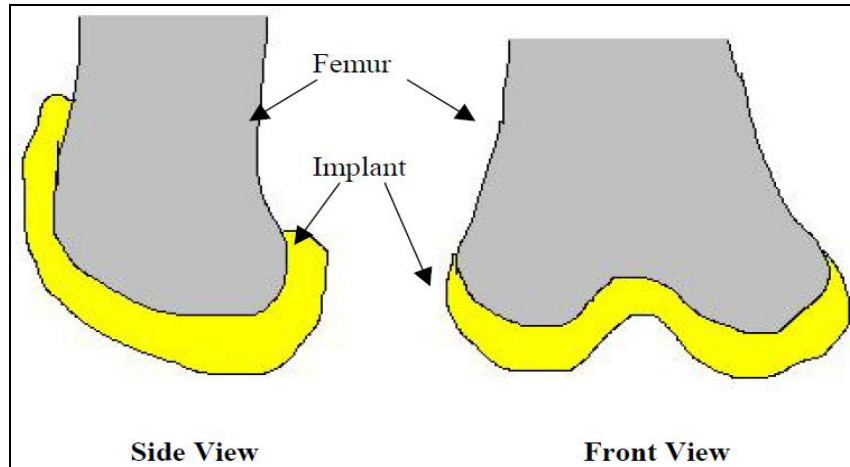


Figure 5.1(d) Schematic sketch of proposed contact surface between implant and femur

Such a parametric interface between implant and femur will make sure that the implant is rigid immediately after the surgery. Due to the presence of curvature in both directions, any displacement as well as rotation will be prevented.

5.2.3 Detailed design steps

For the actual design of the implant based on the above discussed criterion, the very first step was to import the generated 3D model from STL format to a well known usable CAD format. The STEP format was used since it represents a solid model very well. The 3D femur model was imported into the SolidWorks CAD software that was used for the design as shown in figure 5.2.

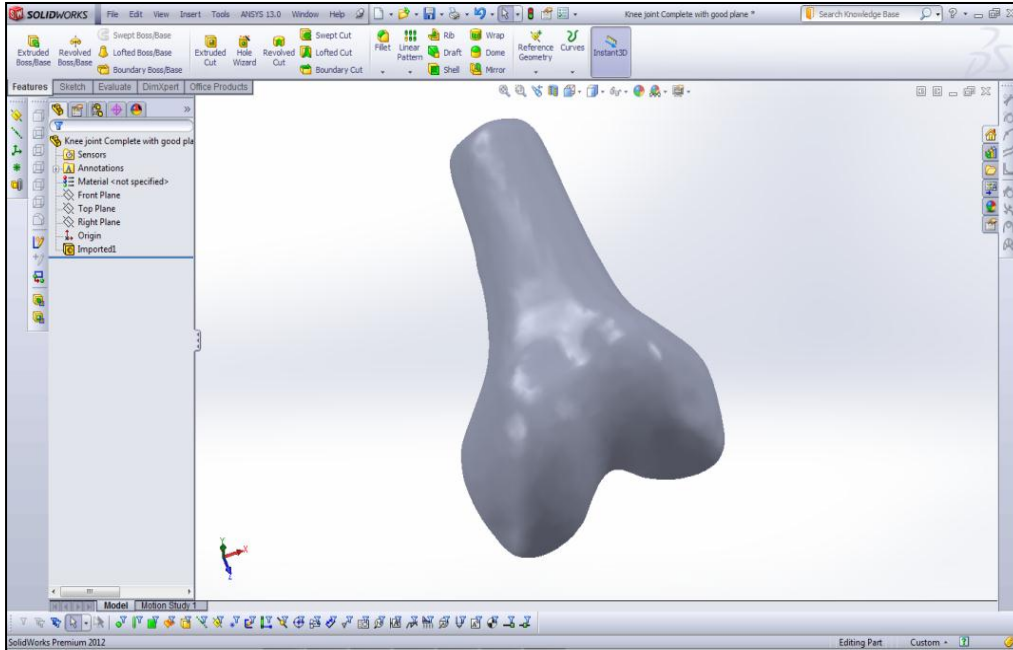


Figure 5.2 Three dimensional CAD model imported to Solidworks

A mid plane was created on this 3D model, which passes through the patella groove, center between the two condyles, and femur. The mid plane was defined by three points, passing through the center of patella groove, center between condyles, and center of femur as shown in Figure 5.3.

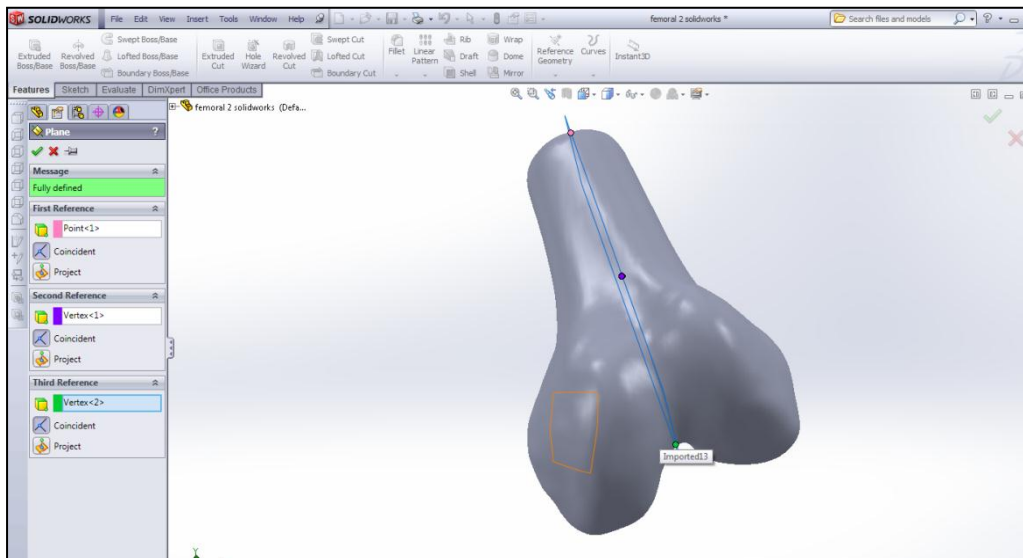


Figure 5.3 Screen-shot from Solidworks, mid plane definition

A sketch was drawn on this mid plane, and the first side cut was generated using the *Cut-Extrude* command. This sketch defines the implant width from the side. Figure 5.4 shows the sketch details. Line L1 and L2 are tangent to curves C1 and C2, respectively. Also, line L1 and L2 make 95° angle with one another. This angle will maintain the insert angle of the implant to be greater than 90° , i.e., 95° . As discussed in the previous section, an insert angle greater than 90° is required to ensure that the implant always slides into the cut bone and has no undercuts. Figure 4.4 also indicates the initial thickness of the implant. The thickness of the implant is 11mm at the articulation, 8.4mm at the patella groove and 5.6mm at the end of the patella groove. This thickness is larger than the minimum thickness required mentioned in Figure 4.1.

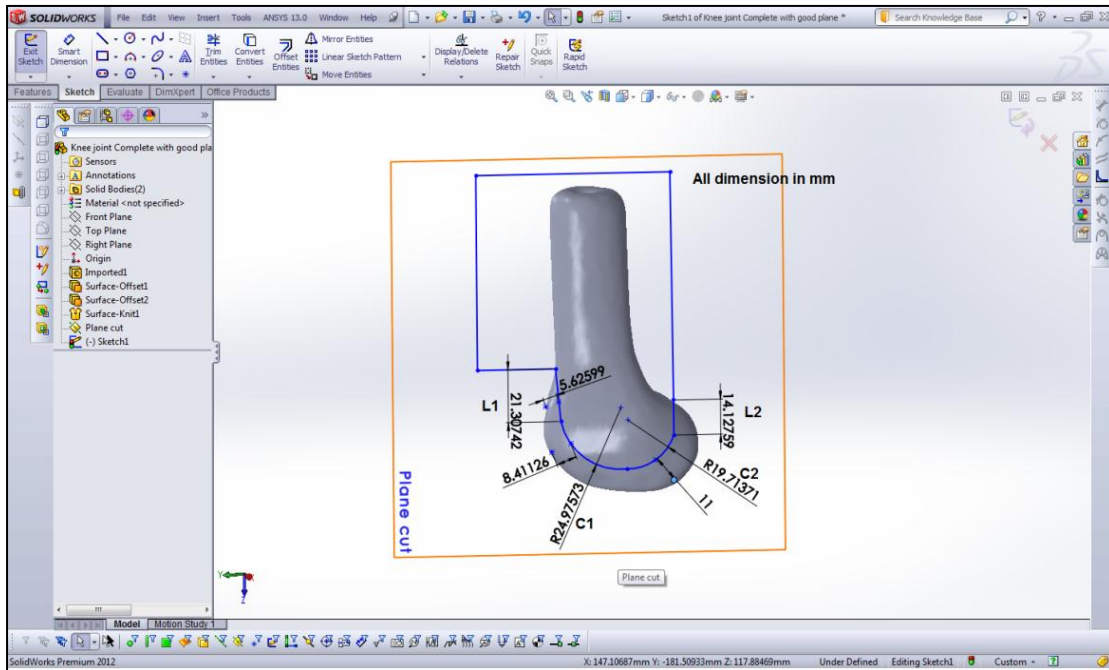


Figure 5.4 Side cut sketch details

The radii of the curves C1 and C2 are 24.97mm and 19.7mm, respectively. These curves are tangent to each other forming a continuous smooth curve. Other lines seen in Figure 5.4 are used to remove the unwanted part of the femur model. Figures 5.5(a) and 5.5(b) show the implant after the *Cut-Extrude* command.

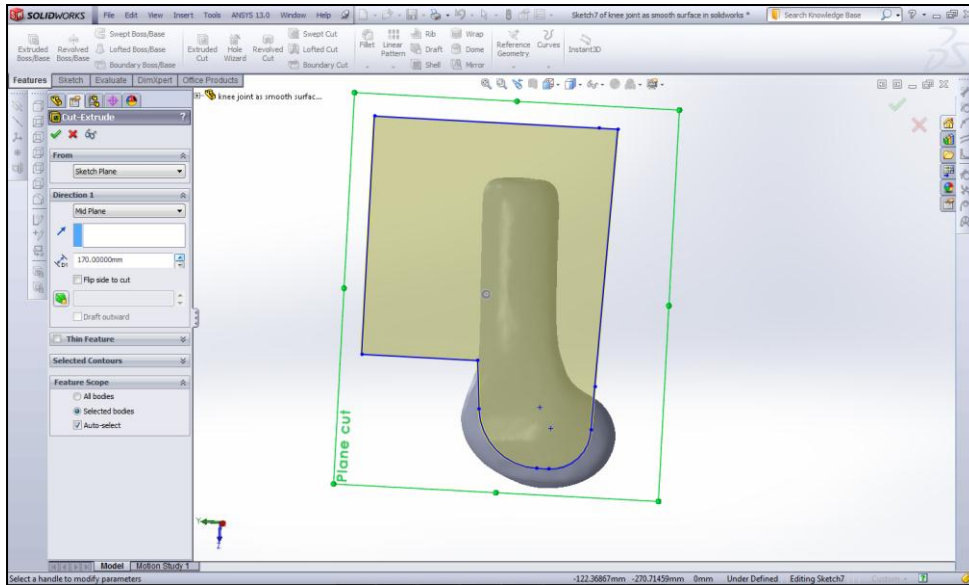


Figure 5.5 (a) Implant during *Side-Cut* command

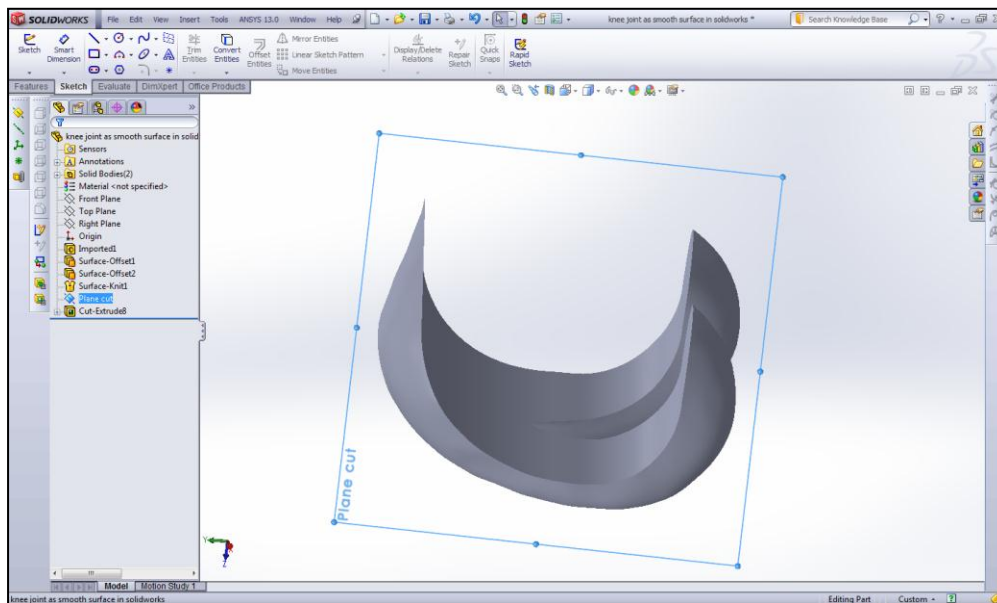


Figure 5.5(b) Implant after *Side-Cut* command

Figure 5.5(b) shows the implant design having a custom articulating surface that exactly replicates the patient's existing articulating surface. It also shows the curved bone-implant surface. In order to promote better bone ingrowth and uniform stress distribution, it was decided that the inner surface needed to be further designed. This was the most challenging task.

Different methods were tried, but most of the methods were not successful or created suboptimal designs with poor surface continuity.

The inner surface as mentioned in the previous section should be parametric as well as nearly define the external surface to get an even distribution of load and uniform thickness. The parametric surface was considered:

- Ease of Surgery
- The feasibility of robotic surgery since femur has to be machined with contour geometry

Considering the above factors, parametric design was chosen for the femur-implant interface.

Different approaches were considered for this parametric design. The only feasible method to generate an inner parametric surface was by using the SolidWorks 3D cutting function *Cut-Loft* along with the use of guide curves. The detailed methodology is explained as follows:

To accurately define the inner parametric surface, six section planes were used to capture the curvature over the entire implant. Figure 5.6 shows the section planes used to generate the inner parametric loft cut. To maintain the continuity of the loft cut, all the planes were passed through the origin. This origin also acts as the center of rotation. The Center of mass (CG) of the imported femur model was considered as the origin to best define the center of curvature of the *sweep cut*. Section planes were named 1st plane, 2nd plane... 6th plane in a clockwise direction for ease of further design.

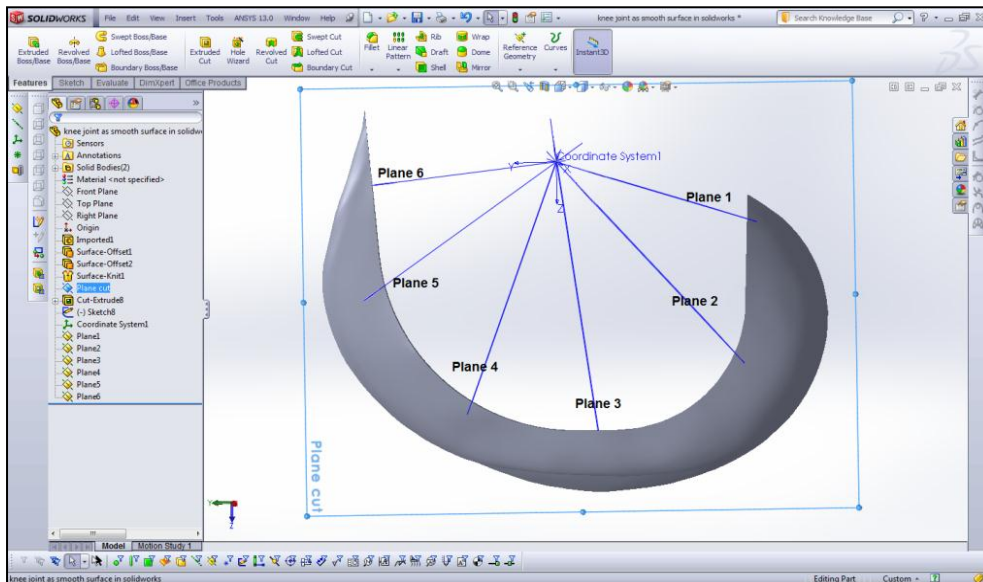


Figure 5.6 six section planes passing through the origin

On each of these six section planes a sketch was drawn, which replicated the external implant curves. This was achieved using the SolidWorks sketch function “Intersection Curve.” These curves shall act as a reference for the inner parametric sketch. Figure 5.7 show one of the six-intersection sketches generated using this command. The curve shown in this figure replicates the external articulating surface of the implant.

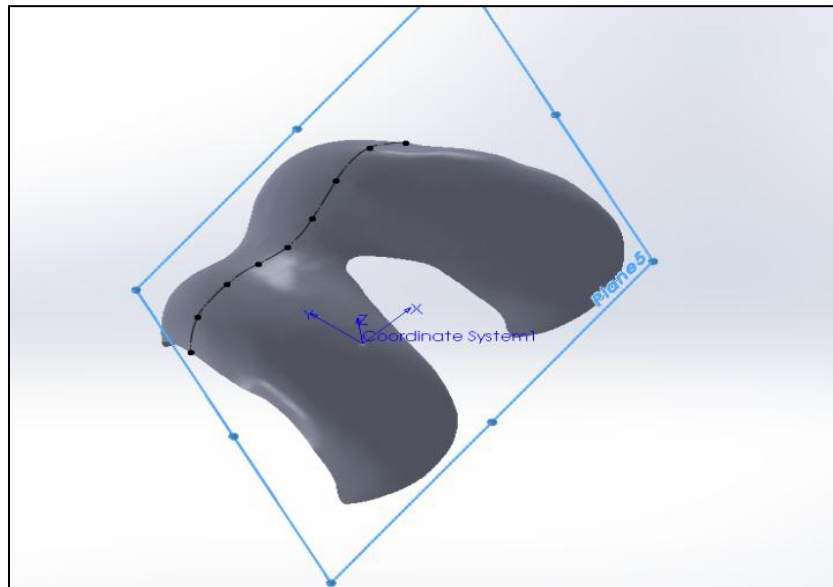


Figure 5.7 typical intersection curves replicating the contour of implant surface

Using these contours from the implant surface, a parametric sketch was defined on each plane. In general, this shape should have the following features:

- It should be parametric i.e., defined using parameterized arcs and lines.
- It should closely follow the shape of section curve similar to Figure 5.7
- The distance between the section curve and parametric curve should define the thickness of the implant. Hence this distance should be maintained equal to or greater than the thickness of cortical bone as discussed in the previous section.
- The generated parametric curve should maintain the continuity i.e., the arcs/lines defining the curve should be tangent to each other. This continuity is required to avoid any step-effect in the design.

Comparing the approximate thickness of cortical bone from Figure 4.1 and following the guideline mentioned above, parametric sketches were generated for all six planes. Figures 5.8(a), 5.8(b), 5.8(c), 5.8(d), 5.8(e), 5.8(f) and 5.8(g) show this detail in each sketch.

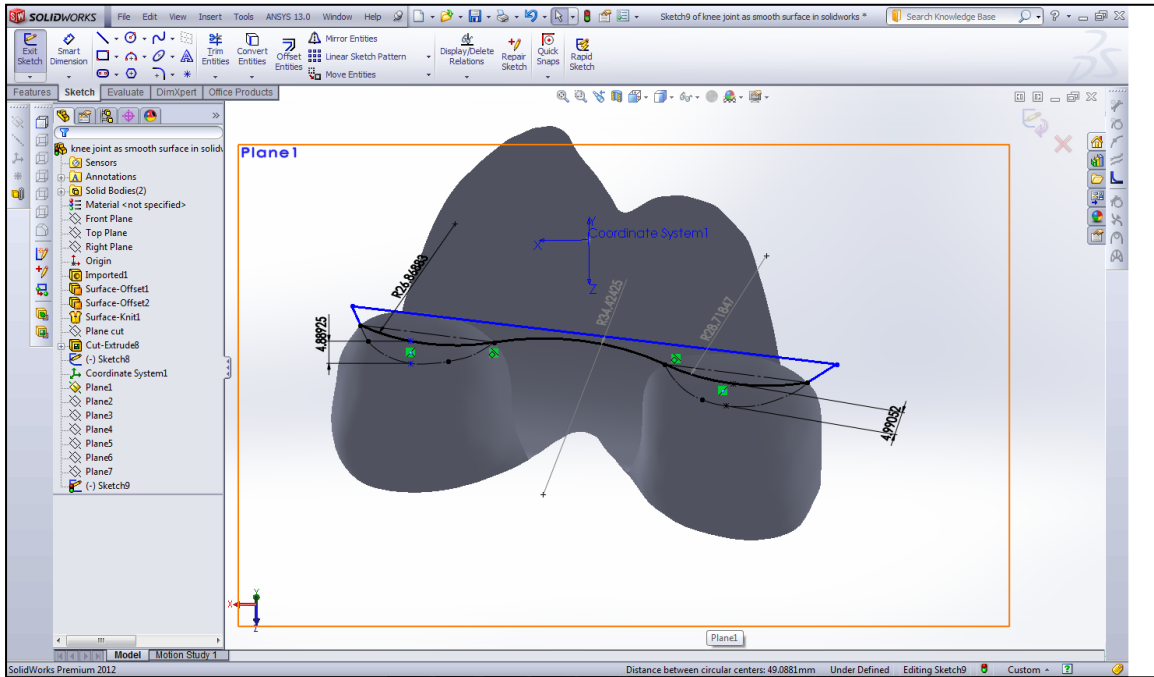


Figure 5.8(a) Parametric sketch details, section plane 1

From Figure 5.8(a), it can be noted that the thickness of the implant shall be 4.889mm and 4.99 mm, respectively for both the condyles. Also the radii of the parametric curve are 26.88 mm, 34.42 mm and 28.718 mm. These radii form a continuous curve by maintaining the tangent. The same is true for all parametric sketches shown in Figure 5.8(b) to Figure 5.8(g). The radii and thickness in each sketch plane were optimized and changed to get the best continuous parametric surface. Also the sketch was closed using lines as shown in Figure 5.8(a) to form a closed loop for *Cut-Loft* function.

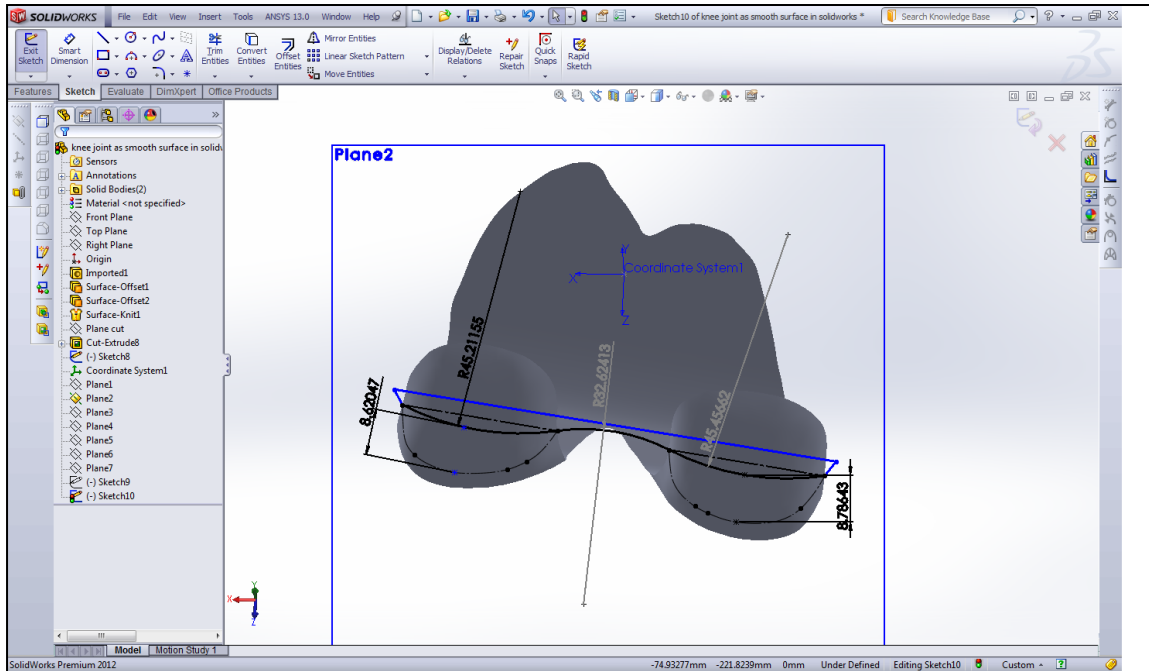


Figure 5.8(b) Parametric sketch details, section plane 2

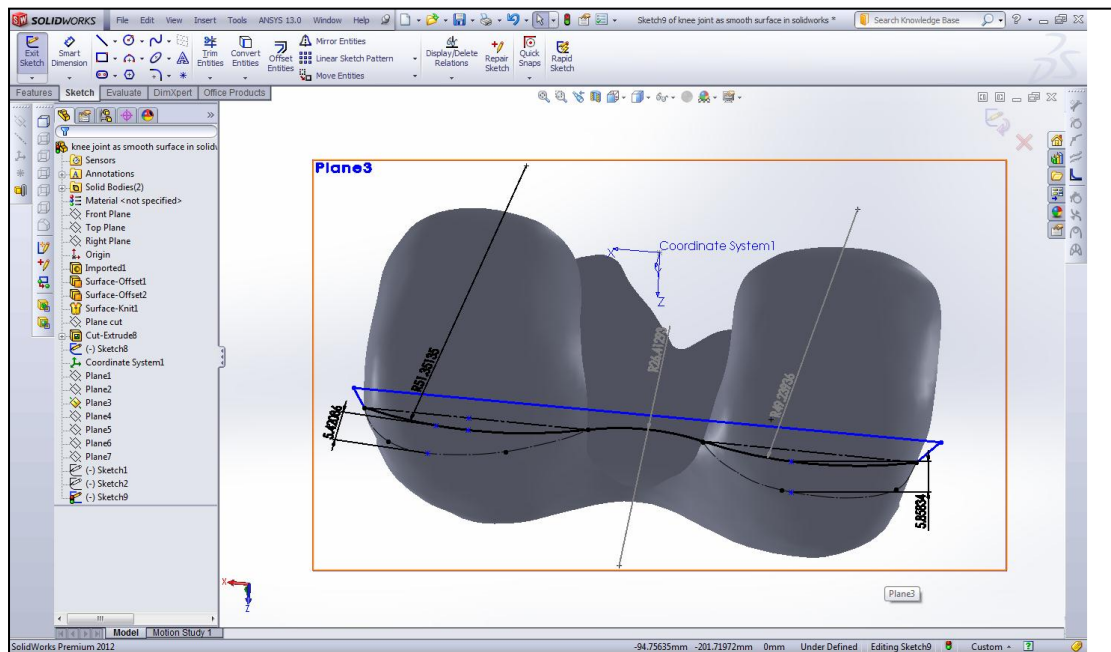


Figure 5.8(c) Parametric sketch details, section plane 3

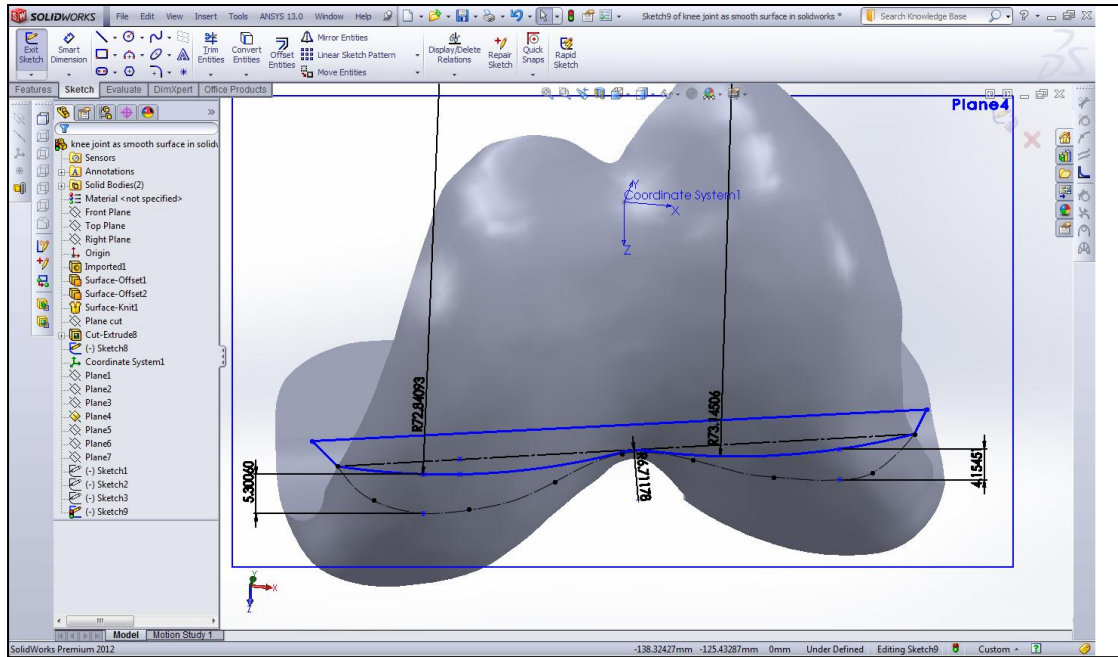


Figure 5.8(d) Parametric sketch details, section plane 4

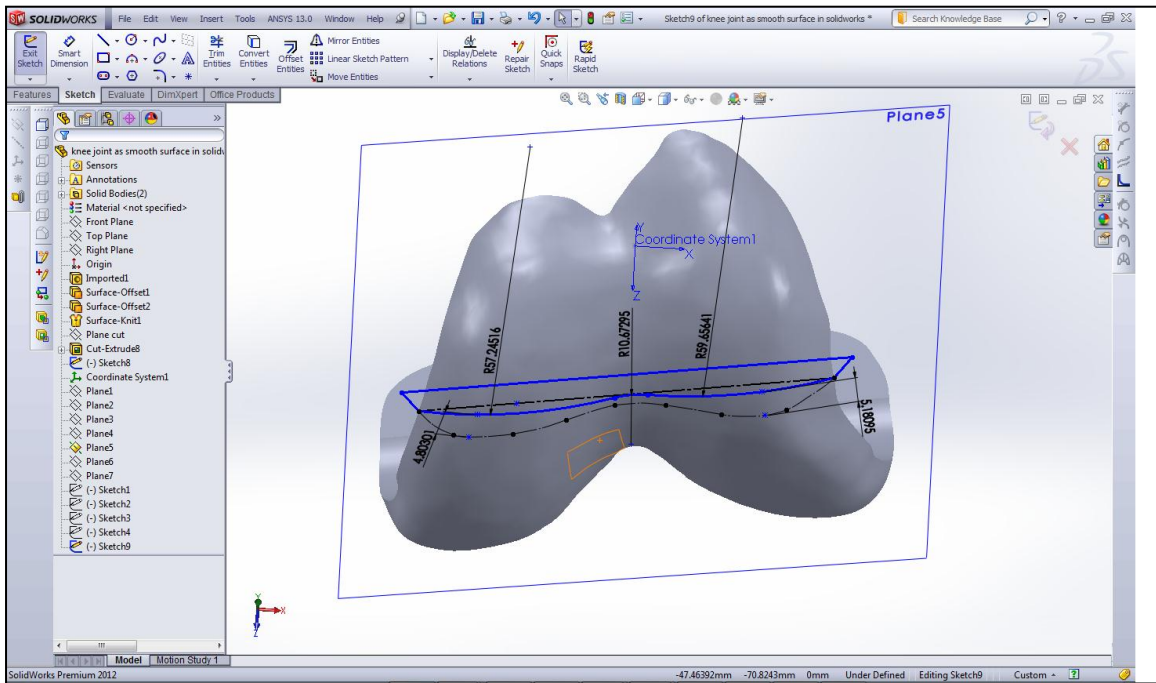


Figure 5.8(e) Parametric sketch details, section plane 5

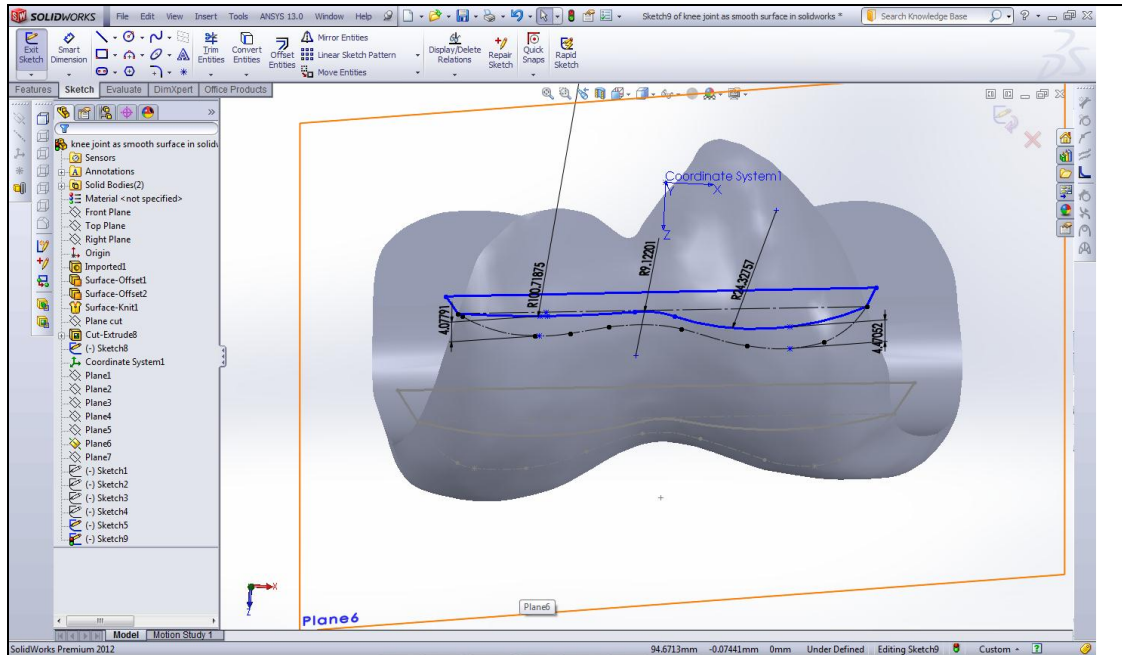


Figure 5.8(f) Parametric sketch details, section plane 6

A summary of all radii and thickness in each section is shown in Table 5.1.

Table 5.1 List of radii and thickness of implant at each section (value in mm)

Sketch Plane	Lateral Thickness	Medial Thickness	Lateral Radius	Central Radius	Medial Radius
1	4.99	4.88	28.7	34.4	26.8
2	8.78	8.6	45.4	32.6	45.2
3	5.8	5.4	49.2	26.4	51.3
4	4.2	5.3	73.1	6.7	72.8
5	5.18	4.8	59.6	10.67	57.2
6	4.4	4.08	24.3	9.1	100.3

These six sketches defined the thickness of the inner parametric shape. 3D guide curves were required for the *Cut-loft* function to generate the parametric inner surface along with these six sketches. These guide curves following the edge of the implant were generated as shown in Figure 4.9. These 3D guide curves are sharp edges generated during the first cut shown in Figure

4.5. The 3D curves were extended at the condylar side to obtain a smooth continuous shape of the *Cut-loft*.

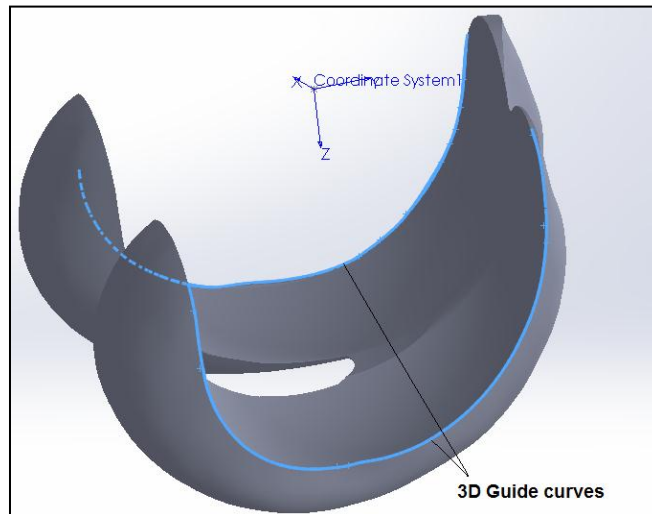


Figure 5.9 Three dimensional guide curves for *Cut-Loft* function

Now we have six sketches and two 3D guide curves to define the inner parametric surface. Using the *Cut-Loft* command in Solidworks, the inner parametric surface was generated in six sweeps. Due to limitations of the software, the cut could not be made in single sweep.

Figure 5.10(a), 5.10(b), 5.10(c), 5.10(d), 5.10(e) and 5.10(f) show the *Cut-Loft* function to generate the inner parametric surfaces, and Figure 5.14(g) shows the final design of the inner parametric surfaced custom human knee implant.

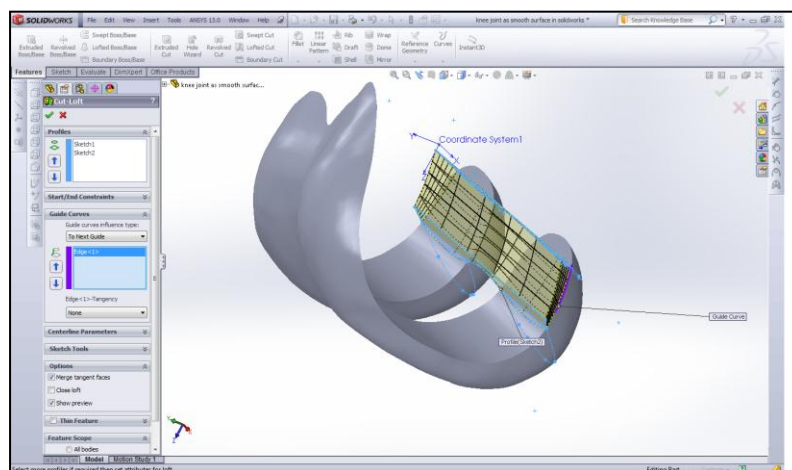


Figure 5.10(a) Screen-shot from Solidworks, First *Cut-Loft* function

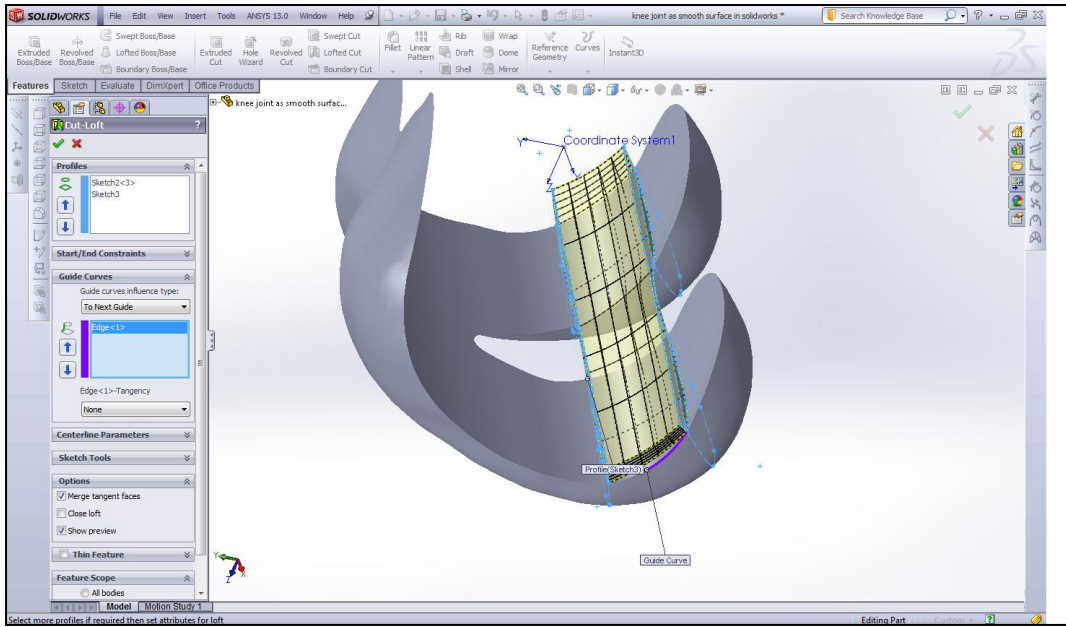


Figure 5.10(b) Screen-shot from Solidworks, Second *Cut-Loft* function

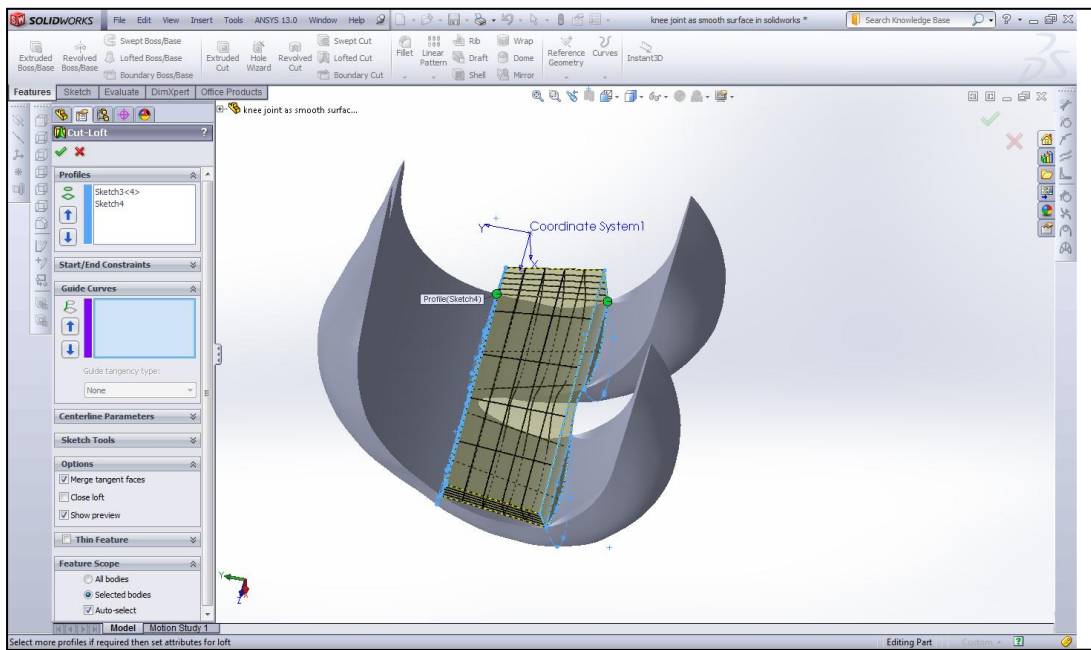


Figure 5.10(c) Screen-shot from Solidworks, Third *Cut-Loft* function

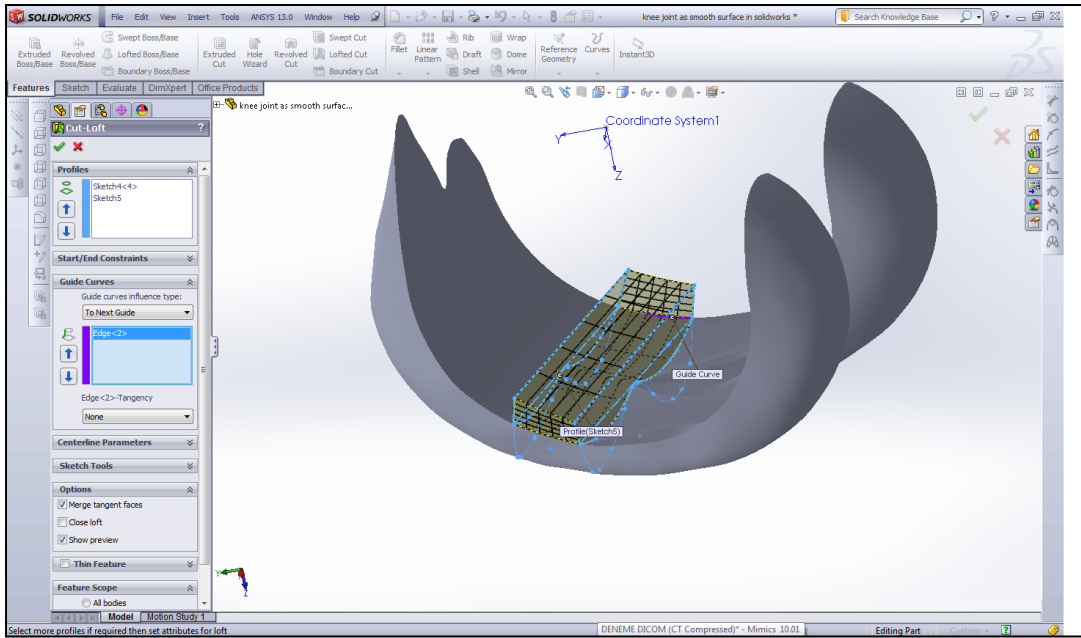


Figure 5.10(d) Screen-shot from Solidworks, Fourth *Cut-Loft* function

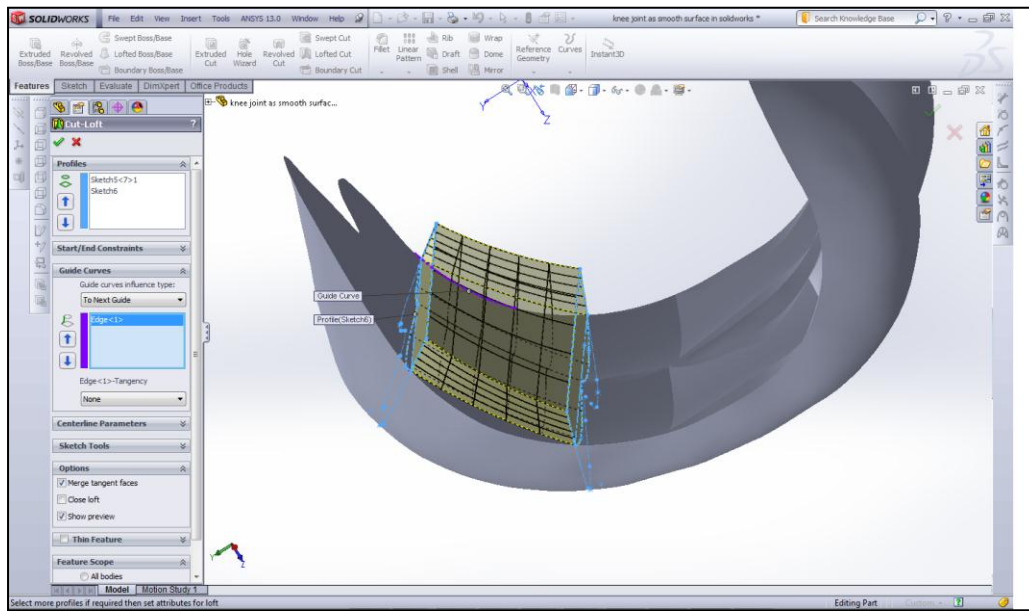


Figure 5.10(e) Screen-shot from Solidworks, five *Cut-Loft* function

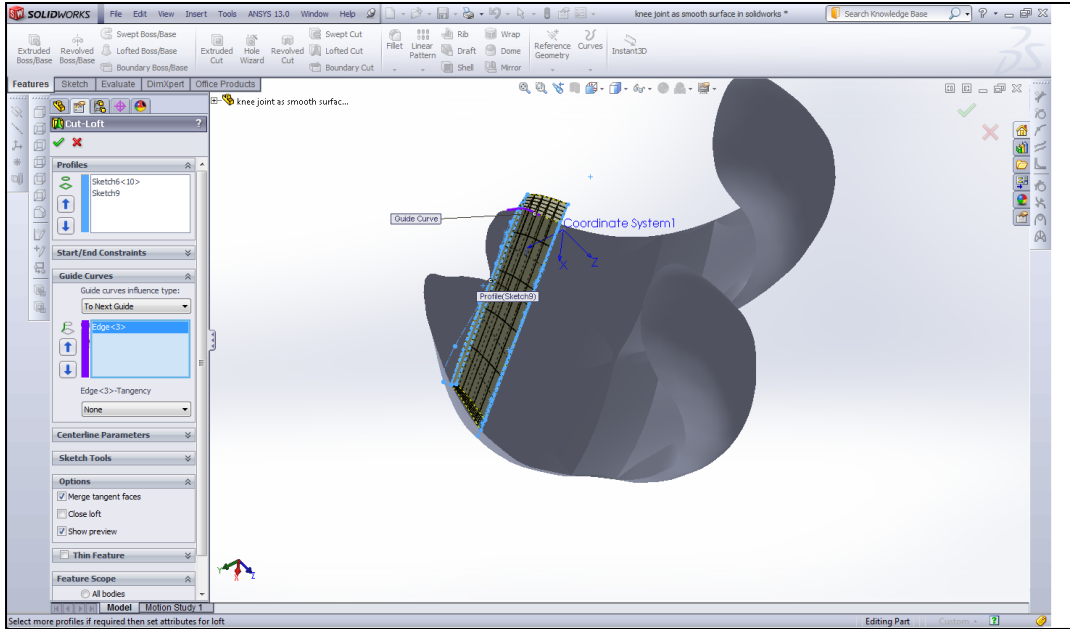


Figure 5.10(f) Screen-shot from Solidworks, Six *Cut-Loft* function

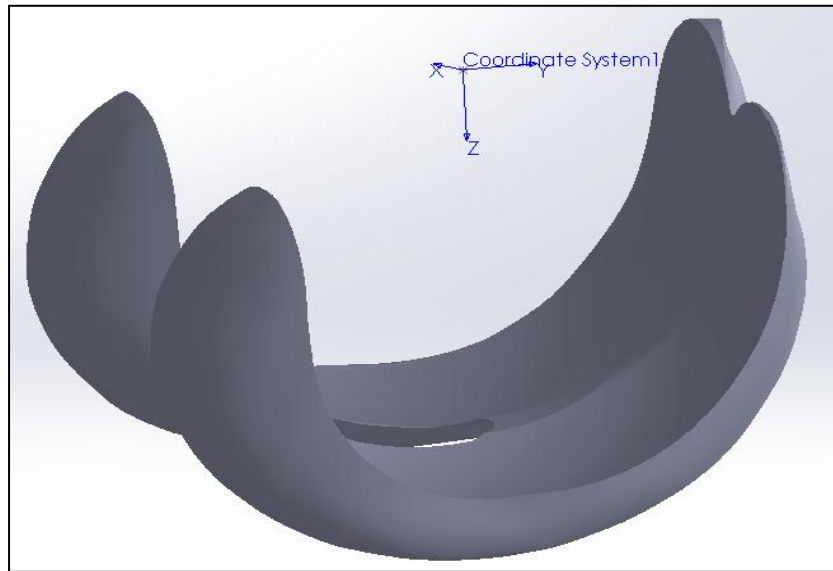


Figure 5.10(g) complete inner parametric surface generated

An important feature of the proposed design is that the shape of the patella groove is replicated. This reduces the need to resurface the patella. It was noted that the designed implant has sharp edges and requires further design modification. Since the patella shall be moving in the patella groove only, the sharp side edges should be avoided. Hence a semicircular cut was made in the region as shown in Figure 5.11

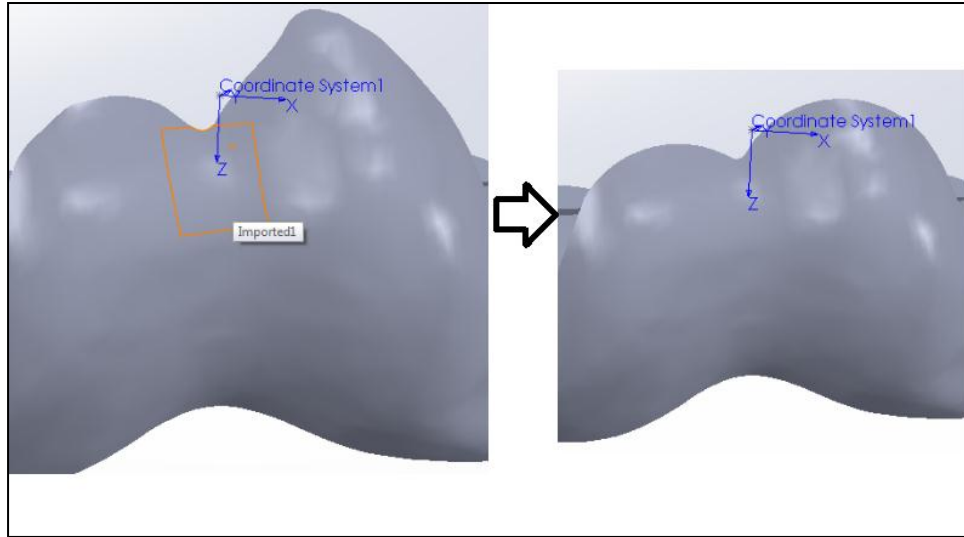


Figure 5.11 Round cut to avoid any sharp edges

5.2.4 Parametric inner surface design of distal femur bone

To check fit and verify the designed parametric custom implant on the distal femur bone, it is necessary that the distal femur also have a similar mating surface. As explained in the previous section, robotic surgery has to be used to obtain this type of contour surface on the distal femur bone. The design of distal femur surface which presented here that must be produced by robotic surgery.

The design of the distal femur surface was obtained using a Boolean operation on the designed implant. Due to limitations in Solidworks, ANSYS Workbench was used to perform this function. The 3D CAD model of designed implant was imported in DesignModeler for ANSYS Workbench as IGES format. Also, the distal femur bone used for the implant design (Figure 5.2) was imported in the same file as shown in figure 5.12. Using the Boolean operation command from creating command in the main tools, select the subtract operation, then select the custom knee implant as tools bodies and the target bodies as distal femur bone (distal femur minus femoral component) to simulate the bone cutting procedure as shown in Figure 5.13, the implant portion of the femur was removed and a parametric distal femur was generated as shown in Figure 5.14.

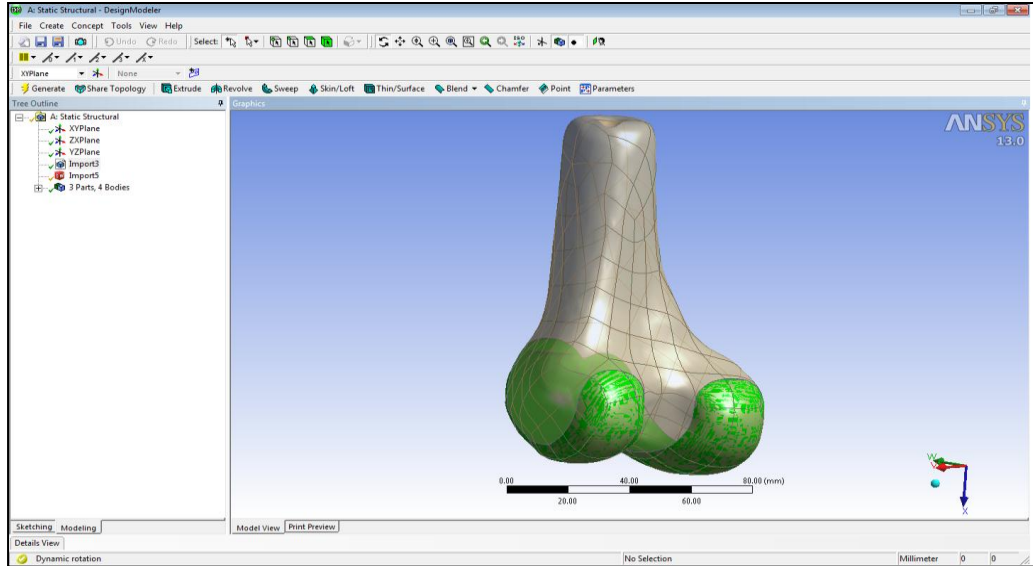


Figure 5.12 three dimensional CAD model of the distal femur bone and femur implant is the same STL file

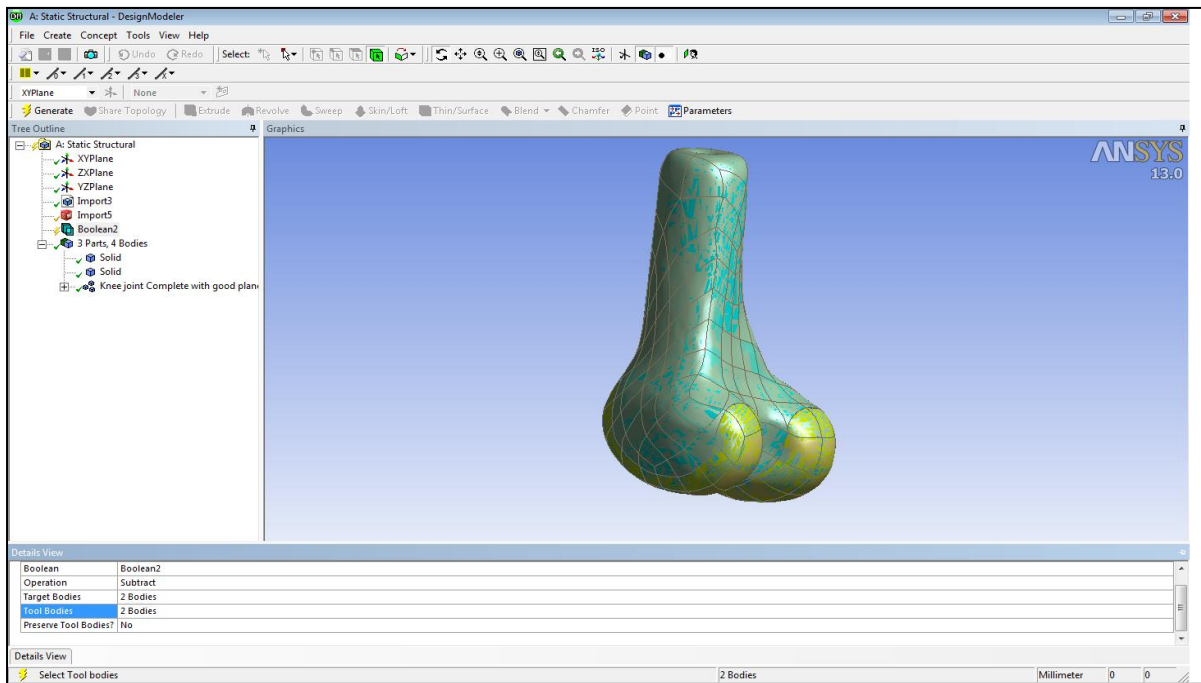


Figure 5.13 Boolean operation commands

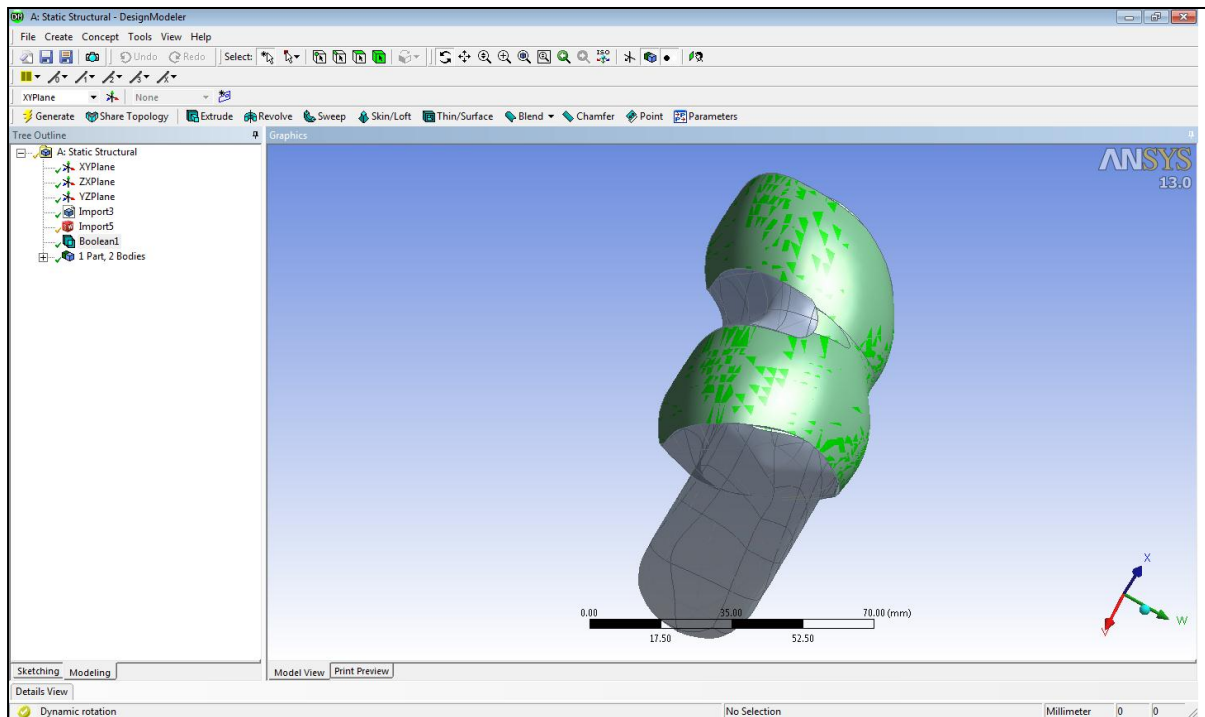


Figure 5.14 Parametric distal femur bone using DesignModeler in ANSYS workbench

5.3 Robotic Surgery

In recent years, robotic surgery systems have been developed for use in orthopedic surgery [93, 94]. The robotic surgery uses an end mill to machine the distal femur bone to fit the implant surface, and the tool path is generated based on a CT-derived Computer Aided Design (CAD) model of the joint and a CAD model of the implant. It was proven that a robot can achieve a much more precise cutting operation than an average orthopedic surgeon can achieve using hand tools and cutting guides. According to a study by Toksvig-Larsen et al. [95], the average contact surface between the distal femur bone and the implant is only about 50% when using conventional methods, which is not sufficient for a cementless implant to ensure prompt and secure fixation. On the other hand, the robots can achieve an average bone-implant contact surface of 95%, which reduces the fixation time and improves the initial stability of the implant. A robot is capable of performing cutting operations of complex freeform surfaces and is not limited to planar cuts, as is the case when using conventional cutting methods. As mentioned previously, a distal femur bone surface was generated by using robotic surgery. Design of such robotic system will help developed confidence in surgeons for using automation in surgery.

5.4 Design of “Standard” femoral component of human knee implant

For comparison purposes, it is necessary to design the standard implant as five cut surface for human knee. Standard implants manufacturer are available for humans and can be used as a reference for designing standard knee implants.

It was decided that the external surface of the implant should be replicated from the CT scan since the study focuses on the interface of femoral component and bone. Hence, the method as shown in the previous section was used to obtain the 3D CAD model of the femur (Figure 5.2).

To design this femoral component of the implant, reference was sought from human implants manufacturer. Unfortunately, since the human implant design is proprietary for every implant manufacturer, such details were not available. A different approach was used to determine approximate knee implant five cut face specifications. The aim of the section was to determine the approximate standard inner face length and angle of implant and to use these values in designing a standard human knee implant.

From the two dimensional drawings/pictures available from the human knee implant manufacturer as shown in Figure 5.15 as example, a comparison table was created. For each implant design, an image was imported in SolidWorks as shown in Figure 5.15, and the length, angle of each face, and thickness at center and edge (a, b, c, d, e, A, AB, B...E and Height) as shown in figure 5.16 were measured.

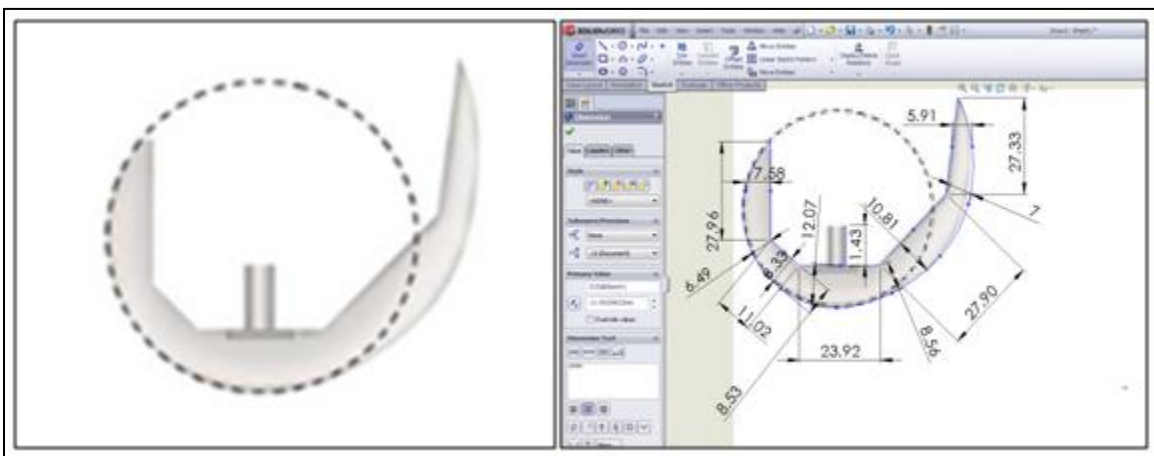


Figure 5.15 Example of image for some manufacturer (right image), and (left image) show import the image in solidworks to find all dimension

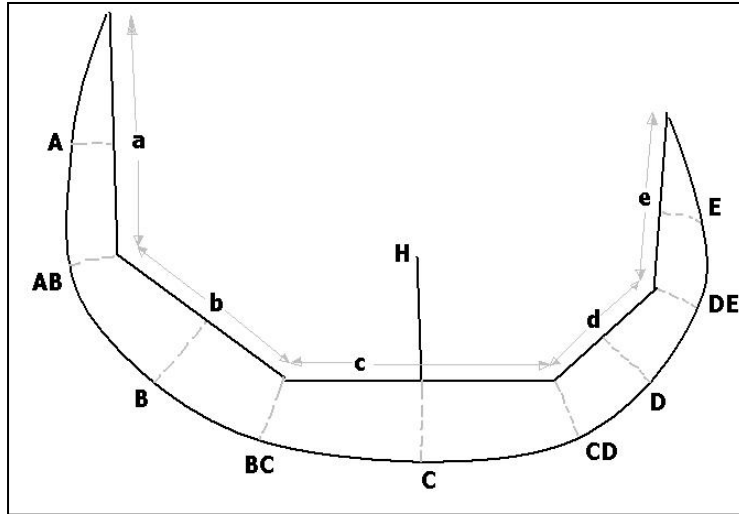


Figure 5.16 Schematic diagram of standard human implant

For every implant manufacturer, a relative width was found for all five faces namely a, b, c, d and e as shown in Figure 5.16. A relative thickness of the implant at the center of each face as well as at the edge was found. Also the relative height of the peg was found and noted as H. Since all the standard implants have 5 to 7 different sizes, a relative number was used to compare the length and thickness. Each face was defined by % of total length and thickness. This can be explained using following equations:

Let a, b, c, d and e is the side lengths of the implant inner face.

Let H be the height of the peg.

Let A, AB, B, BC, C, CD, D, DE and E be the thickness of the implant at the location shown in Figure 4.15.

Let L be the total length of face.

$$L = a + b + c + d + e.$$

Hence relative % length of a = a/L

% Length of b = b/L

% Length of c = c/L

% Length of d = d/L

% Length of e = e/L

The Height H of the peg can also be specified in terms of % total length as H/L

Similarly, relative % thickness at point A = Thickness at A/L and so on....

% thickness at point AB = Thickness at AB/L

% thickness at point B = Thickness at B/L

% thickness at point BC = Thickness at BC/L

% thickness at point C = Thickness at C/L

% thickness at point CD = Thickness at CD/L

% thickness at point D = Thickness at D/L

% thickness at point DE = Thickness at DE/L

% thickness at point E = Thickness at E/L

By using the above method, any effect of size variation of implant can be eliminated. The angle of each face relative to face c was also measured. Since this analysis is approximate, the name of the implant manufacturer is not specified, and it should be noted that these values are for reference purposes only and should not be considered as standard.

Table 5.2 shows the relative length of each face as shown in Figure 5.16. The angle made by each face relative to face c was measured and is shown in Table 5.3. The thickness of the implant at the center of the face and at each edge was also measured relative to the total length and is shown in Table 5.4. Data for peg height for Type 4, 5 and 6 manufacturer was not available.

Table 5.2 Face widths of standard implant in % of Total Length L

Implant Manufacturer →	Type 1	Type 2	Type 3	Type 4	Type 5	Type 6
Face ↓						
a	27%	26%	23%	26%	31%	31%
b	17%	19%	24%	19%	19%	14%
c	26%	23%	20%	27%	18%	23%
d	13%	18%	11%	13%	13%	11%
e	18%	14%	21%	15%	19%	21%
H	12%	12%	13%	N/A	N/A	N/A

Table 5.3 Angle of each face relative to horizontal face c

Implant Manufacturer →	Type 1	Type 2	Type 3	Type 4	Type 5	Type 6
a	96	96	96	90	95	95
b	128	132	131	122	134	134
c	0	0	0	0	0	0
d	138	128	139	138	135	135
e	89	85	88	95	90	90
H	89	90	89	N/A	N/A	N/A

Table 5.4 Thickness of implant at center of face and at edges

Implant Manufacturer →	Type 1	Type 2	Type 3	Type 4	Type 5	Type 6
A	7%	6%	8%	6%	6%	6%
AB	6%	6%	7%	5%	6%	6%
B	7%	6%	10%	6%	8%	7%
BC	6%	5%	7%	5%	6%	6%
C	9%	8%	9%	10%	7%	7%
CD	7%	6%	7%	7%	6%	6%
D	9%	9%	7%	7%	7%	7%
DE	5%	6%	6%	6%	6%	6%
E	6%	7%	7%	6%	7%	7%

Based on the above data, the average of all these implant types was taken and is summarized in Table 5.5 and Table 5.6

Table 5.5 Average of % Face widths and angle

Face	Average Length	Average Angle
a	27%	95
b	19%	130
c	23%	0
d	13%	136
e	18%	90
H	12%	90

Table 5.6 Average of Implant Thickness

Face / Edge	Average %relative thickness of implant
A	7%
AB	6%
B	8%
BC	6%
C	9%
CD	7%
D	8%
DE	6%
E	7%

Our aim is to design a standard human femoral component of implant based on the data from Tables 5.5 and 5.6.

As explained in the previous section, a 3D model in STEP format was imported in SolidWorks for the flat, femoral component knee implant design as shown in Figure 5.2. A mid plane was also created using the same concept as shown in Figure 5.3. A sketch was drawn on this mid plane as shown in figure 5.17, and the first side cut was generated using *Cut-Extrude* command. The idea was to make a sketch based on the above values as a reference.

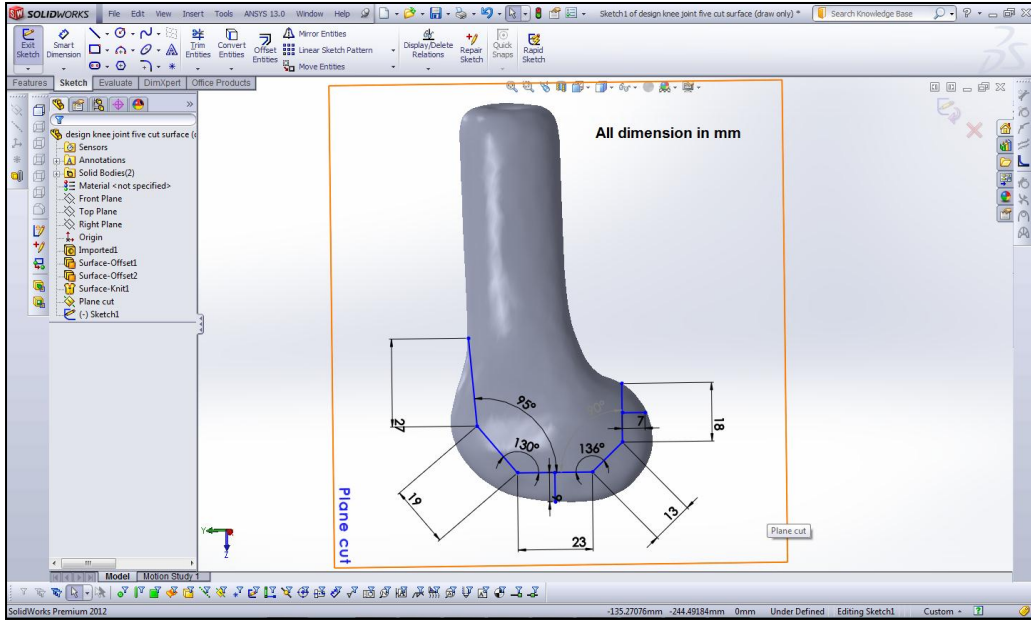


Figure 5.17 Sketch for flat implant obtained using data from Table 4.5 and Table 4.6

Based on the above sketch details, the implant was made using *Cut-Extrude* command in SolidWorks. Figure 5.18(a) and 5.18(b) shows the implant design having a custom articulating surface, exactly replicating the patient and flat inner surface. This design constrains displacement and rotation of the implant in one direction (direction perpendicular to the cut). The implant can still slide along the cut axis. This movement shall be constrained by pegs on each condyle.

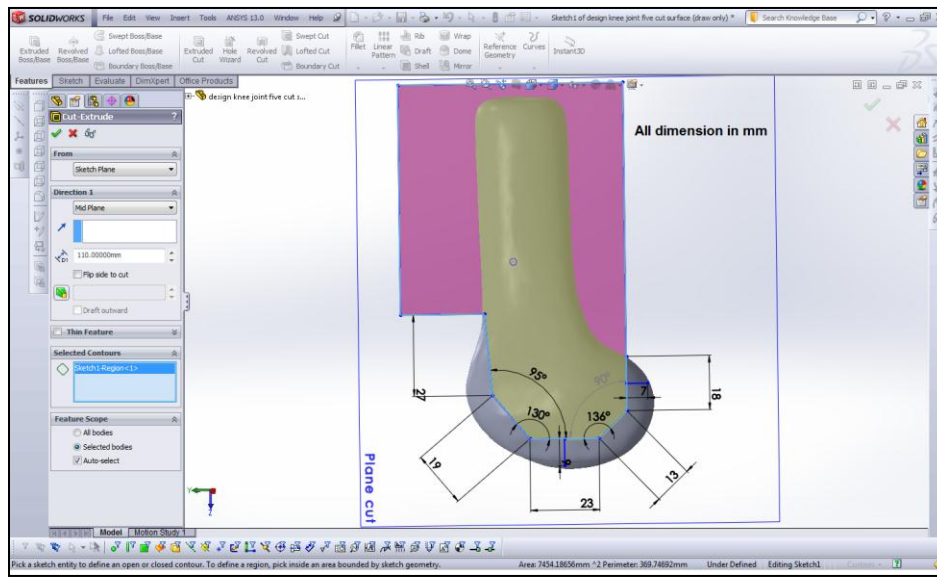


Figure 5.18 (a) Standard implant during *Side-Cut* command

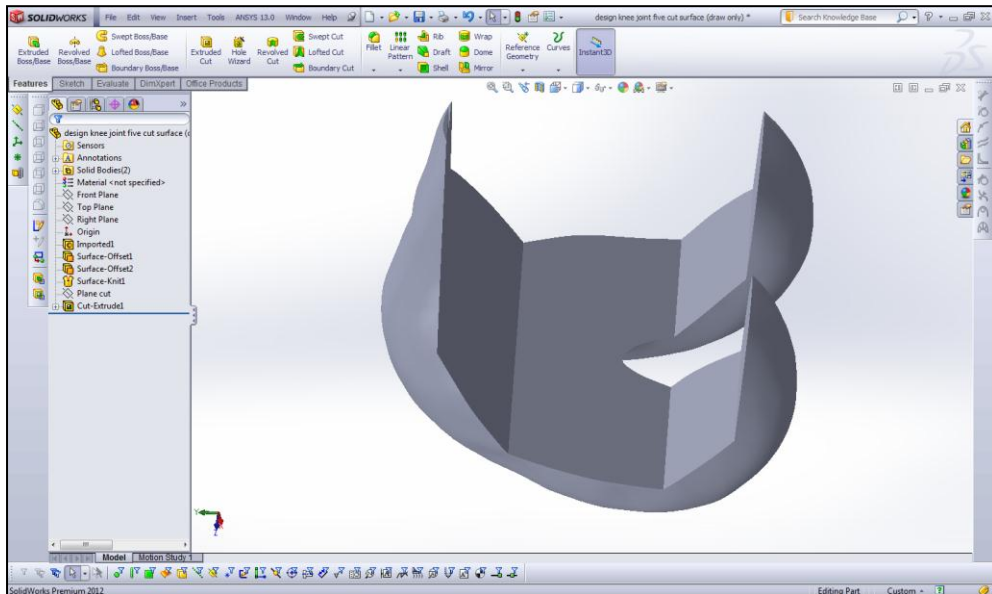


Figure 5.18(b) Standard implant after *Side-Cut* command

On the flat surface perpendicular to the mechanical axis of the joint, a sketch was created as shown in Figure 5.19(a). The peg with 3mm diameter was chosen. These pegs were modeled at the center of the condylar face as well as parallel to the insert angle. The pegs have to be parallel to the insert angle for implant to be inserted in femur. This sketch was extruded using the *Base-Extrude* command. The pegs were created of 7mm length. This is shown in Figure 5.19(b)

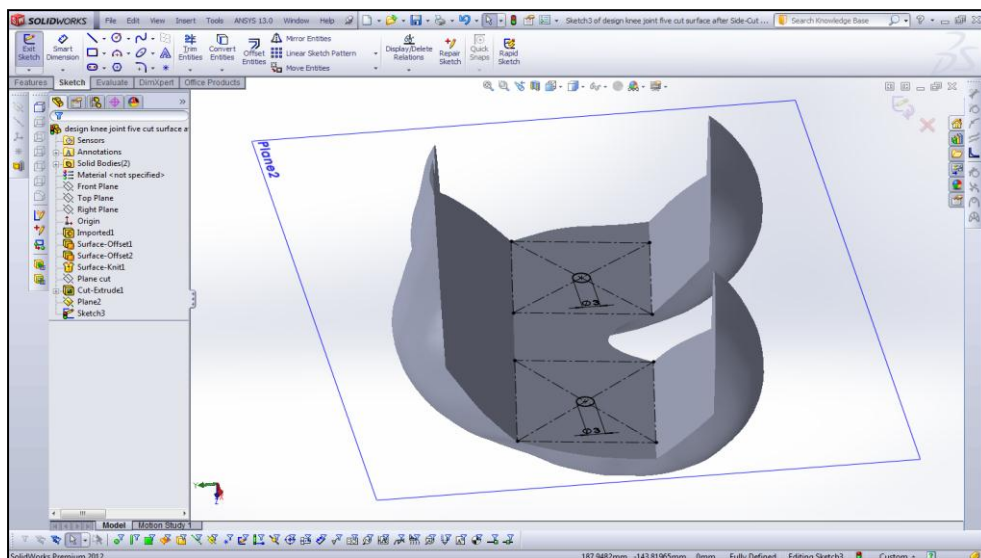


Figure 5.19(a) Sketch for generating pegs

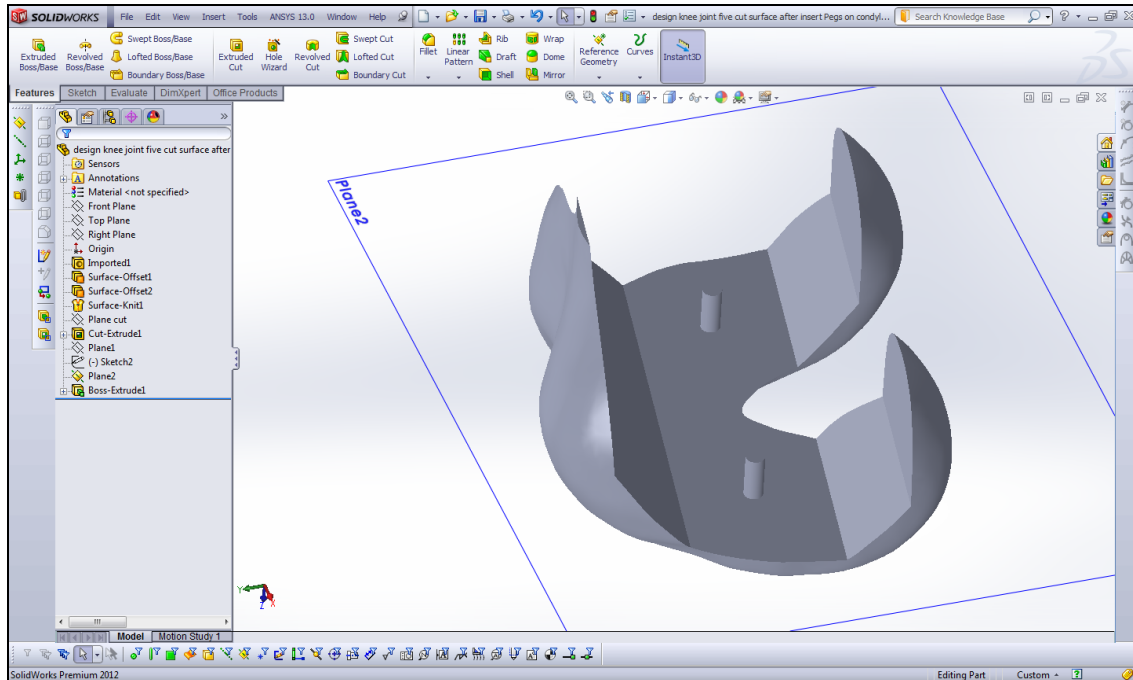


Figure 5.19(b) Pegs on condylar face

As the case with the custom parametric designed implant, the sharp edges on the side of patella groove were changed to semi-circular edge using a cut with radius of 14.5mm as shown in Figure 5.20.

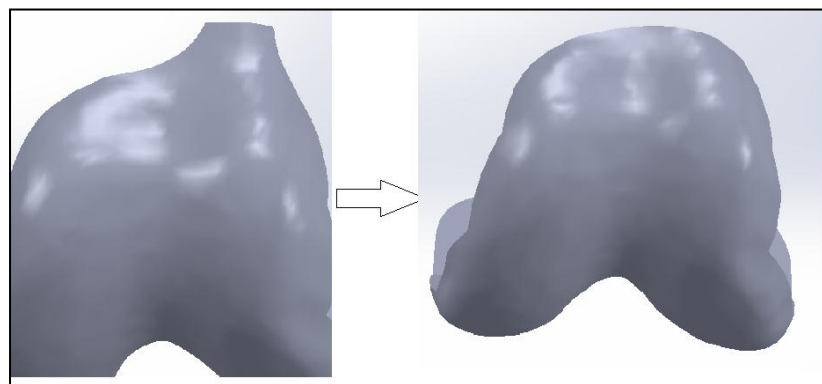


Figure 5.20 Round cut to avoid any sharp edges on flat implant

Tissue damage cannot be avoided in this type of design, and it is necessary to sacrifice the cranial-cruciate ligament and caudal cruciate ligament. Also, the design of the femur with a flat

surface is not required in this design, since the femur is cut using a flat guide saw to fit the implant shown above.

The final design of the faceted femoral component of human knee implant with custom articulating surface is shown in Figure 5.21.

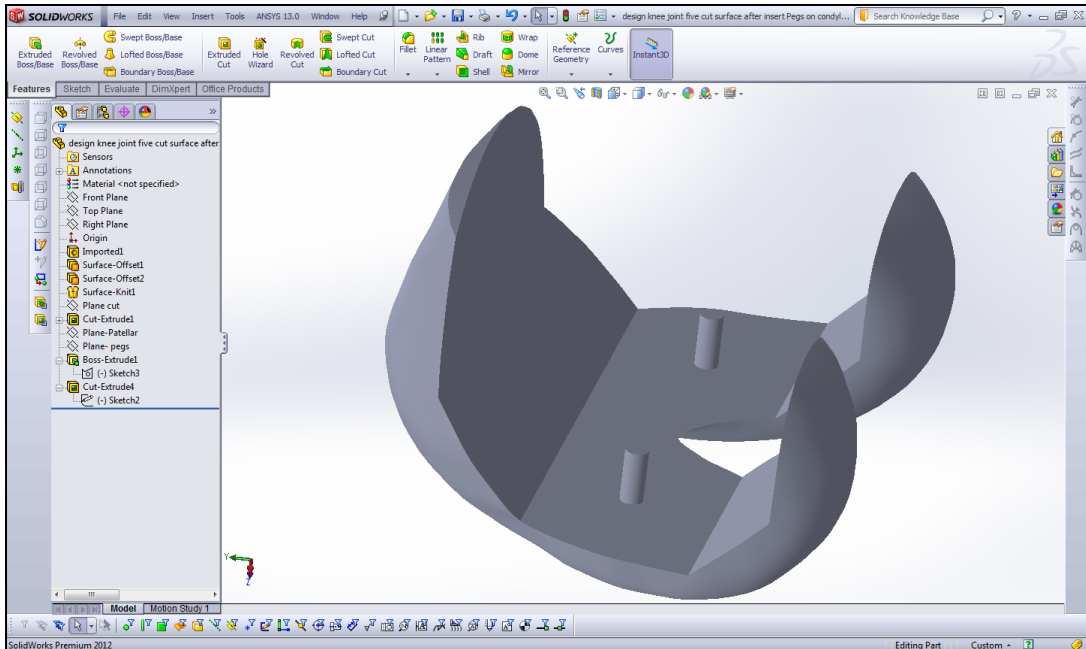


Figure 5.21 Standard human femoral component of implant

5.3.1 Parametric inner surface design of distal femur bone

To check fit and verify the designed parametric standard implant on the distal femur bone, it is necessary that the distal femur also have a similar mating surface. As explained in the previous section 5.2.4 in this chapter for using Boolean operation command to make similar mating surface as the implant surface. Using the same steps in as the previous section, the final design of the distal femur surface was obtained as shown in figure 5.22. This represents the surface that must be produced by the surgeon.

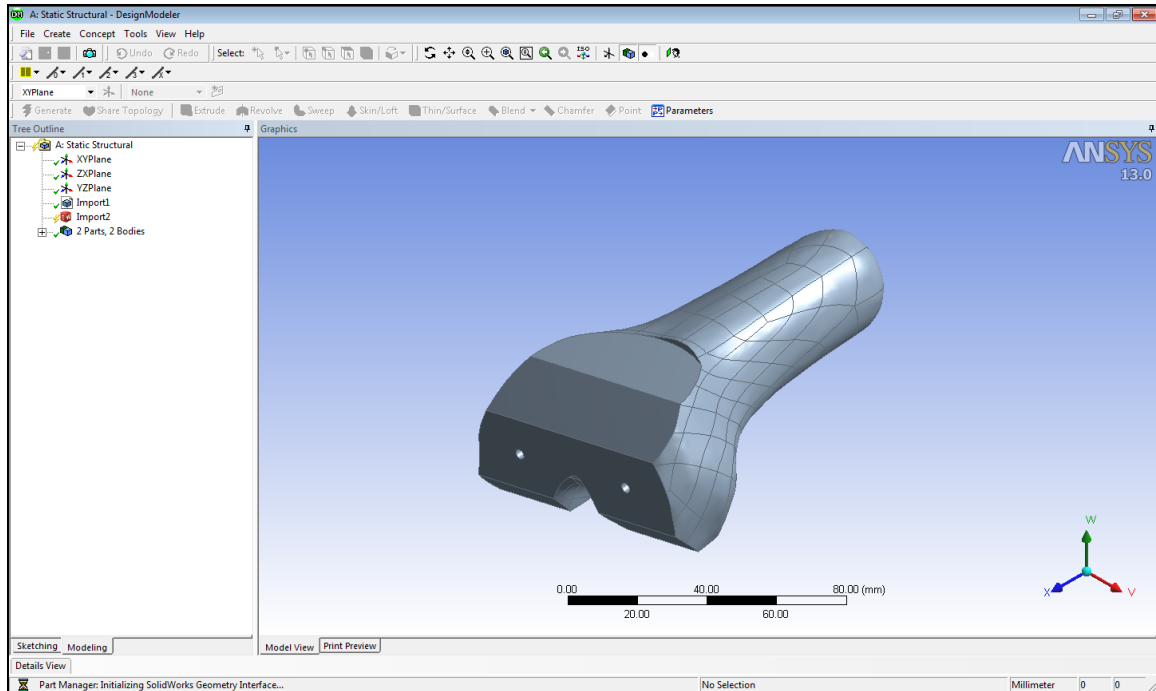


Figure 5.22 parametric distal femur bone for standard femoral implant

5.4 Finite Element Analysis

To test the custom design smooth surface of femoral component implant that proposed bone-implant interface will provide more even stress distribution, finite element analysis (FEA) were performed. FEA used for confirming the uniform load distribution over the entire surface of bone-implant interface.

Two implant femoral component of knee joint were designed with the same articulating surface as discussion before in this chapter. One bone implant interface surface were designed with the conventional five cut flat surface, and the other bone-implant surface was designed with the proposed custom smooth surface.

5.4.1 Creation of FE models with ANSYS

ANSYS Workbench 13.0 (ANSYS Inc., Southpointe, PA, USA) was used to create the FE models in this thesis rather than ANSYS Mechanical APDL 13.0. Although both software are technically same, ANSYS Workbench has more user friendly interface.

Once ANSYS Workbench was opened, Static Structural was chosen as Analysis Systems as show in figure 5.23. Once the Static Structural is chosen, the square box appears in the Project Schematic. Material properties, geometries, boundary/loading conditions were specified in the specific programs activated by clicking the rows such as Engineering Data, Geometry, and Model respectively.

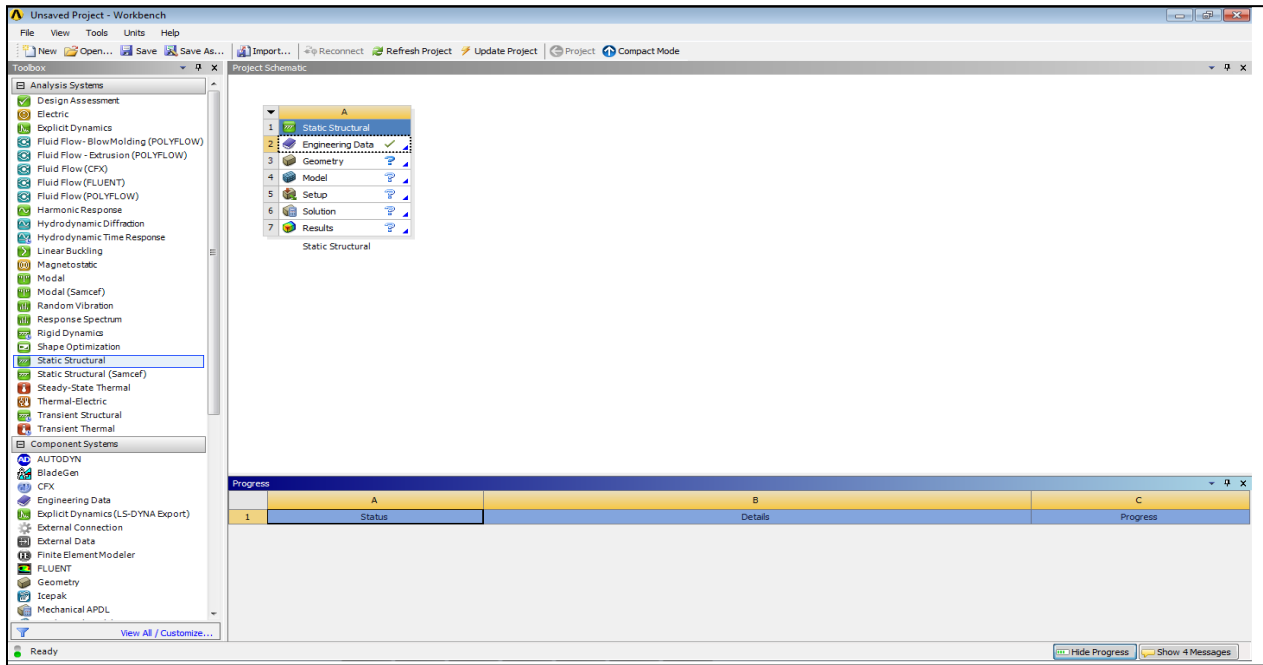


Figure 5.23 Typical View of ANSYS Workbench. Static Structural can be chosen from the left column.

5.4.1.1 Assigning Material Properties

Material properties for each cortical bone, trabecular bone for the distal femur bone and titanium for the implant can be specified in *Engineering Data* in shown in Figure 5.24. In this Engineering Data, homogeneous isotropic elastic material properties were specified into the cortical and trabecular bone separately and also titanium material for the implant. Two properties such as Young’s modulus and Poisson’s ratio were needed to be specified manually. Then, Bulk and Shear Modulus shown in Figure 5.22 were automatically calculated. Based on the literature review in the section 2.8, the densities of the cortical and trabecular bones were assumed to 1.8 g/cm³ and 0.5 g/cm³ respectively. Using these density values, Young’s moduli were obtained

from the following equations in the previous section 2.8: $E_{\text{cortical}} = -6.142 + 14\rho$ and $E_{\text{trabecular}} = 0.58\rho^{1.3}$, where ρ was the density (the unit of trabecular bone density was converted from g/cm^3 into kg/m^3 before putting it into the latter equation). Throughout this process, the Young's modulus of 19GPa and 1871MPa were obtained and assigned into the cortical and trabecular bone respectively. Poisson's ratio of 0.3 and 0.12 were also adopted from the literature [64], and then assigned into cortical and trabecular bones respectively. While the material property of the implant has assigned as 110GPa for Young's modulus and poisson's ratio is 0.3 approximating some grades of Titanium alloy Ti6Al4V [96]. Summaries for the material properties used for the analysis are specified in Table 5.7.

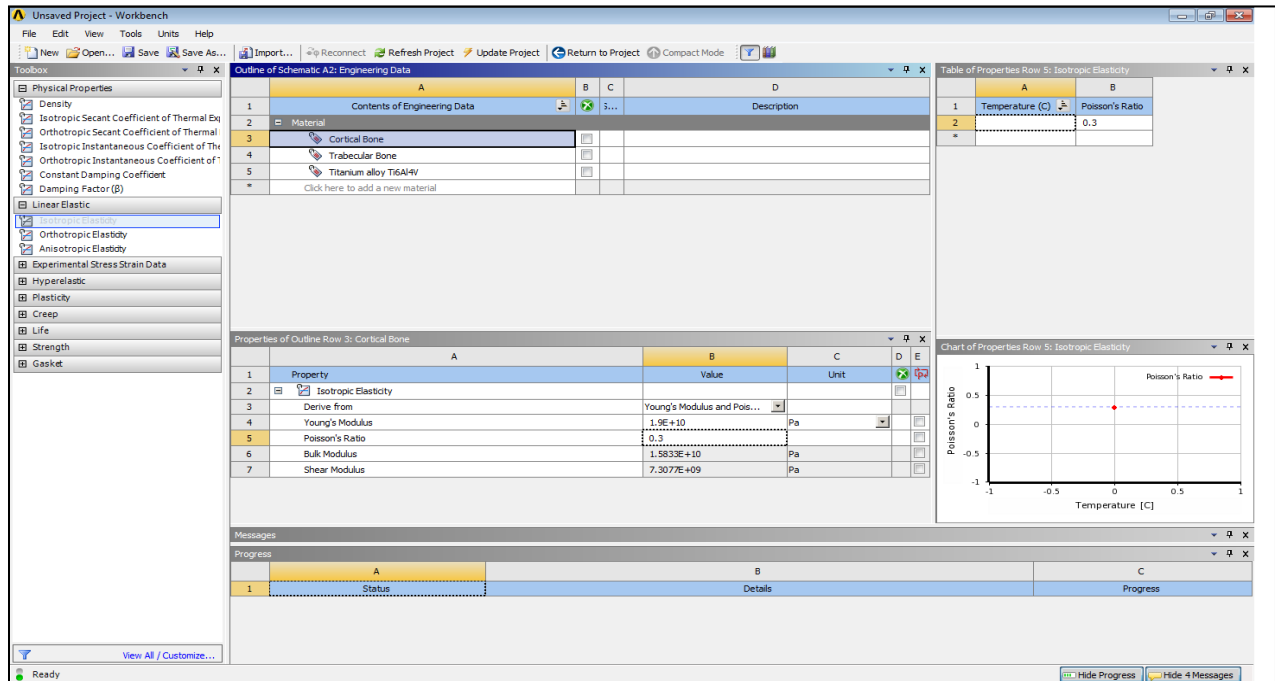


Figure 5.24 Assignment of material properties in the Engineering Data in the Workbench for cortical bone

Figure 5.24 shows the view of the Engineering Data where material property assignment was performed. Isotropic Elasticity was chosen from Linear Elastic from the left column, then two material properties (Young's modulus and Poisson's ratio) were specified separately for the cortical bone, trabecular bone and titanium material for the implant.

Table 5.7 show the summaries of the material properties used for analysis [64, 96].

Material	Modulus of elasticity	Poisson's ratio
Cortical bone	19 GPa	0.3
Trabecular (Cancellous) bone	1871 MPa	0.12
Titanium alloy Ti6Al4V	110 GPa	0.3

5.4.1.2 Geometry

Geometry was then imported into the CAD program called *DesignModeler* in the ANSYS WorkBench. This DesignModeler was opened by right clicking the *Geometry* in the square box in Figure 5.23. In the Design Modeler, each geometry as IGES file format was imported separately. Parametric distal femur bone in the figure 5.14 which discussion in the chapter 5 was imported and then import the femoral implant in the same file as shown in figure 5.25.

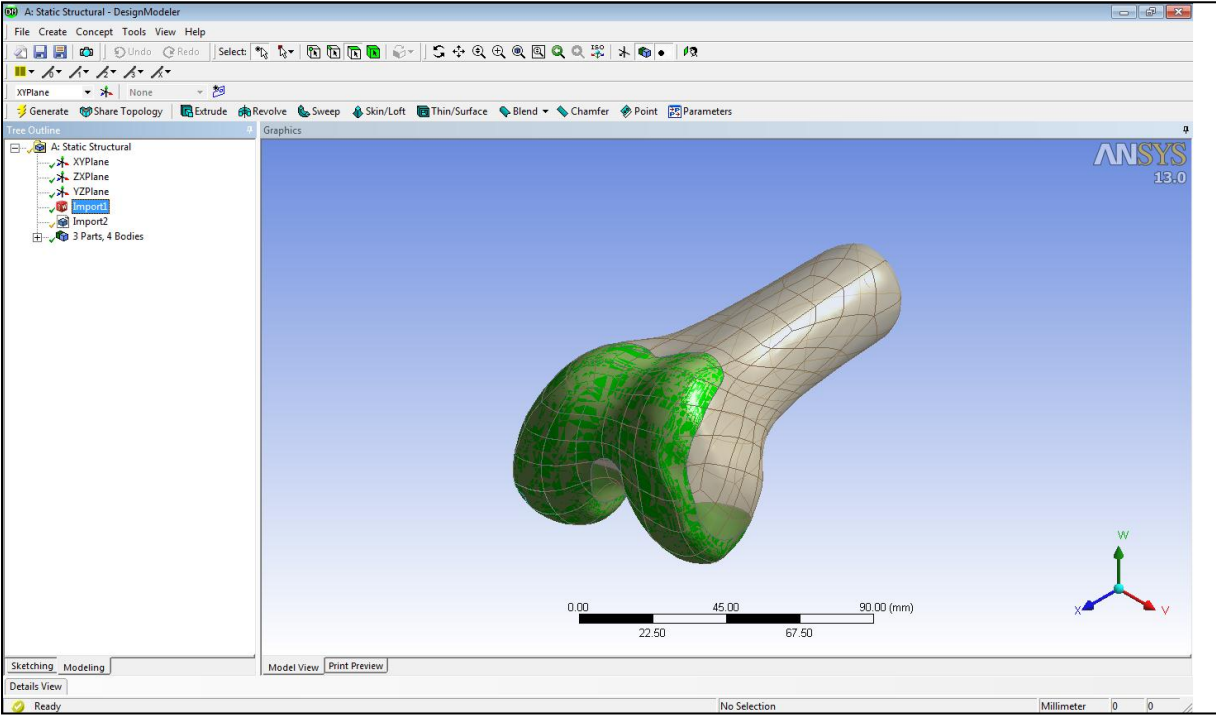


Figure 5.25 Imports of Geometries

5.4.1.3 Meshing the geometry

Once the geometries were imported into the ANSYS Workbench, meshing was taken place again. Segmented image was already meshed earlier as described in the section 4.3.5. This earlier meshing was necessary process only to convert CT data based geometry into the importable file format to the ANSYS Workbench. However, once these meshed geometries were imported into the ANSYS Workbench, the geometries were recognized as unmeshed solids constructed by many tetrahedrons by the ANSYS Workbench. Therefore, additional meshing was required. In order to model complex geometry of the distal femur, tetrahedron was chosen as the element shape again. *Patch Conforming* was selected as meshing algorithm. Element size was set to the default setting “coarse”. Element growth rate and transition ratio were set to 1.2 and 0.272 respectively. If meshing geometries with these specifications was failed, another meshing algorithm called *Patch Independent* algorithm was selected.

Also the same steps was done for the conventional femur implant as five cut straight of bone-implant interface, the femur implant with pegs as shown in figure 5.21 is imported in ANSYS workbench, and the femur bone as five cut face import in the same file. Also the assigned materials for each model as the same discussion when using the femoral implant as smooth bone-implant interface. Number of nodes and elements used for each model in table 5.8. Two models after imported and meshed FE model can be show in figure 5.26.

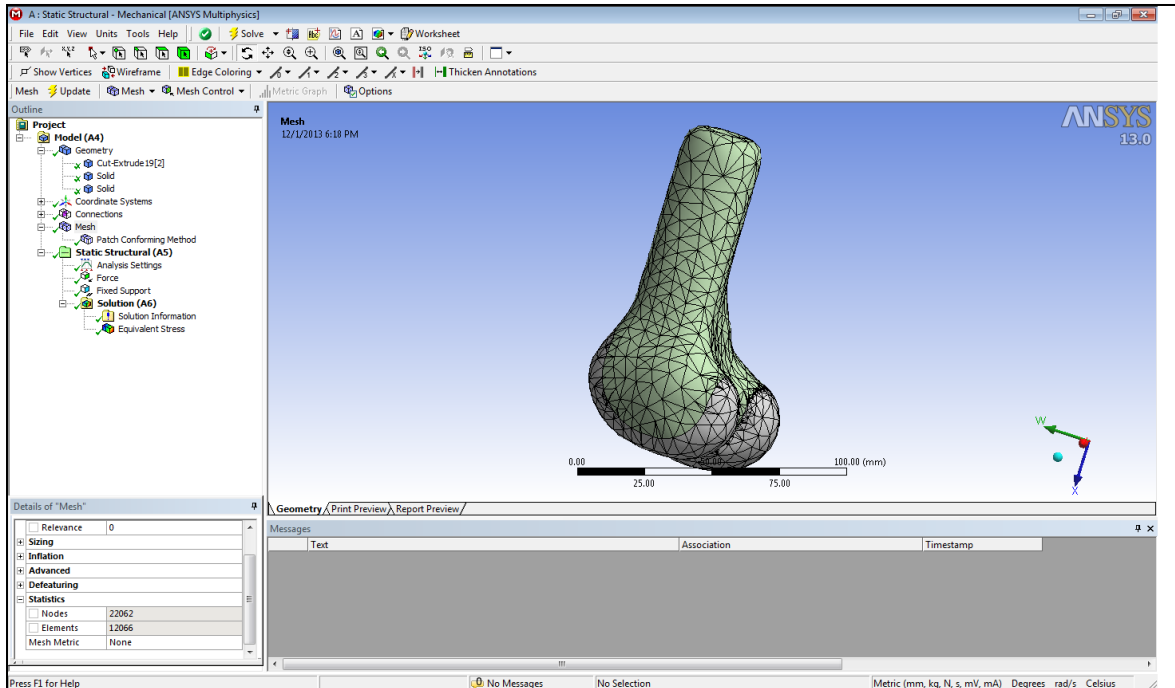


Figure 5.26 Meshed Finite Element Model.

Table 5.8 Number of nodes and tetrahedral elements used for each element

FEA Model	Number of nodes	Number of elements
Custom design implant	7102	3395
Custom femur	16310	9368
Standard design implant	7046	3445
Standard femur	12576	7190

5.4.1.4 Boundary/loading Condition

Once meshing the geometry was completed, the boundary condition was specified in the software called Mechanical in the ANSYS Workbench. It can be opened by right clicking the Model in the square box shown in Figure 5.23.

For these analyses, three cases different positions out of a gait cycle were simulated. The center position, middle position and back position as shown in the figure 5.27.

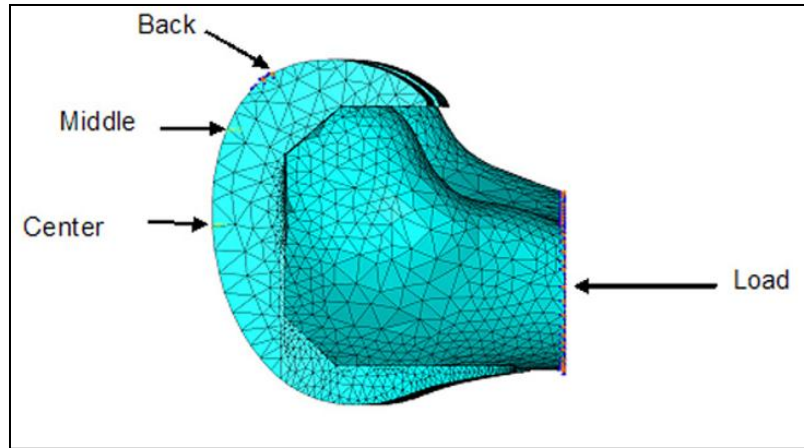


Figure 5.27 Load and reaction force used for all finite element analysis models.

Case I: The center position for the reaction force represents a standing position or starting position of a gait cycle (straight position).

Case II: The middle position represents the end of a normal walking gait cycle.

Case III: the back position represents an extreme position for climbing stairs.

The vertical axial load was applied at the proximal end of femur bone and there are ground reaction forces where the femoral component interacts with the tibial component. These reaction forces can be seen as point forces or distributed over a fairly small area.

Axial loading and restraints were applied to the meshed assemblies as described before. The assembly was restrained by restricting motion along center position, middle position and back position as shown in the figure 5.27. This assembly was loaded axially with 2100N at the proximal-most end of the femur, representing approximately 3 times a nominal body weight of 70 kg. Many researchers have estimated that the maximum vertical load on the proximal end of the femur during natural gait falls within from 2 to 4 times of the body weight [97, 98, 99 and 100], so 2100 N is reasonably typical test load. This load for my thesis compares well with the 2200 N used by Chu [103], 2200 N axial force used by Godest et al. [101] and 2000 N used by Villa et al. [102].

The angle of the load during the middle and back position was adjusted to better simulate the correct conditions. The femur bone was created which bonded contact with the femoral implant. The gait cycle loads were applied on the proximal end femur bone. The boundary conditions (reaction force) were defined as narrow surfaces going across the implant of an approximately

width of 2–3 mm. This represents the limited surface contact between the femoral component and the tibial tray as shown in Figure 5.27.

The interaction contact between the implant and the end distal femur bone was defined as augmented Lagrange contact which chooses from the bonded contact command. Boundary conditions needed to be specified were following: 1) *force* (including magnitude, direction, and location), 2) *fixed support*, 3) *reaction force*, and 3) *contact* which specifies the boundary condition between the implant and distal femur bone boundaries.

CHAPTER 6

RESULTS AND DISCUSSION

6.1 RESULTS

It is important to conduct a finite element analysis for confirming the uniform load distribution over the entire surface of bone-implant interface. As mentioned previously, a closed solid CAD model of the implant as well as cut femur is required for Finite Element Analysis study. The purpose of an FEA study is to examine the stress distribution on in implant.

The plots for all finite element analysis were done in at the same stress scale level. All stresses plotted in this thesis were von Mises. Most importantly, results of this thesis show that the stresses were highly concentrated along the sharp edges for the conventional implant design, while the custom implant design showed a more uniform stress distribution. This can be clearly seen in all Figures from 6.1 to Figure 6.3. The custom design implant generated much lower maximum stress for all cases.

For the center position which describes the standing position out of gait cycle, the vonMises stress values of the conventional standard implant and custom femoral knee implant approximately from 0.00576MPa to 50MPa and from 0.00422MPa to 26.054MPa respectively as shown in figure 6.1(a) and 6.1(b). For the conventional implant design, the average stresses at the sharp edges were 16MPa during the center position case; and for the custom implant smooth surface design, the average stresses were 6.687MPa in the contact region. The red color represents the maximum stress and the green color represents the average stress.

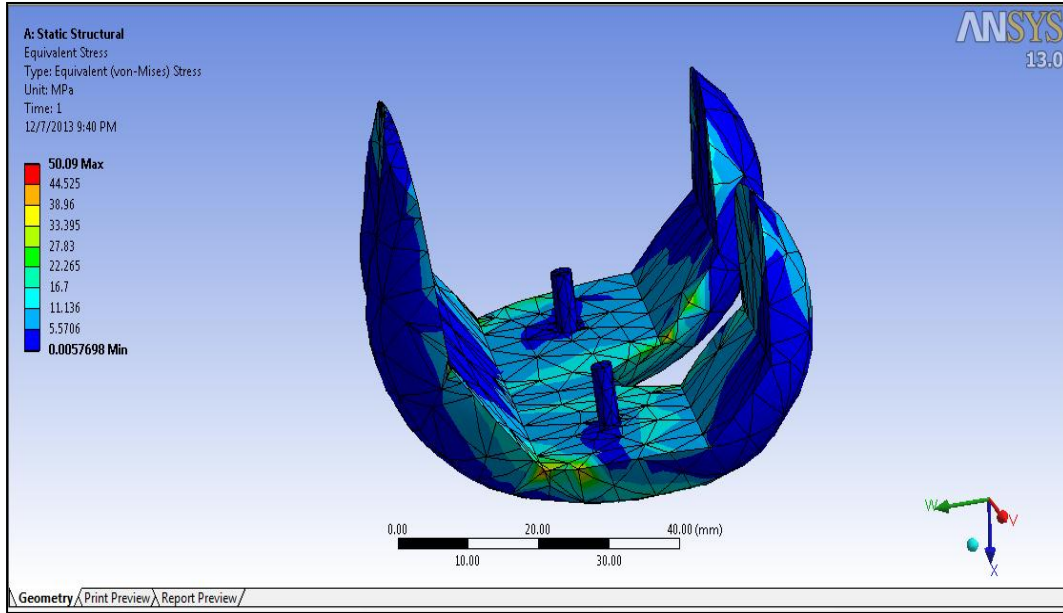


Figure 6.1(a) the vonMises stress distribution (MPa) in the conventional implant as five cut surface for case I.

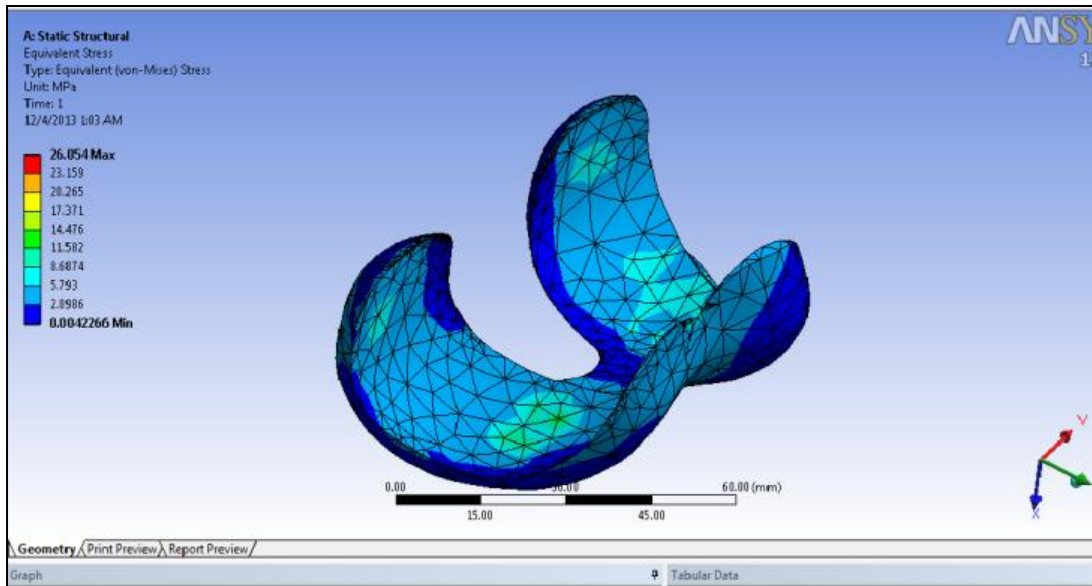


Figure 6.1(b) the vonMises stress distribution (MPa) in the custom implant as smooth surface for case I.

Also for the middle position case, the vonMises stress values for the conventional standard implant and custom implant approximately from 4.691×10^{-6} MPa to 24.54 MPa and from 0.0005605 MPa to 18.657 MPa respectively as shown in Figure 6.2(a) and 6.2(b).

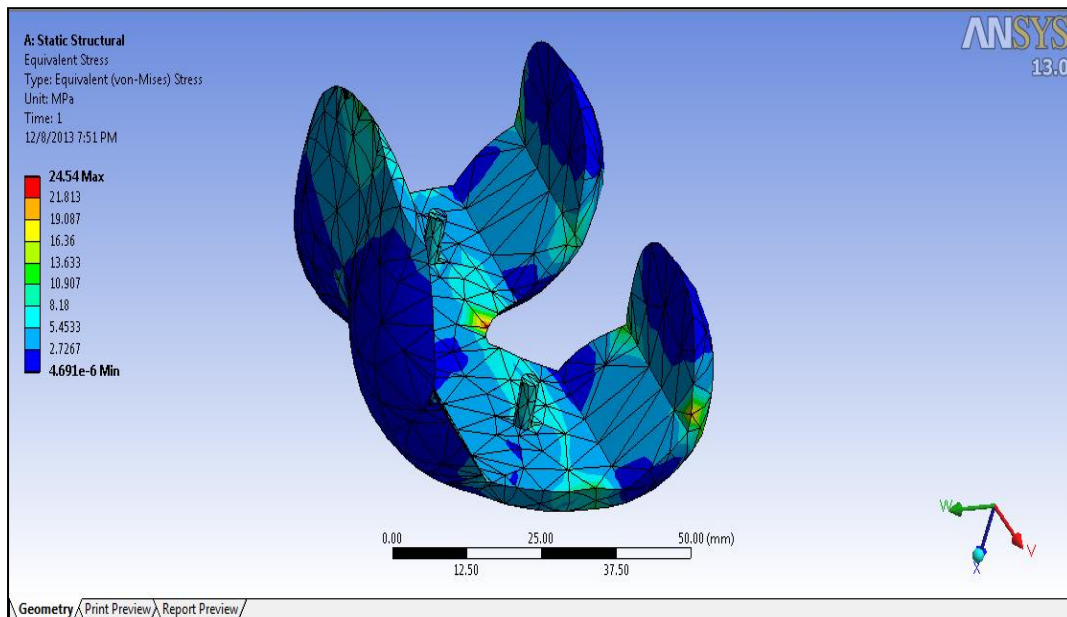


Figure 6.2(a) the vonMises stress distribution (MPa) in the conventional implant as five cut surface for case II.

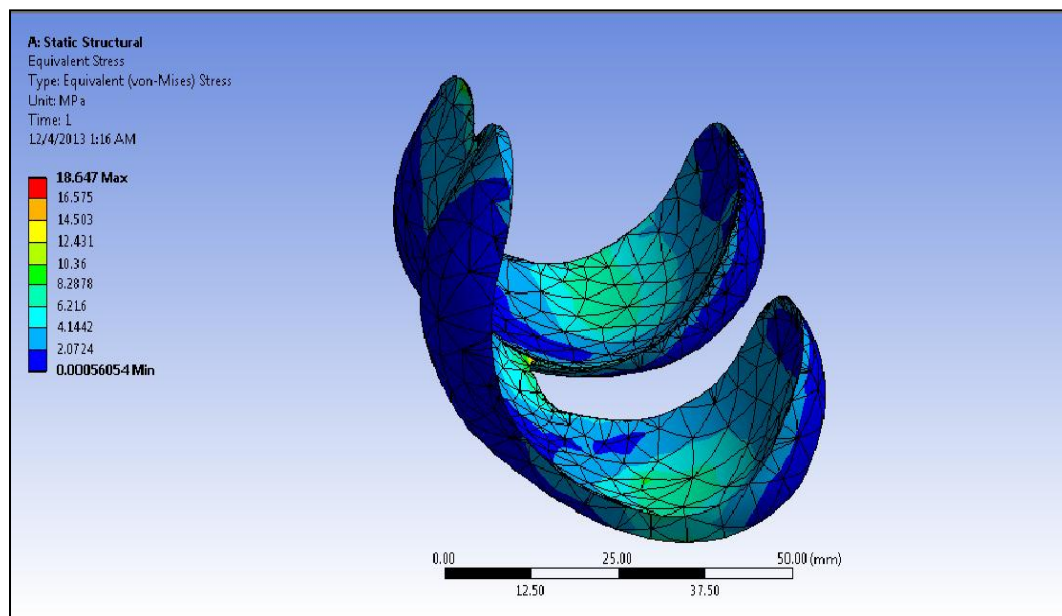


Figure 6.2(b) the vonMises stress distribution (MPa) in the custom implant as smooth surface for case II.

Finally for the back position, the vonMises stress values for the conventional standard implant and custom implant approximately from 6.1857×10^{-6} MPa to 40.144MPa and from .0004324 MPa to 22.881MPa respectively as shown in Figure 6.3(a) and 6.3(b).

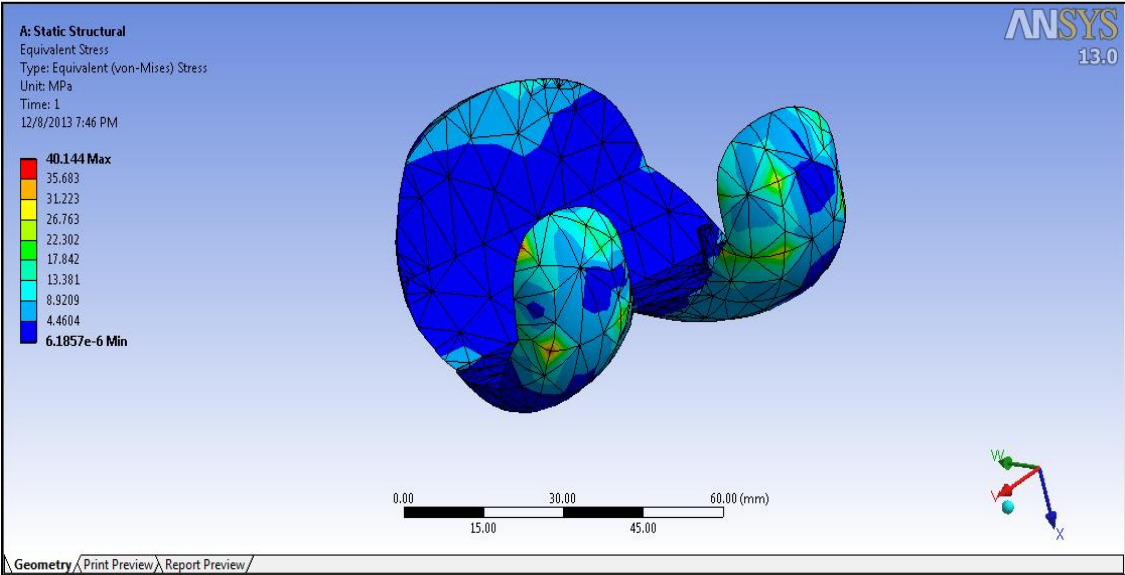


Figure 6.3 (a) the vonMises stress distribution (MPa) in the conventional implant as five cut surface for case III.

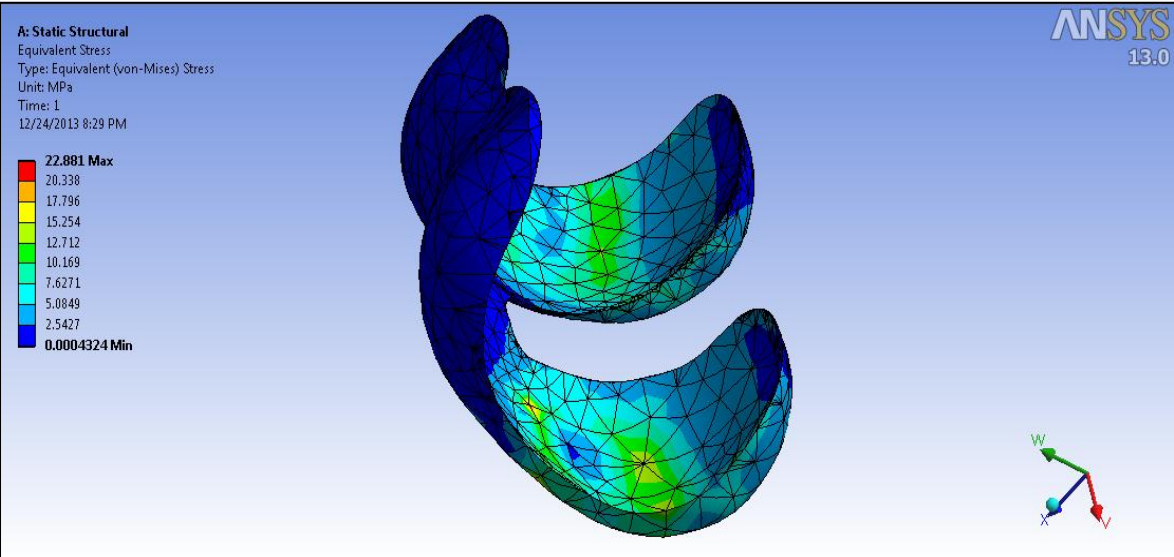


Figure 6.2(b) the vonMises stress distribution (MPa) in the custom implant as smooth surface for case III.

6.2 Discussion

In the current research, the femoral component of a customized knee implant system is proposed. Further design of the tibial component can be easily done with a similar approach. The process from converting CT data to CAD model was already available; however, the process of parametric inner surface design was not available. This research developed a detailed methodology on how to design such a parametric surface. Previously, generating parametric inner surfaces was tried using contours from a CT scan; this research used complete surface, which gives an added advantage of uniform thickness of the implant and better continuity.

The finite element analyses presented here were based on a perfect fit between the femoral implant and the distal femur bone because Boolean operations were used to simulate the cuts. This parametric distal femur was done in ANSYS workbench by using Boolean operation command. However, a perfect match of the contact surfaces is not very common when preparing them using hand tools and cutting guides. As discussed before, the average contact surface between bone and the implant is only about 50% when using conventional standard knee implant, meaning that the actual loading of the joint was probably worse than what is reported here. It is anticipated that the true surface pressures on the standard implants would be higher. Also from the results above, it can be seen that a custom implant as smooth surface with bone would provide a more even stress distribution on the implant-bone interface than the conventional femoral components implant. As discussed before from some previous study and also with the result above, when using the conventional femoral components, the stress concentrations along the sharp edges causes bone remodeling and increased bone density, while the areas between the sharp edges experience stress shielding that leads to bone resorption. This uneven bone remodeling is thought to lead to premature aseptic loosening, but it also increases the complexity of a revision surgery due to missing bone.

On the other hand, the downside of using custom-designed implant components is the time and cost associated with the design, as well as the need for a robotic surgical to perform and cut the distal femur bone. However, with time and experience, the design of custom femoral components based on a CT scan could become highly streamlined, and the total time and cost could be reduced to a minimum. To produce custom designed implant components at a reasonable cost has always been a problem and has discouraged this approach in the past. Recent developments

in direct metal fabrication using Rapid Prototyping technologies can radically change the situation.

With the production of custom implants now feasible in an EBM machine, there is a drastic reduction in cost as well as time to manufacture such implants. The technology is promising, the cost of manufacturing is comparable with the standard procedure currently followed, and the time for manufacturing is 1/3 of the current technique.

An Electron Beam Melting (EBM) machine is capable of producing 10–15 custom implant components in less than 15 hours in either titanium or cobalt-chromium at a reasonable cost [104]. The finishing operation is very similar to conventional implant fabrication and would not add significantly to the total cost. One advantage of producing a femoral implant component using the EBM technology is the ability to produce the porous bone ingrowth surface simultaneously. This will save time and cost otherwise associated with the sintering operation of titanium or cobalt-chromium beads, which is normally done in multiple steps and requires manual labor.

The cutting operation of the femur bone for the custom design prosthesis can be performed by using orthopedic robots. These robots can produce the freeform bone-implant interface using a rotating mill cutter that would produce an almost perfect fit between the distal femur bone and the femoral implant.

The proposed custom femoral component is not for every patient but can be applied to younger patients and those who have a more active lifestyle and will therefore depend on the implant for a long time. It is anticipated that custom-designed implants will increase the longevity and that the added cost can be justified for these younger, more active patients.

CHAPTER 7

CONCLUSION AND FUTURE WORK

7.1 Conclusion

This research provides a new method for custom design femoral component implant.

The proposed custom design of femoral component as smooth interface between the bone and the implant has the following advantages compared with a conventional standard femoral component.

- i. The articulating surface of custom femoral component design closely mimics the shape of the distal femur, there is no need for resurfacing of the patella and the gait cycle is not change.
- ii. Owing to the resulting uniform stress distribution, bone remodeling for the proposed custom design is even and the risk of premature loosening may be reduced.
- iii. For the implant design, the need for surgical interventions and fitting of filler components is reduced because the bone-implant interface can accommodate anatomical abnormalities at the distal femur.
- iv. The bone-implant interface for the custom implant is customized; about 40% less bone must be removed compared to the conventional standard knee joint prosthesis surgery procedures.

The primary disadvantages are;

- i. Time.
- ii. Cost required for the design, and
- iii. The possible need for robots to perform and cut the distal femur bone.

These disadvantages may be eliminated by the use of rapid prototyping technologies, especially the use of Electron Beam Melting technology for quick and economical fabrication of custom implant components.

This research only studied the stress distributions in the implant interface for the custom design and the conventional standard femoral implant; the wear and materials of the implant is not

within the scope of this research. For the conventional implant design, the stress distributions along the sharp edges, while the custom implant design showed a more uniform stress distribution.

7.2 Future work

This research introduces first of its kind custom femoral implant as smooth surface with the distal femur bone and a new manufacturing technique for producing proposed design. The research focuses only on design of custom implant femoral component and finite element analysis for examine the stress distribution on the implant. Significant work still remains in this area to successfully implant such system and get successful results. Following are some of the major area highlighted in which further research is required:

1. Design of custom tibial component of implant
2. Finite Element Analysis for total knee joint
3. Implant materials research
4. Robotic Surgery

The above mentioned areas of future research are now discussed in detail:

7.2.1 Design of custom human tibial component of implant

The design of custom tibial component shall contain mainly two components: The plastic component and the metal component. Design of these components can be done in very similar fashion as femoral component. Another aspect that has to be considered in design of tibial component is design of interface between plastic and metal components. Generally Ultra High Molecular Weight Polyethylene (UHMWPE) is used for manufacturing plastic component. This component shall have exact mat surface of femoral component of implant to ensure proper articulation. This component could either be injection molded or machined.

However, since this component is customized, creating a mold may not be economical and machining of such component could easily be achieved. The metal component, which is inserted in the tibia, should be designed to retain ligaments and have a parametric inner surface. It is proposed that this parametric surface could be concave or convex. A study has to be initiated to

know which type of surface (convex or concave) could give better results in terms of uniform stress distribution over the entire surface. This tibia component however can be manufactured using EBM technique.

7.2.2 Finite Element Analysis for total knee joint

After understanding the knee joint mechanics, a Finite Element Analysis of femoral component implant and femur bone could be carried out. This shall reveal the stress distribution pattern at the bone-implant interface. Once the tibial component of the custom human knee implant system is designed, a complete finite element analysis of the artificial knee joint can be done. This study will reveal important areas of improvement. The design then can be modified and optimized accordingly. Closed solid CAD model is already available for femoral component. Using similar approach, a CAD model can also be generated for tibial components and FEA could be carried out.

7.2.3 Implant materials research

In current research, a Titanium based alloy was used in implant design (Ti6Al4V) and was used in FEA for test the stress distribution on bone-implant interface for femoral component and it may be used in production of femoral component on EBM Machine.

Currently different implant materials like Chromium-Cobalt, Ceramic are used. Machine parameters on EBM should also be determined for materials like Chromium-Cobalt and a comparison should be carried out on which material is better, particularly using this technology.

7.2.4 Robotic Surgery

Robotic surgery has been used in many area of medicine including orthopedic. The current design of custom knee implants required to have a parametric contour based femur surface. As mentioned previously, a femur component surface of design implant was generated for robotic surgery.

Design of such robotic system will help developed confidence in surgeons for using automation in surgery. A robot acts as an extension of the surgeon's eyes and hands in a minimally invasive surgery to design femoral knee component surface as shown in figure 7.1 [105].



Figure 7.1 Surgical robotics (orthopedic robots)

APPENDIX

Appendix A: Segmentation Procedure and 3D model

MIMICS works on the concept of stacking the two-dimensional images in order to convert it into three -dimensional images. Three-dimensional modeling process of knee prosthesis consisted of some main steps. Figure A.1 is the flow chart regarding the construction of knee geometry model.

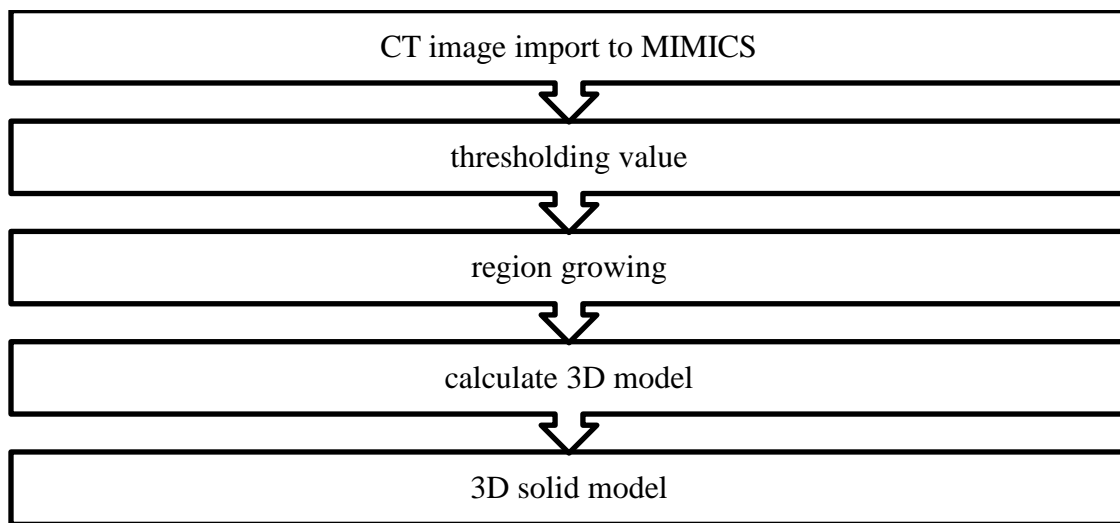


Figure A-1 knee geometry model construction flow chart

A.1 Computed tomography scan

As illustrated, modeling was started using computed tomography (CT scan) images. The medical images were exported from the CT equipment in the DICOM format. The DICOM (Digital Imaging and Communications in Medicine) file format is the standard method for the transmission of medical images and their associated information. These DICOM image files were retrieved from the CT scanner workstation and copied on a CD. DICOM image files are imported into MIMICS 10.01. Mimics divide the screen into three views: the original axial view of the image, and resliced data making up the coronal and sagittal views. Cropping operation of CT images in all three views reduces the chances of segmenting unwanted geometry and fixes the region of interest that has to be a segment of the remaining part.

A.2 Thresholding Value

Once the images are imported, the next stage is to select the correct threshold value for the region growing function. Profile line is used to determine the appropriate threshold value for the 3D reconstruction. It was drawn in axial view between two extremities of cortical bone in the distal femur part as shown in Figure A.2 (a).

The selection of the threshold value is important for the accuracy of the resulting model, enhances the image and focuses only on the area of interest. If the value is selected too low, then the resulting model will be smaller than the actual knee joint. The threshold function will separate the soft tissue from the hard tissue isolating the bone structure only.

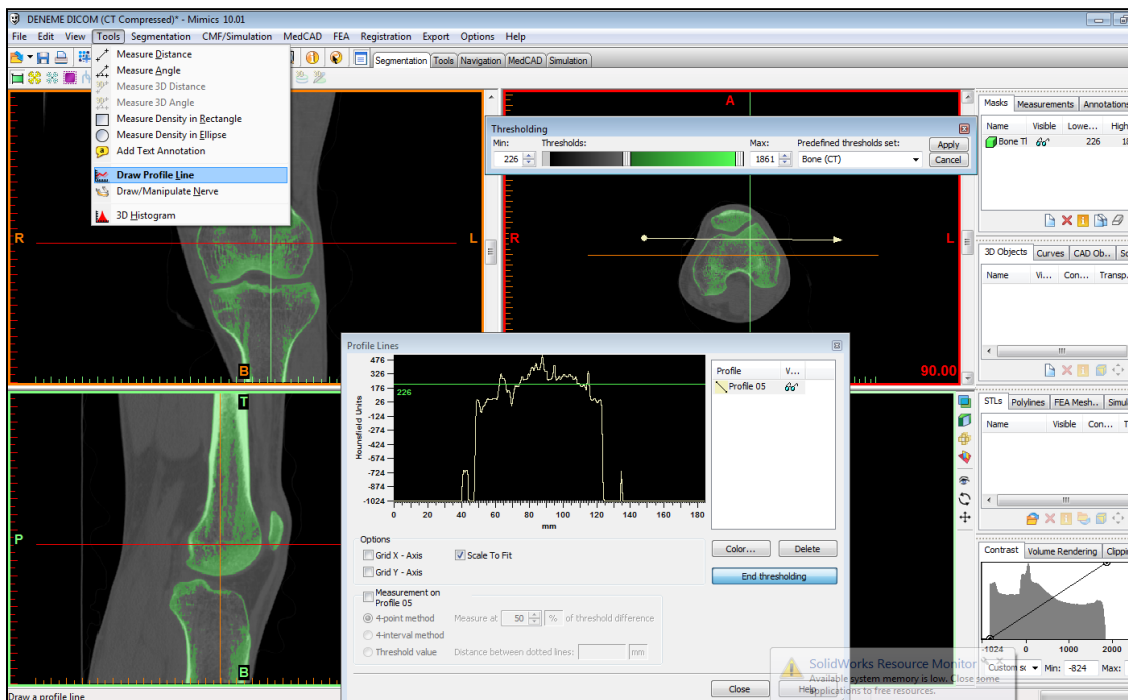


Figure A.2 (a) Profile line drawn on axial view.

Based on profile line value, which gives the Hounsfield unit variation over the line drawn; thresholding operation was performed to create a mask which connects all the regions of the same threshold range.

The green mask as shown in Figure 4 was created automatically which falls inside the cropped region after the accomplishment of thresholding operation by select thresholding in the main

toolbar and click apply with the standard settings as for Bone (CT), then rename the mask "Bone Thresholding" by clicking green in the mask tab .

Selection of the threshold value is very important and plays a vital role in the accuracy of the model generated. The value of the threshold shown in the Hounsfield unit varies from -1024 to 476. The area below 226 indicates the start of soft tissue. If the threshold value is too high, cancellous bone is neglected. If the value is selected too low, then unwanted soft tissues are included and the resulting model will be smaller than the actual knee joint. The threshold function will separate the soft tissue from the hard tissue isolating the bone structure only, also separate each bone from the bone structure.

The 3D Histogram as shown in Figure A.2 (b) can be used to identify the boundary between soft tissue and bone. The 3D Histogram is the histogram of the complete data set. The X-axis lists the gray values; along the Y-axis the number of pixels that is displayed. The range of these axes can be user defined or automatic (all values). The Y-range can be logarithmic or decimal. The (yellow) line(s) correspond to the threshold value(s) of the active mask selected. These values vary with every person since they have different bone densities.

The range of correct threshold value of soft tissue from 200 to 1125, and the range bone of gray value (threshold value) from 1125 to 2701 as shown in figure A.2 (b).

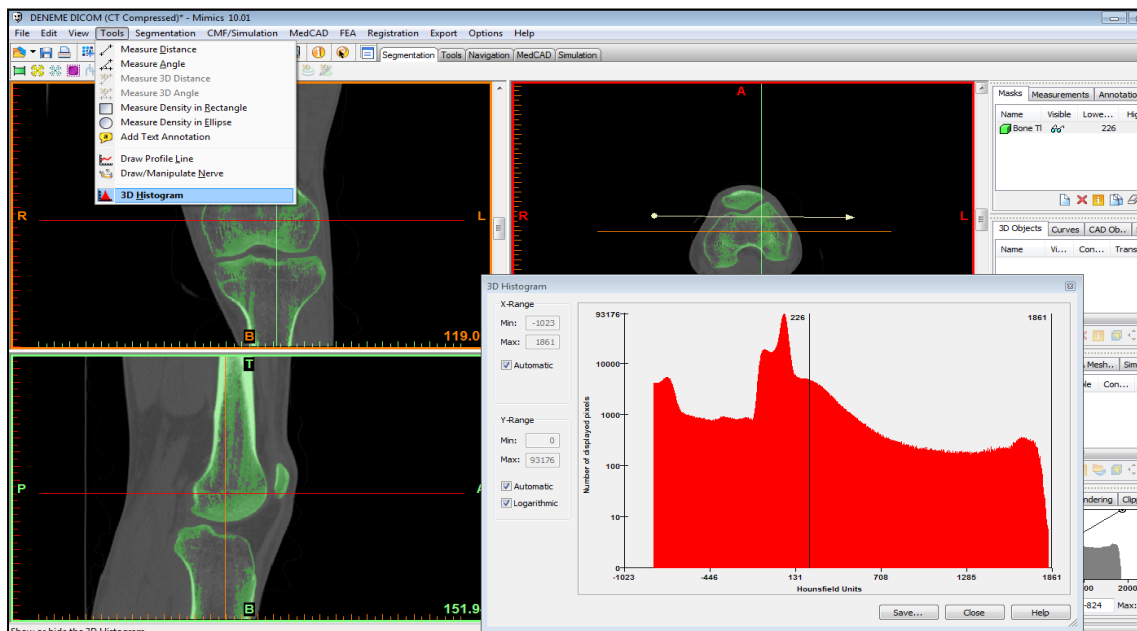


Figure A.2 (b) typical range of gray value for human knee (3D histogram)

A.3 Region growing

To complete the isolation of the hard tissue, the "Region Growing" function was used. This function connects all volumetric pixels (voxels) within the threshold that are physically connected to the initially selected voxel. During the process of 3D reconstruction, each pixel on every image is converted into a voxel (Volume element). During region growing, the color of the mask is selected in an image and all the images connected to that mask get selected and copied in a new mask. While operating region growing function, termination of all connectivity between distal femur and proximal tibia part should be strictly followed. Because the distal femur and the proximal tibia are not connected, multiple region growings were applied using different masks and colors as shown in figure A.3.

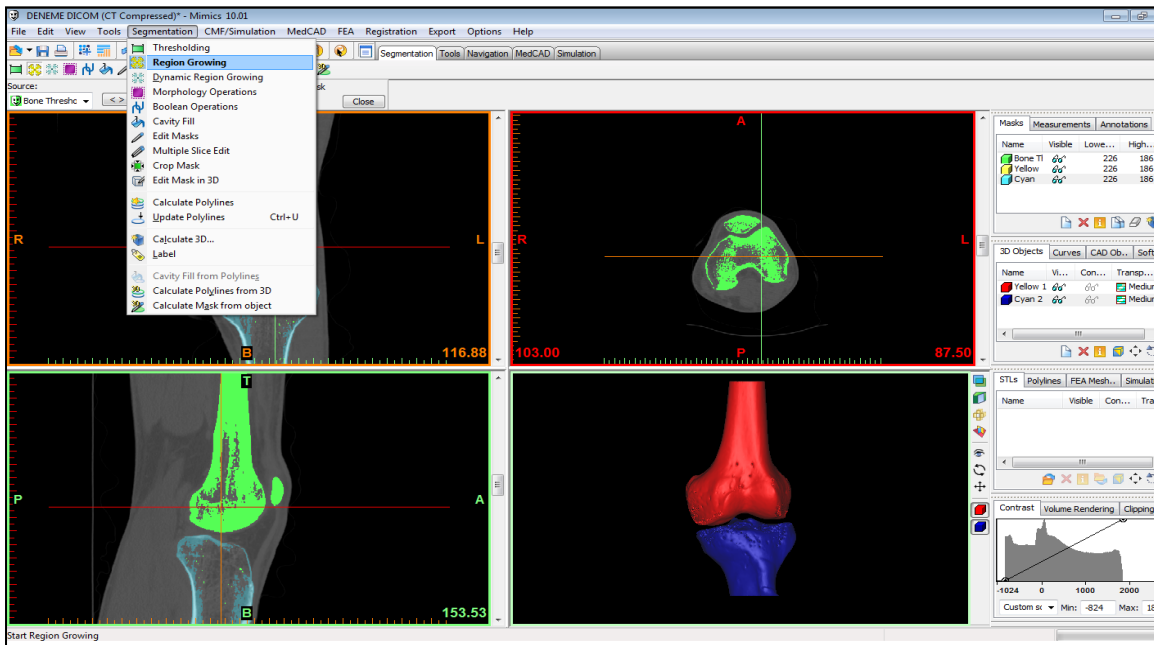


Figure A.3 Region growing operation

A.4 Three dimensional reconstructions

Following region growing, the model is now ready for 3D reconstruction. Each mask was converted into a 3D model using the "calculate 3D" function as shown in figure A.4. Because of the thresholding function, some of the cancellous bone was not included; and this created

unwanted internal voids in the model. "Calculate 3D" function was called to convert the green mask into three-dimensional surface. A complete solid model was desired for the custom design phase, and editing of the masks was necessary from the segmentation menu of MIMICS 10.01.

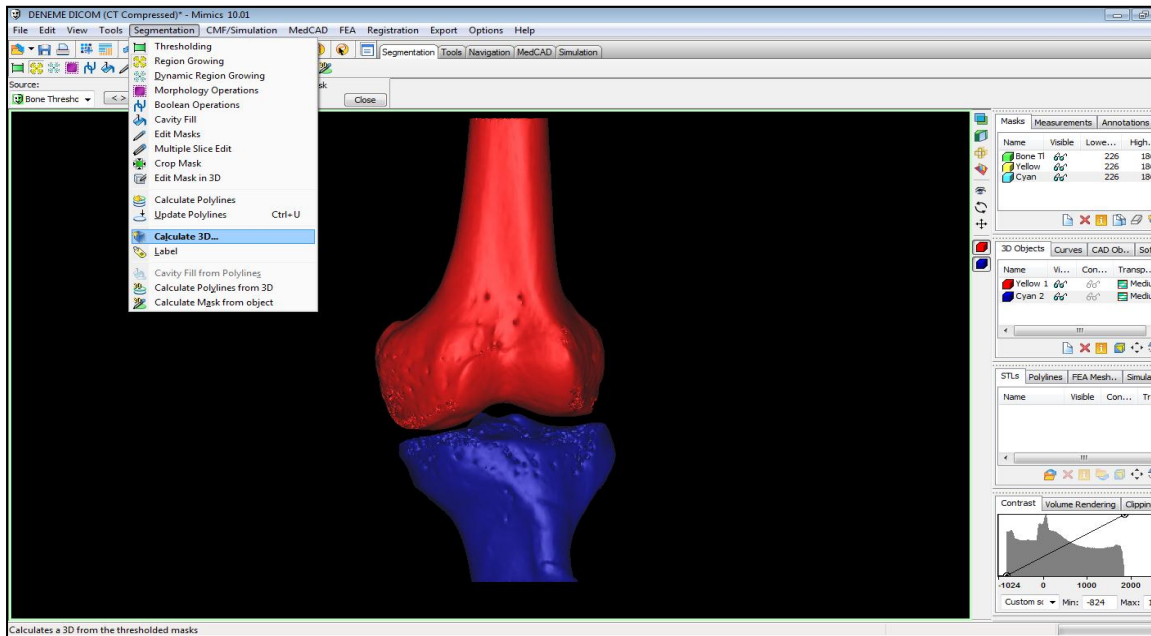


Figure A.4 Three- dimensional CAD model of knee generated in MIMICS

By means of creating and modifying these segmentation masks in Mimics, the 3D CAD models of the knee are obtained. MIMICS use a smoothing algorithm during the 3D reconstruction phase to create a more realistic model. The model will be the anatomical reference for the design of the prosthesis. It is also the base for the surgical instrumentation design and the surgical operation planning.